

NOAA Technical Memorandum ERL GLERL-49

INVESTIGATION OF THE CURRENTS
AND DENSITY STRUCTURE OF LAKE ERIE

James H. Saylor
Gerald S. Miller

Great Lakes Environmental Research Laboratory
Ann Arbor, Michigan
July 1983



**UNITED STATES
DEPARTMENT OF COMMERCE**

Malcolm **Baldrige**,
Secretary

NATIONAL OCEANIC AND
ATMOSPHERIC ADMINISTRATION

John V. Byrne,
Administrator

Environmental Research
Laboratories

Vernon E. Derr,
Acting Director

NOTICE

Mention of a commercial company or product does not constitute an endorsement by NOAA Environmental Research Laboratories. Use for publicity or advertising purposes of information from this publication concerning proprietary products or the tests of such products is not authorized.

CONTENTS

	Page
Abstract	1
1. INTRODUCTION	1
2. DESCRIPTION OF MEASUREMENTS	4
3. RESULTS	12
4. SUMMARY AND DISCUSSION	48
5. REFERENCES	51
Appendix A.--LOW-PASS FILTERED WIND STRESS VECTORS FOR THE PERIOD OF THE CURRENT MEASURING PROGRAM, MAY 1979 THROUGH JUNE 1980.	55
Appendix B.--WATER TEMPERATURE ISOTHERMS (°C) DRAWN FROM THERMISTOR CHAIN RECORDINGS AT MOORINGS 9, 11, 19, AND 21 IN THE CENTRAL BASIN OF LAKE ERIE FOR MAY THROUGH SEPTEMBER 1979.	60
Appendix C.--VECTOR-AVERAGED LAKE ERIE CURRENTS COMPUTED ON A MONTHLY BASIS FOR MAY 1979 THROUGH JUNE 1980.	66

FIGURES

	Page
1. Lake Erie bathymetry and instrument mooring locations.	2
2. Typical configuration of a Lake Erie current meter mooring.	5
3. Lake Erie surface water temperature observed in 1979 compared to a climatological mean calculated by Felt and Goldenberg (1976).	13
4. Vector-averaged lake currents observed on May 24-25, 1979, during a storm with winds from the north-northeast . The arrowhead indicating direction of flow is not included as a part of the current speed scale. Open arrowheads show currents closest to the bottom on moorings that had three current meters.	14
5. Movements of Woodhead sea surface drifters released and recovered in Lake Erie in 1979.	17
6. Lake Erie resultant current vectors for the period July 1 through September 20, 1979.	22
7. Lake Erie resultant current vectors for the period October 1 through December 31, 1979.	23
8. A drawing of the Woodhead seabed drifter. It is weighted at the tail so that it stands upright on the lake bottom; bottom currents fill the umbrella-shaped head and drag the drifter along. The surface version floats head downward.	24
9. Movements of Woodhead seabed drifters released in Lake Erie in 1979 and subsequently recovered.	24
10. Lake Erie resultant current vectors for September 17-23, 1979. Clockwise circulation prevails in both the central and eastern basins.	28
11. Lake Erie resultant current vectors for October 3-7, 1979. Anticlockwise circulation prevails throughout the central basin and the northern half of the eastern basin.	29
12. Generalization of the third dominant circulation pattern observed in the Lake Erie current charts.	31

13. Kinetic energy spectra computed from hourly averaged current velocity recordings at station 17 during May through October 1979. Both the rotary components and the total kinetic energy are presented. 32
14. Rotary spectra of the hourly wind stress vectors computed by Schwab (1982) from National Water Research Institute buoy wind measurements during May through October 1973. 33
15. Transport streamline pattern at different phases of a gravest mode vorticity wave in an elliptic paraboloid. 35
16. The rotary components of kinetic energy spectra computed from 4-h-averaged current velocity recordings during May through November 1979 at three moorings situated on a cross section of the eastern basin of Lake Erie. 36
17. Low-pass filtered, hourly-averaged current velocity vectors (drawn at 2-h intervals) from a middle of the eastern basin (mooring 28) current meter at 33 m depth for the month of August 1979. 36
18. Kinetic energy spectra computed from 4-h-averaged current velocity recordings at mooring 15 during May through December 1979. 38
19. Kinetic energy spectra computed from hourly-averaged current velocity recordings at mooring 6 during May through October 1979. 38
20. Hourly water levels at Toledo (solid line) and Buffalo and the current velocity component parallel to the channel axis at moorings 4, 5, and 6, August 1-15, 1979. 39
21. Low-pass filtered water levels at Toledo (solid line) and Buffalo and the current **velocity** component parallel to the channel axis at moorings 4, 5, and 6, August ~~29-~~September 27, 1979. 41
22. Water temperature recordings at moorings 23, 25, and 26 on a cross section of Lake Erie at the Pennsylvania Ridge. 43
23. Low-pass filtered wind stresses computed for Lake Erie in **July** 1979 (Schwab, 1982) and currents (both **hourly-**averaged but plotted at 2-h intervals) across the Pennsylvania Ridge. 44

24.	Low-pass filtered Lake Erie wind stresses and currents at the Pennsylvania Ridge in September 1979.	45
25.	Lake Erie stream function (top) for a 5.2 m s^{-1} west wind.	47
26.	Low-pass filtered wind stress vectors for May, June, July, and August 1979.	56
27.	Low-pass filtered wind stress vectors for September, October, November, and December 1979.	57
28.	Low-pass filtered wind stress vectors for January, February, March, and April 1980.	58
29.	Low-pass filtered wind stress vectors for May and June 1980.	59
30.	Water temperature isotherms ($^{\circ}\text{C}$) drawn from thermister chain recordings at moorings 9, 11, 19, and 21 in the central basin of Lake Erie for May 1979.	61
31.	Water temperature isotherms ($^{\circ}\text{C}$) drawn from thermister chain recordings at moorings 9, 11, 19, and 21 in the central basin of Lake Erie for June 1979.	62
32.	Water temperature isotherms ($^{\circ}\text{C}$) drawn from thermister chain recordings at moorings 9, 11, 19, and 21 in the central basin of Lake Erie for July 1979.	63
33.	Water temperature isotherms ($^{\circ}\text{C}$) drawn from thermister chain recordings at moorings 9, 11, 19, and 21 in the central basin of Lake Erie for August 1979.	64
34.	Water temperature isotherms ($^{\circ}\text{C}$) drawn from thermister chain recordings at moorings 9, 11, 19, and 21 in the central basin of Lake Erie for September 1979.	65
35.	Vector-averaged Lake Erie currents for May 1979. The arrowhead indicating direction of flow is not included as a part of the current speed scale; open arrowheads show currents closest to the bottom. Monthly averaged water temperatures recorded in current meters nearest the surface and at 2.3 m above the bottom are also displayed.	67
36.	Vector-averaged Lake Erie currents for June 1979. The arrowhead indicating direction of flow is not included as a part of the current speed scale; open arrowheads show currents closest to the bottom. Monthly averaged water temperatures recorded in current meters nearest the surface and at 2.3 m above the bottom are also displayed.	68

37. Vector-averaged Lake Erie currents for July 1979. The arrowhead indicating direction of flow is not included as a part of the current speed scale; open arrowheads show currents closest to the bottom. Monthly averaged water temperatures recorded in current **meters** nearest the surface and at 2.3 **m** above the lake are also displayed. 69
38. Vector-averaged Lake Erie currents for August 1979. The arrowhead indicating direction of flow is not included as a part of the current speed scale; open arrowheads show currents closest to the bottom. Monthly averaged water temperatures recorded in current meters nearest the surface and at 2.3 **m** above the bottom are also displayed. 70
39. Vector-averaged Lake Erie currents for September 1979. The arrowhead indicating direction of flow is not included as a part of the current speed scale; open arrowheads show currents closest to the bottom. Monthly averaged water temperatures recorded in current meters nearest the surface and at 2.3 **m** above the bottom are also displayed. 71
40. Vector-averaged Lake Erie currents for October 1979. The arrowhead indicating direction of flow is not included as a part of the current speed scale; open arrowheads show currents closest to the bottom. Monthly averaged water temperatures recorded in current meters nearest the surface and at 2.3 **m** above the bottom are also displayed. 72
41. Vector-averaged Lake Erie currents for November 1979. The arrowhead indicating direction of flow is not included as a part of the current speed scale; open arrowheads show **currents** closest to the bottom. Monthly averaged water temperatures recorded in current meters nearest the surface and at 2.3 **m** above the bottom are also displayed. 73
42. Vector-averaged Lake Erie currents for December 1979. The arrowhead indicating direction of flow is not included as a part of the current speed scale; open arrowheads show currents closest to the bottom. Monthly averaged water temperatures recorded in current meters nearest the surface and at 2.3 **m** above the bottom are also displayed. 74
43. Vector-averaged Lake Erie currents for January 1980. The arrowhead indicating direction of flow is not included as a part of the current speed scale; open arrowheads show currents closest to the bottom. Monthly

- averaged water temperatures recorded in current meters nearest the surface and at 2.3 m above the bottom are also displayed. 75
44. Vector-averaged Lake Erie currents for February 1980. The arrowhead indicating direction of flow is not included as a part of the current speed scale; open arrowheads show currents closest to the bottom. Monthly averaged water temperatures recorded in current meters nearest the surface and at 2.3 m above the bottom are also displayed. 76
45. Vector-averaged Lake Erie currents for March 1980. The arrowhead indicating direction of flow is not included as a part of the current speed scale; open arrowheads show **currents** closest to the bottom. Monthly averaged water temperatures recorded in current meters nearest the surface and at 2.3 m above the bottom are also displayed. 77
46. Vector-averaged Lake Erie currents for April 1980. The arrowhead indicating direction of flow is not included **asa** part of the current speed scale; open arrowheads show currents closest to the bottom. Monthly averaged water temperatures recorded in current meters nearest the surface and at 2.3 m above **the** bottom are also displayed. 78
47. Vector-averaged Lake Erie currents for May 1980. The arrowhead indicating direction of flow **is** not included as a part of the current speed scale; open arrowheads show currents closest to the bottom. Monthly averaged water temperatures recorded in current meters nearest the surface and at 2.3 m above the bottom are also displayed. 79
48. Vector-averaged Lake Erie currents for June 1980. The arrowhead indicating direction of flow is not included **as** a part of the current speed scale; open arrowheads show currents closest to the bottom. Monthly averaged water temperatures recorded in current meters nearest the surface and at 2.3 m above **the** bottom are also displayed. 80

TABLES

	Page
1. Location and makeup of the Lake Erie current meter moorings and the interval of data collections.	6
2. Release and recovery information for Lake Erie surface drifters.	18
3. Release and recovery information for Lake Erie seabed drifters.	25

INVESTIGATION OF THE CURRENTS AND DENSITY STRUCTURE OF LAKE ERIE*

James H. Saylor and Gerald S. Miller

Currents and water temperatures were recorded at a large-scale grid of fixed moorings in Lake Erie from May 1979 through June 1980. Thermistor **chains** were used to record the complete development and decay of central basin stratification. First a fragile stability develops, which is very susceptible to high wind stress. For example, strong wind impulse in late May 1979 completely mixed the central basin and postponed the development of stable stratification for 3 weeks. Currents measured in **the** lower half of **the** central basin water column were mostly return flows (beneath **the** surface wind drift) driven by the surface pressure gradient. We often observed a complex system of Lake Erie circulation gyres as predicted by models, although we noticed a frequent tendency for one of the central basin gyres to become dominant and envelop the whole basin in either uniform clockwise or anticlockwise flow. It is not clear why one of the circulation cells grows as opposed to the others. The currents appear to be somewhat more barotropic than predicted by full Ekman layer current models. Tidal-like currents driven by the longitudinal seiches of Lake Erie control the island-filled passages between **the** western and central Lake Erie basins, with currents across the **whole** island chain very much in phase. Processes of hypolimnion volume entrainment are suggested from the central basin temperature recordings. Large quantities of water were exchanged between the central and eastern basins over long periods; this occurred mostly after the shallow ridge **that** separates them had become unstratified. These and other topics are discussed as we explore the large data set generated from the experiment.

1. INTRODUCTION

We measured currents and water temperature distributions in Lake Erie from May 1979 through June 1980. The measurements were undertaken as a contribution to the Lake Erie **Surveillance** Program performed for **the** International Joint Commission (**IJC**) by the Environmental Protection Agency (**EPA**), and the EPA provided partial funding for this work. Because of research interest in the large-scale lake circulation processes, our measurements were made on a lake-wide grid of stations as shown in figure 1. Fit into **this** lake-wide grid were several area-specific concentrated water temperature and current measuring programs performed by Canada's National Water Research Institute (**NWRI**). Their studies were locally intensive and **process-**oriented (e.g., diffusion of oxygen across **the** thermocline in the central basin). Data collection schedules and station configurations were generally

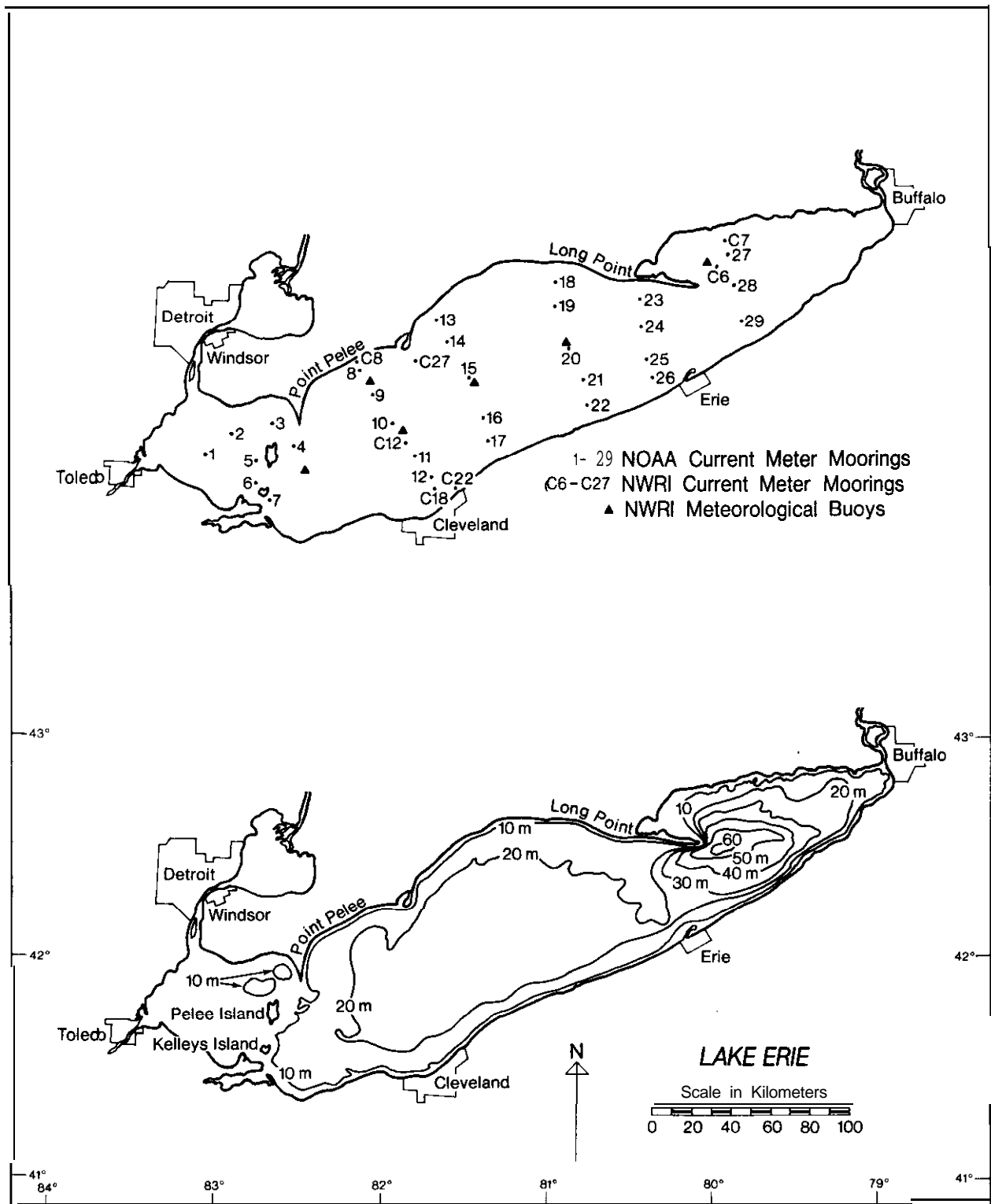


FIGURE 1.--Lake Erie bathymetry and instrument mooring locations.

coordinated prior to the experiment. Following completion of the field experiments, F. M. Boyce of NWRI organized regular workshops involving discussions of progress and goals in data analyses.

In the past, Lake Erie current measurements were mostly qualitative in nature, originating with the whole-basin drift bottle studies of **Harrington** (1895). Current studies using similar methods of measurement have been made sporadically ever since, focusing primarily on the western basin and island region. Olson (1950) studied surface currents using drift cards (an innovative technique at that time) to trace the Detroit River inflow and patterns of movement about **Pelee** Island. **Verber** (1953, 1955) used drift cards, current drogues, and a current meter in the inter-island channels to describe rotational water circulations in the western basin and around the islands. Several other studies of a similar nature have produced patterns of interest (c.f., Wright, 1955, and O'Leary, 1966); we will discuss how our studies agree with some of these earlier results in later chapters.

Distributions of water temperature, turbidity, and alkalinity have been used to infer circulation patterns. Powers *et al.* (1960) investigated the whole basin, while Hartley *et al.* (1966) concentrated on the western basin. Hamblin (1971) studied summer water temperature distributions in the eastern basin and suggested a strong cyclonic flow during the stratified season based on geostrophy.

The first extensive studies of lake currents using direct methods were made by the U.S. Public Health Service in 1964 and 1965 (FWPCA, 1968). They moored current meters and water temperature recorders on a lake-scale grid and reported some general patterns of mid-depth and near-bottom current flows deduced from their observations. The measurements were made with early versions of self-contained **Savonius** rotor current meters that recorded on photographic film. The data were difficult to transcribe from the film in an orderly and accurate fashion, even with the automated light dot scanner developed by the instrument manufacturer. Thus, long time series of reliable current velocity recordings at numerous open lake stations recorded simultaneously have generally been unavailable for model comparisons or verification.

Hamblin (1971) studied the PWPCA data extensively and reported **vector-**averaged current observations on a monthly basis throughout the year. He discussed the observations in relation to prior studies in each of the three Lake Erie basins and made some comparisons with currents inferred from water density distributions obtained from synoptic surveys performed from research vessels.

Near-bottom currents in the central basin were measured during Project Hypo in 1970 (**Blanton** and Winklhofer, 1971 and 1972). With an array of moorings in place during July and August of that year, the same current recording instruments as used in the PWPCA studies referred to above were used to measure movements of the oxygen deficient **hypolimnion** water mass. These investigations revealed a dynamic **thermocline** surface separating the surface and bottom layers; it is pushed deeper along the southern shore of the lake in response to prevailing southwesterly winds and with upwelling of the

hypolimnetic layer along the northern shore. This semipermanent tilt of the thermocline during those 2 months was associated with northwesterly flow of bottom water across the basin, conforming to bottom current patterns suggested by movements of seabed drifters released in the central basin during 1965 by Hartley (1968). In the Project Hypo studies, dissolved oxygen concentrations were monitored thoroughly throughout the central basin and factors influential in causing anoxia, such as sediment oxygen demand and bacterial processes, were looked at simultaneously. The investigations were instrumental in confirming the seriousness of the oxygen depletion problem in this area of the lake and effective in underscoring the dynamical forces controlling the movements of the bottom waters. Important inferences were drawn concerning the role these forces play in causing hypolimnion volume changes that may also result in oxygen enrichment.

One process of bottom water renewal suggested by the results of Project Hypo was a deep inflow of hypolimnion water from the eastern basin to the central basin through the deep channel south of the Pennsylvania Ridge. Comprehensive current velocity, water temperature, and dissolved oxygen profiles across this ridge and extending into both the eastern and central basins were measured by NWRI in 1977 and 1978 and reported by Boyce *et al.* (1980) and Chiochio (1981).

The objectives of this report are to present the characteristic flow patterns and their persistence as derived from analyses of our new measurements in Lake Erie and to relate the patterns to the driving forces. We will describe how these new data fit into the existing circulation knowledge base and how they relate to what is known of the water volume exchange processes between the three basins. We will also compare our results with several earlier numerical simulations of currents in Lake Erie and discuss some of their similarities and differences.

2. DESCRIPTION OF MEASUREMENTS

Currents and water temperatures were measured with an array of EG&G vector averaging current meters. These current meters accumulate in electronic storage registers the east and north components of the current flow past the meter for a preselected fixed interval of time; this interval was 15 min in Lake Erie. Computation of the direction vector is triggered eight times for each revolution of the Savonius rotor current speed sensor. For example, in a 50 cm s^{-1} current, 10,400 current vector computations are completed in a 15-min sampling period. The averaged current vector, together with a reading of the ambient water temperature, is then read onto a magnetic tape cassette at the end of the interval.

The Savonius rotor has been used to measure current speed for many years and its characteristics are relatively well known (e.g., Gaul *et al.*, 1963). Threshold speed in the EG&G version is about 2.5 cm s^{-1} . A thermistor located inside the current meter housing is used for the water temperature measurement and is accurate to $\pm 0.1^\circ\text{C}$.

In May 1979, we deployed 29 current metering stations in Lake Erie at locations shown in figure 1. The deployments were made from the EPA Research Vessel *Rachel Carson*. All of the stations consisted of a series of current meters stretched in a taut line and suspended in the water column beneath a subsurface float (fig. 2). This mooring arrangement minimizes the vertical movements of the current meters, since it is well known that the Savonius rotors tend to overspeed with vertical accelerations of the meters. The subsurface buoys were placed deep enough to be beneath significant wind wave orbital velocities for all but the most intense Lake Erie storms. In the shallow western basin of the lake, only one current meter per mooring was placed at stations 1 through 7. With the thought that these moorings would be recovered in fall 1979, a surface float was attached to the anchor at the end of the ground line. The other 22 moorings had more than one current meter and were also equipped with EG&G acoustic releases placed in the current meter strings just above the railcar wheel anchors. No surface markers were attached to these moorings.

Configurations of the individual stations are given in table 1. Outside the western basin, a current meter was deployed 10 m below the water surface at each station. Each of these stations also had a current meter as close to the bottom as the fastening hardware and acoustic release length would permit, with the current sensor itself thus placed at 2.3 m above the bottom. (This was the design depth; actually the anchor settles into the bottom some unknown distance and the measurements are somewhat closer to the lake floor). Several stations in water deeper than 20 m had a third current meter between the 10-m depth and the bottom meter. The table also gives the length of the water temperature and current velocity record obtained from each meter.

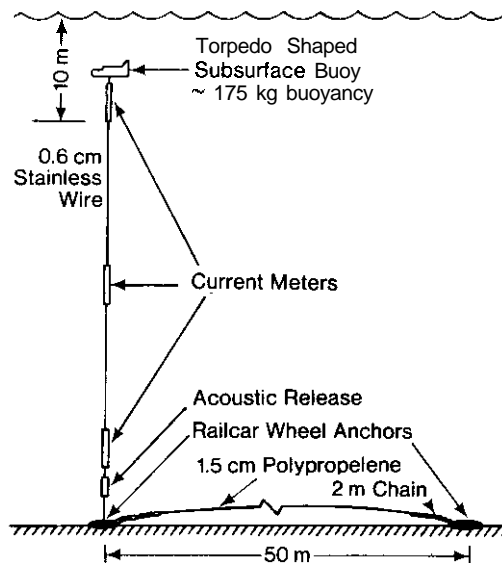


FIGURE 2.--Typical, configuration of a Lake Erie current meter mooring.

TABLE 1.--Location and *makeup* of the Lake Erie current meter moorings and the interval of data collections. The prefix C indicates NWRI stations that we used in this report. Thermistor chain moorings are also listed.

Mooring	Position		Water depth	Meter depth	Current	Data interval	
	(°N)	(°W)	(m)	(m)		Temperature	
1	41°46.1'	83°04.0'	10.0	6.0	--	130/1979-294/1979	
2	41°51.7'	82°54.2'	11.3	6.9	--	130/1979-294/1979	
3	41°54.5'	82°39.6'	11.6	6.7	--	--	
4	41°49.0'	82°30.7'	12.2	6.7	130/1979-294/1979	130/1979-294/1979	
5	41°44.2'	82°44.8'	11.0	6.0	132/1979-339/1979	132/1979-339/1979	
6	41°38.3'	82°44.8'	15.9	7.4	132/1979-297/1979	132/1979-297/1979	
7	41°33.8'	82°40.6'	12.5	6.7	--	--	
8	42°10.0'	82°07.6'	20.4	10.0 18.1	-- --	-- --	
9	42°03.1'	82°02.6'	22.9	10.0 20.6	128/1979-207/1980 128/1979-276/1980	128/1979-207/1980 128/1979-276/1980	
10	41°55.6'	81°55.0'	24.4	10.0 17.3 22.1	128/1979-154/1980 -- 128/1979-154/1980	128/1979-154/1980 128/1979-343/1979 128/1979-154/1980	
11	41°46.5'	81°47.3'	23.5	10.0 21.2	128/1979-144/1980 128/1979-217/1980	128/1979-144/1980 128/1979-217/1980	

TABLE 1.--Location and *makeup* of the Lake Erie current meter moorings and the interval of *data collections*. The prefix C indicate8 NWRI stations that we used in this report. Thermistor chain moorings are also tinted. (Cont.)

Mooring	Position		Water depth (m)	Meter depth (m)	Current	Data interval	
	(°N)	(°W)				Temperature	
12	41'39.6'	81'41.0'	19.8	10.0 17.5	129/1979-217/1980 --	129/1979-217/1980 129/1979-015 /80	
13	42°23.0'	81'40.0'	18.3	10.0 16.0	129/1979-156/1980 --	129/1979-129/1979 --	
14	42°17.1'	81'35.6'	23.5	10.0 21.2	129/1979-156/1980 271/1979-156/1980	129/1979-156/1980 271/1979-156/1980	
15	42'07.7'	81°28.2'	24.4	10.0 16.7 22.1	129/1979-231/1980 ¹ 129/1979-231/1980 129/1979-360/1979	129/1979-231/1980 129/1979-231/1980 129/1979-231/1980	
16	41°56.6'	81'22.7'	23.5	10.0 21.8	129/1979-218/1980 129/1979-351/1979	129/1979-218/1980 129/1979-218/1980	
17	41°50.6'	81'19.8'	20.4	10.0 18.1	129/1979-311/1979 222/1979-365/1979	129/1979-311/1979 222/1979-365/1979	
18	42'33.8'	80°55.5'	17.4	10.0 15.1	126/1979-242/1979 126/1979-155/1980	126/1979-242/1979 126/1979-155/1980	
19	42°27.6'	80'55.8'	20.4	10.0 18.1	126/1979-155/1980 ₂ 126/1979-155/1980 ²	126/1979-155/1980 126/1979-155/1980	
20	42°15.8'	80°50.1'	22.5	10.0 20.2	-- --	-- --	

TABLE 1.--Location and *makeup* of the Lake Erie current meter moorings and the interval of *data* collections. The prefix C indicates NWRI stations that we used in this report. Thermistor chain moorings are also listed. (Cont.)

Mooring	Position		Water depth (m)	Meter depth (m)	Current	Data interval	
	(°N)	(°W)				Temperature	Temperature
21	42°07.3'	80°45.5'	23.5	10.0 21.2	125/1979-161/1980 125/1979-161/1980	125/1979-161/1980 125/1979-161/1980	125/1979-161/1980 125/1979-161/1980
22	42°00.7'	80°43.9'	21.0	10.0 18.7	-- --	-- --	-- --
23	42°29.0'	80°24.2'	16.8	10.0 14.5	122/1979-080/1980 --	122/1979-015/1980 --	122/1979-015/1980 --
24	42°22.2'	80°23.7'	16.8	10.0 14.5	123/1979-151/1979 123/1979-151/1979	123/1979-151/1979 123/1979-151/1979	123/1979-151/1979 123/1979-151/1979
25	42°12.7'	80°22.0'	21.3	10.0 19.0	-- --	123/1979-103/1980 123/1979-080/1980	123/1979-103/1980 123/1979-080/1980
26	42°08.0'	80°19.9'	19.8	10.0 17.5	123/1979-241/1980 123/1979-338/1979 ³	123/1979-241/1980 ---	123/1979-241/1980 ---
27	42°40.9'	79°51.8'	35.4	10.0 33.1	122/1979-268/1979 --	122/1979-268/1979 --	122/1979-268/1979 --
28	42°33.0'	79°49.3'	56.4	10.0 32.7 54.1	123/1979-012/1980 123/1979-154/1980 123/1979-241/1979	123/1979-012/1980 123/1979-154/1980 123/1979-154/1980	123/1979-012/1980 123/1979-154/1980 123/1979-154/1980
29	42°22.7'	79°46.5'	40.2	10.0 25.0 37.9	123/1979-173/1980 123/1979-163/1980 123/1979-284/1979	123/1979-173/1980 123/1979-173/1980 123/1979-159/1980	123/1979-173/1980 123/1979-173/1980 123/1979-159/1980

TABLE I.--Location and makeup of the Luke Erie *current* meter moorings and the interval of data collections. The prefix C indicates NWRI stations that we used in this report. Thermistor chain moorings are also tinted. (Cont.)

Mooring	Position		Water depth (m)	Meter depth (m)	Data interval	
	(°N)	(°W)			Current	Temperature
C6	42°38.9'	79°55.7'	41.5	10.0	131/1979-303/1979 ⁴	131/1979-303/1979
				17.0	131/1979-303/1979 ⁵	131/1979-303/1979
				19.0	131/1979-303/1979 ⁵	131/1979-303/1979
				37.0	208/1979-303/1979	208/1979-303/1979
c7	42°44.5'	79°53.0'	22.5	10.0	131/1979-202/1979	131/1979-202/1979
				15.5	131/1979-295/1979	131/1979-295/1979
				17.2	131/1979-295/1979	131/1979-295/1979
C8	42°11.8'	82°08.7'	16.5	10.0	129/1979-213/1979	129/1979-213/1979
C12	41°51.8'	81°54.8'	23.8	10.0	129/1979-300/1979	129/1979-300/1979
				15.0	129/1979-300/1979	129/1979-300/1979
				19.5	129/1979-300/1979	129/1979-300/1979
				21.2	129/1979-300/1979	129/1979-300/1979
C18	41°37.6'	81°40.1'	17.0	10.0	130/1979-302/1979	130/1979-302/1979
				14.0	130/1979-302/1979	130/1979-302/1979
				15.7	130/1979-229/1979	130/1979-229/1979
c22	41°37.9'	81°31.9'	12.2	10.0	130/1979-300/1979	130/1979-300/1979
C27	42°12.4'	81°47.2'	21.0	16.5	129/1979-299/1979	129/1979-299/1979
				18.0	129/1979-299/1979	129/1979-299/1979
Thermistor moorings						
9T	42°03.3'	82°02.3'	22.9	6.7-20.7		127/1979-299/1979
11T	41°46.9'	81°46.8'	23.5	4.5-21.8		127/1979-299/1979

TABLE 1.--Location and makeup of the Lake Erie current meter moorings and the interval of data collections. The prefix C indicates NWRI stations that we used in this report. Thermistor chain moorings are also listed. (Cont.)

Mooring	Position		Water depth (m)	Meter depth (m)	Current	Data interval	
	(°N)	(°W)					Temperature
19T	42°27.3'	80°55.4'	20.4	5.4-18.4			125/1979-244/1979
21T	42°07.0'	80°45.2'	23.5	6.5-21.9			124/1979-265/1979

¹Gap Feb. 22-Apr. 21 1980.

²Large gaps in data.

³Data quality below average.

⁴178-208/1979 missing.

⁵201-208/1979 missing.

Thermistor chains were moored separately close to the current meters at stations 9, 11, 19, and 21. These moorings had a configuration similar to those for current meters, with the string of thermistors stretched between a subsurface float and an anchor and with a surface float attached to the end of the groundline. The thermistor chain itself consisted of 11 thermistors spaced at 2-m intervals. The recording package was attached to the anchor and the 20-m-long chain was tied to the mooring cable and then wrapped back again on itself. Thus near the top of the string, the measuring interval was somewhat less than 2 m. Water temperature was recorded once each hour, with the accuracy of the measurement again being $\pm 0.1^{\circ}\text{C}$.

We exchanged data with NWRI, and current meter records from several of their 1979 stations have been used to fill holes in our own data set. These locations are shown in figure 1 and the station particulars listed in table 1. Although the instruments vary somewhat from those described earlier, the mooring techniques are similar and the data are compatible. These data are used throughout this paper without distinction as to where they came from, but we do certainly acknowledge their source with gratitude.

It was originally planned that the moorings outside the shallow western end of Lake Erie would be deployed for about 1 year. The acoustic releases used to retrieve the moorings had proven themselves to be very reliable in past overwinter placements, but in Lake Erie misfortune struck; a batch of defective acoustic release batteries were received from the instrument manufacturer. On the recovery trip in June 1980, only a few more than one-half of the stations released on command of the shipboard acoustic control. Several other of the acoustic devices released randomly some time after the initial command for interrogation and release; these surfaced a week or two later and were found by passing small boats or lake freighters.

Faced with many remaining stations with defective acoustic releases, we spent the latter half of summer 1980 looking for the moorings by both searching with a side-scanning sonar device and grappling for the ground lines. This search was only partially successful and five stations, with a total of nine current meters, were ultimately lost to the lake. The search was difficult for two reasons. Several moorings on the Canadian side of the lake were apparently moved by fishing vessels trawling very intensively for smelt. Two moorings were actually recovered by these fishermen, one recovery in summer 1981 was of a mooring (station 9) that had been dragged off station in either 1979 or 1980. The second complication was that, in the eastern half of the lake, several of the moorings in the relatively shallow water of the central basin apparently walked along the bottom in response to intense fall and winter storms. Without very precise positions, backup recovery methods were essentially useless. Had the acoustic releases worked, these would not have been insurmountable problems because their range for interrogation and position finding has generally exceeded 5 miles. But their failure insured equipment losses and, together with malfunctioning current meters, accounts for the holes in the data collected column of table 1.

NWRI deployed six meteorological buoys dispersed throughout Lake Erie in 1979 (fig. 1). They measured wind speed and direction and air and water surface temperature continuously from early May through late October. Schwab

(1982) used these observations to compute an hourly wind stress vector that he then compared with the stress determined inversely from the recorded Lake Erie wind tides. His computed wind stresses from the meteorological data are shown in appendix A to give the reader a ready reference to the seasonal, monthly, or episodic forcing. The period from late October 1979 through June 1980 is shown with overwater wind stresses computed by the methods of **Resio** and Vincent (1977) and Schwab (1978). We used the wind observations from Toledo and Cleveland, Ohio; Erie, Pa.; Buffalo, **N.Y.**; and London, **Ont.**, to determine these values.

3. RESULTS

3.1 Thermal Structure

Water temperatures were measured with both thermistor chains and a thermistor integral to each current meter. Temperature recordings at the four central basin thermistor chain moorings (stations 9, 11, 19, and 21) are illustrated on five figures, one for each month from May through September 1979, in appendix **B**. We averaged current meter recordings of water temperature for each month, and they are displayed on the monthly-averaged current charts shown in appendix **C**. Temperature **distributions** were also recorded on whole-lake water quality monitoring surveys as reported by Rathke et al. (1983). but we will not use those data here.

A general picture of the annual cycle of water temperature variations in Lake Erie can be constructed from the monthly averages. The shallow **western** basin warms quicker in spring than the rest of the lake. It also cools faster in fall and is well mixed, with the observed temperatures revealing unimportant horizontal gradients. Past studies have shown vertical stratification here rare and short-lived (**Carr et al.**, 1965). In summer the deeper central and eastern basins do stratify, as the monthly data illustrate. The eastern basin is perhaps more like Lake Ontario and the other Great Lakes than the other two Lake Erie basins, for it stratifies for certain in June and remains so into November. The central basin, which is remarkably flat-bottomed and has a mean depth a little less than 20 m, reveals more transient stratification. Mid-depth versus bottom temperature recorders in May and June show slight gradients, and in July and August, stable stratification that vanishes by the end of September. In all other months it is nearly isothermal, cooling to 0°C in winter.

The dynamics of central basin stratification are very important to the biology and chemistry of the bottom water. Some insights into the physical processes can be gained from study of the thermistor chain records in appendix B. The uppermost thermistor on each chain was 5 to 6 m below the water surface. Therefore we show the daily average of surface water temperature recorded at NWRI buoys (fig. 3). For reference, compare this average to the **climatological** mean given by Felt and Goldenberg (1976). For the most part, the temperature structure in the upper 5 m is not critical in charting the progress of stratification.

May reveals a most interesting sequence of events in the warming of the central basin. We see an almost month-long steady increase in surface layer

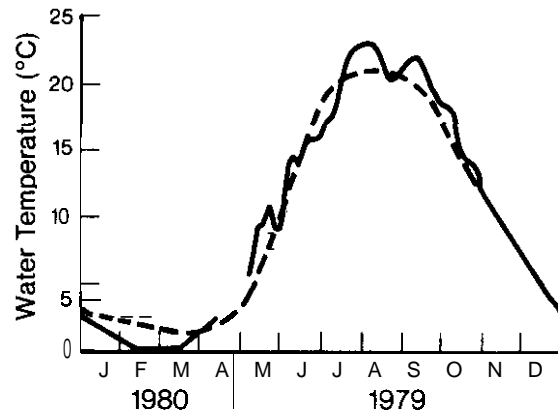


FIGURE 3.--Lake Erie surface water temperature observed in 1979 compared to a climatological mean calculated by Feit and Goldenberg 119761.

warming, starting from water nearly isothermal throughout the basin at about 5°C. A fragile stability gradually developed as surface heated water expanded downward in the water column. The moderate wind impulses on May 12 and 16 are recorded in the temperature structure as upper layer thickening and mixing processes that intensify the density differences between the top and bottom layers, but the stratification process ended abruptly with the wind storm that began on May 24. Intense winds from the north-northeast quickly mixed the whole central basin water mass. The computed wind stresses for the interval show that this was the most intense storm of the 1979 stratified season, with the stress approaching 3 dynes cm^{-2} at the peak of the 3-day-long episode. Currents measured in the lake during the period are shown in figure 4. They are typical of those observed with strong winds transverse to the lake's major axis throughout the entire year. *i.e.*, basically return flow at 10-m depths and below, against the wind stress but with and driven by the surface pressure gradient.

The disruption in the development of stratification must play an important role in the following sequence of eventual hypolimnion formation and the risk that pertains to late summer bottom water anoxia. The thermal structure is assuredly very sensitive to climatic variations and lake levels (Charlton, 1980, and Lam *et al.*, 1982). We can easily envision years in which frequent and intense meteorological systems would cause a short stratified season or quiescent years that would cause a long stratified season. Lake levels may greatly influence the annual variations in hypolimnion volume by stretching or shrinking the water column as much as 5 percent.

June 1979 was a month for rebuilding the thermocline and for establishing stable stratification. The major wind events of the month on the 10th and 11th, the 18th, and 23rd and 24th resulted in upper layer mixing and thermocline deepening. The process continued into July, and we notice that the wind stresses during the 1st through the 5th caused a nearly isothermal surface layer to form above a distinct thermocline that retains its identity for the

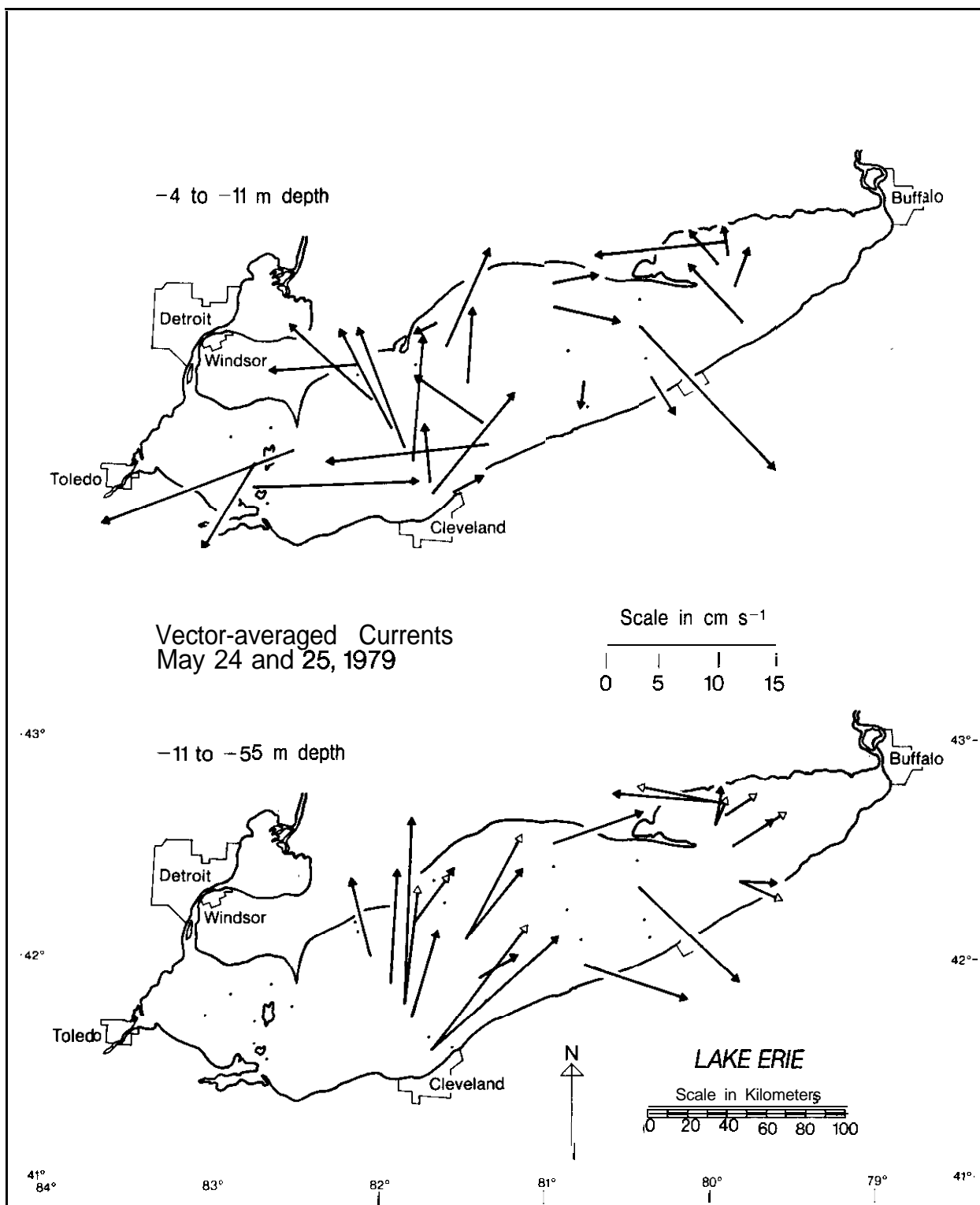


FIGURE 4.--Vector-averaged *lake currents* observed on *May 24-25, 1979*, during a storm *with winds* from the north-northeast. The arrowhead indicating direction of flow is not included as a part of the current speed scale. Open arrowheads show currents closest to the bottom on moorings that had three current meters.

balance of the month. Continued surface heating and light winds through the remainder of July produced a varied temperature structure throughout the basin. At stations 9 and 11, surface heating and light to moderate wind mixing caused a thick thermocline (with a temperature gradient of about $1.3^{\circ}\text{C m}^{-1}$ at the end of July) with moderate temperature gradients to be established in the lower half of the water column. At station 19 a sort of double **thermocline** evolved in mid-July that by month's end merged into a structure similar to that at stations 9 and 11, i.e., a thick layer of modest temperature gradients. The biggest difference at station 19 is that this layer was pushed up higher in the water column, perhaps showing advection of a thick lens of cooler hypolimnion water past this site. We will later show that a large influx of hypolimnion water to the central basin (from the eastern basin) occurred during July 21-25 across the Pennsylvania Ridge. The bottom current meter at station 19 and results of earlier studies (Boyce *et al.*, 1980, and Chiochio, 1981) show the influx to be directed northwestward along a proper course to influence conditions in this part of the lake.

In July station 21 showed the clear development of a double thermocline that persisted into early August. The three-layered density structure encouraged a host of interesting physical processes that we won't go into here; its development is a somewhat curious feature not widely researched in the Great Lakes. The disappearance of this structure on August 2 seems firmly related to the wind storm on that day; the mixing process elevates the lower thermocline and submerges the upper. In the same time interval, there was a process of hypolimnion entrainment to the west in Lake Erie (between **thermistors** chains 9 and 11), wherein the hypolimnion volume and temperature increased as a thick thermocline layer was compressed to a thin layer of stronger temperature gradients (Ivey and Boyce, 1982). In the transition, the lower layer captured a part of the water formerly in the thermocline. Can it be that the process was more widespread than the area looked at by Ivey and Boyce? Perhaps the process is more general than first thought.

August 1979 was a month of intensifying thermocline temperature gradients coupled with deepening and clear definition of a hypolimnion layer just 2- or 3-m thick. The major wind stress impulses during the month are clearly evidenced in the thermal data, and temperature gradients are as high as 6°C m^{-1} . On both lake cross-sectional pairs of stations, the thermocline tilts downward to the south but not greatly so, the southerly stations recording temperature structure perhaps on average just 1- or 2-m deeper for the month. Larger tilts were recorded by Blanton and Winkhofer (1972) from results of ship **surveys**. The monthly temperature averages from current meters at 10-m depth also showed cooler water during July and August along the north shore (appendix C). The thermistor chain in the shallowest water at station 19 revealed the weakest stratification. The pulse of bottom water cooling and thermal gradient relaxation here that started on August 21-22 again appeared **correlated** with a large volume pulse in inflow from the eastern basin across the Pennsylvania Ridge on August 17-20. By August 31 stratification was weakening in the northeastern part of the central basin (station 19), since close to the bottom the temperature was already in **excess** of 14°C .

September thermistor chain recordings document the end of the 1979 central basin stratification. The hypolimnion disappeared at station 21 on

September 11 in response to wind-driven mixing associated with the stress impulse on that and the previous day. It survived the September 13-15 wind storm at stations 9 and 11 in the western part of the basin, but succumbed to the stress just a few days later, disappearing at these two stations on September 19. The central basin was nearly isothermal for the remainder of the year, with major cooling events taking a form similar to the in-phase temperature reduction occurring on September 22. Later we will see that the near-bottom currents support the theory that summer stratification should persist longest in the western part of the central basin.

3.2 Current Flows

Efforts to measure water currents and to derive resulting circulation patterns in Lake Erie are at best frustrating. As noted earlier, **past** efforts have been split into distinct groups, either the drift bottle, drift card, or what-have-you type of surface water drift measurement on the one hand, or the fixed current meter approach on the other. The problem that arises is that in shallow Lake Erie the two measurement techniques are measuring different fields of flow and no one has yet been able to **measure** the two together with any success.

The lake is divided into three distinct and very different basins and these differences complicate the observer's dilemma. The shallow western basin has an average depth of about 8 m, all but ruling out useful deployments of fixed current meters. (**Most** state-of-the-art current meters just do not perform close to the surface where wind waves are large.) Moreover, it is separated from the rest of the lake by a string of islands that strongly influences basin interactions through the restricted passages. The central basin accounts for almost two-thirds of Lake Erie's surface area, but it, too, is relatively shallow and very flat, with a mean depth slightly less than 20 m. The oxygen depletion problem has made the region a productive area for hydrodynamic research, and current meter studies are certainly feasible in the lower half of the water column. The upper half, however, gives the same problems as encountered in the western basin, with the added complication that large ships in commercial trade are free to travel almost anywhere without fear of grounding. (The navigation routes in the western basin are clearly restricted by water depths.) We experienced major problems with ships in our studies. One mooring was retrieved after being caught by a ship's rudder and dragged 15 km; another had the subsurface buoy pierced by a ship's **propellor**.

The eastern basin has an average depth of nearly 24 m and is a **bowl-**shaped depression with maximum depth in the center of about 64 m (fig. 1). It is separated from the central basin by the Pennsylvania Ridge, which trends southerly from the north shore to the west of Long Point. The deepest communication between the basins occurs through the narrow channel in the southerly reaches. The eastern basin also appears somewhat isolated in its dynamical characteristics as we will see in this chapter, although water volume exchange processes across the sill are of great interest in the study of central basin stratification, as noted earlier.

In this report, we were constrained for whole-lake currents to use surface currents suggested by historical drift object studies or inferred from numerical simulation. Results of our own launching of Woodhead surface drifters in the central and eastern basins of Lake Erie during current meter deployments are shown in figure 5. Travel times and percentages of recovery are summarized in table 2. The courses of drift resemble earlier results closely; the surface drift is eastward with the prevailing wind stress. Hamblin (1971) summarized many of the earlier drift studies pictorially, and the reader is referred to his report for comparative results.

3.2.1 Currents During Central Basin Stratification

The bulk of our current measuring program was directed toward dynamics of the central basin, which (as discussed earlier) is strongly stratified for just a short part of the year. In 1979 this was clearly not much longer than July, August, and the first two-thirds of September, having no doubt been shortened by the wind-driven whole-basin mixing episode of late May.

Vector resultant currents computed on a monthly-averaged basis are shown in appendix C. We present all of the months from May 1979 through June 1980

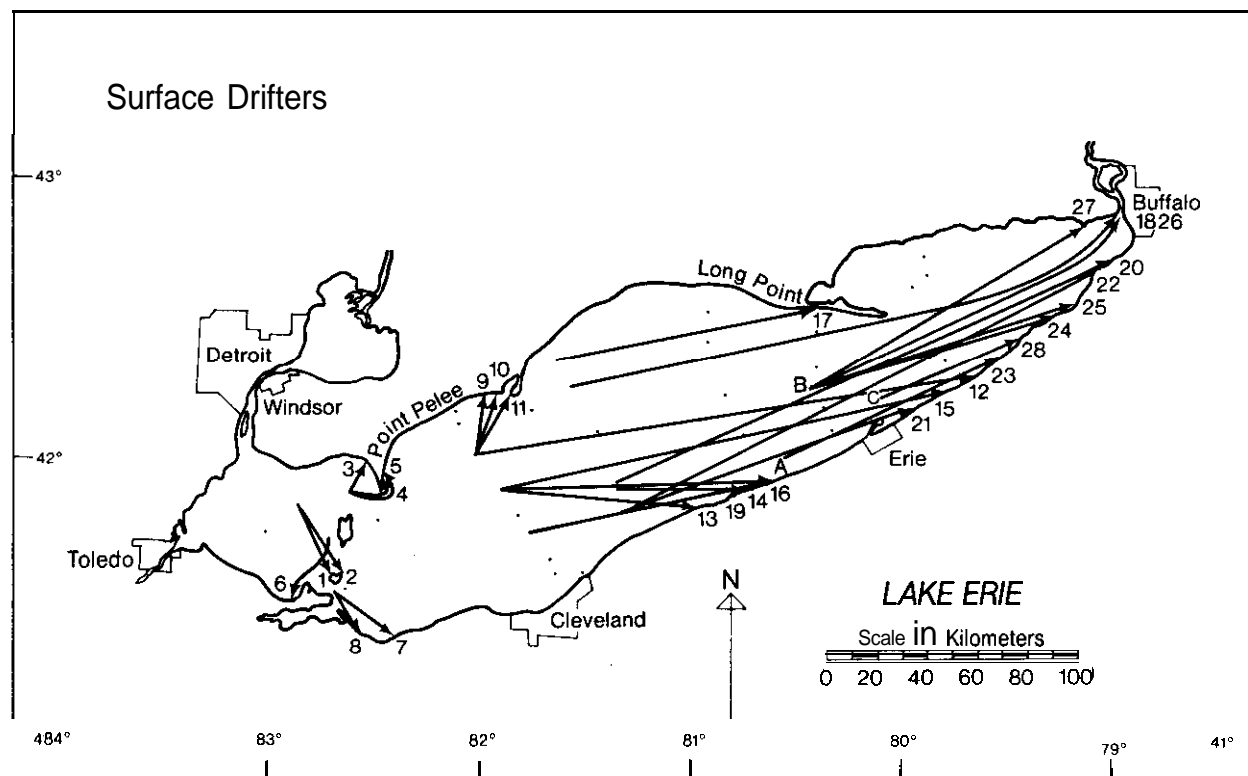


FIGURE 5.--Movements of Woodhead sea surface drifters released and recovered in Lake Erie in 1979.

TABLE 2.--*Release and recovery information for Lake Erie surface drifter8*
(83 released, 28 recovered)

Date	Deployment		Recovery		Time in water (days)	Distance traveled (km)	Speed (cm s ⁻¹)
	Position	Number	Date	Position			
5/10/79	2	5	6/2/79	1	23	32	1.61
			4/5/80	2	366	34	0.17
5/10/79	3	5	5/15/79	3	5	13	3.01
			5/18/79	4	8	17	2.46
			5/23/79	5	13	20	1.78
5/10/79	4	5	--	--	--	--	--
5/11/79	5	5	5/26/79	6	15	27	2.08
5/11/79	6	5	--	--	--	--	--
5/11/79	7	5	5/16/79	7	5	30	6.94
			5/22/79	8	11	21	2.20
5/7/79	8	3	--	--	--	--	--
5/7/79	9	5	6/9/79	9	33	24	0.84
			6/9/79	10	33	25	0.88
			6/18/79	1 1	42	28	0.77
			8/16/79	1 2	101	202	2.31
5/7/79	10	5	7/27/79	1 3	81	85	1.21
			8/15/79	1 4	100	110	1.27
			8/16/79	1 5	101	183	2.09
5/7/79	11	5	8/20/79	1 6	105	105	1.15
5/8/79	12	5	--	--	--	--	--
5/8/79	13	4	6/16/79	1 7	39	85	2.25
5/8/79	14	4	7/15/79	1 8	68	235	4.00
5/8/79	16	5	6/25/79	1 9	48	57	1.37
			7/5/79	20	58	215	4.29
5/8/79	17	5	7/5/79	21	58	129	2.57
			7/7/79	22	60	217	4.19
7/27/79	A	4	8/15/79	2 3	19	93	5.66

TABLE 2.--*Release and recovery information for Lake Erie surface drifter8*
(83 released, 28 recovered) (Cont.)

Date	Deployment		Recovery		Time in water (days)	Distance traveled (km)	Speed (cm s ⁻¹)
	Position	Number	Date	Position			
7/27/79	B	5	8/19/79	24	23	108	5.43
7/27/79	B	5	8/19/79	25	23	112	5.63
			8/22/79	26	25	148	6.85
			9/1/79	27	36	126	4.05
7/27/79	c	3	8/15/79	28	19	68	4.14

for completeness, but it is obvious **that the** number of working current meters steadily decreased from early on until very few were giving useful data in the last several months. The charts are separated into two parts, one showing the near-surface currents (mostly at 10 m) and the other near-bottom flows. We do this to help the reader sort out the flows at different levels, since they are even more confusing when plotted all together on one chart. The **monthly-**averaged currents yield a complicated set of charts on which concise and strong flow patterns do not persist for lengthy intervals of time stretching into many months, but they do sort into several frequently observed **catagories** that are of great interest.

During July, August, and September, there developed in the central basin a consistent pattern of near-bottom flow that was also evidenced in the 10-m measurements, especially in August and September. It consisted of a **west-**southwestward flow of bottom water that flowed parallel to the south coast of the lake. It started to develop a little in the eastern half of the basin in July and intensified and dominated the flows of August and September. The same pattern appeared at the 10-m level also, with August revealing a **whole-**basin clockwise flow that strengthened and even enveloped most of the eastern basin circulation in September. The shear between **midlevel** and bottom level currents does not tend to be large. The flows bore close **resemblance** to those reported during the same part of the stratification cycle by **Blanton** and **Winklhofer** (1972). Their measurements were also near the bottom and were concentrated in the center of the lake, where the currents are more northwesterly (in the cross-lake flow, central part of our whole-basin pattern). Our measurements have extended the reach of westward flow along the entire southern shore and have closed the loop in a clockwise fashion with definite eastward currents along much of the northern shore. The bottom waters are transported northward across the lake in the western part of the basin and southward in the eastern part. The circulation is similar to one given by FWPCA (1968) for bottom flow (labeled "prevailing annual bottom flow" . . . fig. 35).

August and September were somewhat unusual when compared with most of the other months, for the only other month in which clockwise circulation filled the central basin was February 1980. We notice that the epilimnion circulation at 10 m did not differ substantially from the near-bottom flow even during the most intensely stratified months, although there are a few obvious exceptions, such as at stations 18 and 19 in July. The stronger circulations of August and September do appear to have lessened the extent of the flow oppositions.

In the eastern basin, the monthly-averaged currents were essentially cyclonic from the time of current meter deployment in May through August. In most patterns the basin appeared quite isolated from the currents of the central basin, and this is the case also in daily-averaged current charts that we have closely examined for the entire data collection interval. Cyclonic flow during this season in the eastern basin was suggested by **Hamblin** (1971) because of a constantly shallower thermocline in the basin's center and geostrophy, and **our** measurements confirm this distribution. It was not until September that this pattern broke down and clockwise flow from the central basin spilled over and surrounded the eastern basin as well.

It is of interest to integrate the circulation for the entire season of intense central basin stratification, i.e., from say July 1 through the first two-thirds of September. Results of this integration are shown in figure 6. The current pattern that emerges is one of a general clockwise flow encircling the central basin and represented in both the mid-depth **epilimnion** currents and the near-bottom flow.

The part of the lake that deviates most from this description is in the northeastern part of the central basin, where the deep flow at station 19 is northwesterly (the average is greatly influenced by the strong northwesterly flow observed here in July) and where currents at station 18 are bi-modal, with no strong component parallel to the lake's major axis over the averaging interval. Bottom currents of a few centimeters per second on average may appear to be rather slight, but we should recall that the steady flows portrayed by the vector averaged currents lead to a length of over 50 km of water transported past a current meter in just a 1-month interval with a 2 cm s^{-1} current speed and that this value is typical of the current speeds observed through the stratified season of 1979.

3.2.2 Currents During the Unstratified Season

Following the breakup of central basin stratification, the three nearly isothermal months of October, November, and December exhibited a similarity in current flows. We have averaged them all together and the resultant vectors are shown in figure 7. Most remarkable is the continuation of near-bottom current flows with directions comparable to and magnitudes slightly greater than those of the **summer** season. Most different in the pattern of bottom currents is the contraction of the clockwise central basin cell to the northeastern two-thirds of the basin, while in the southwestern third an **anticlockwise** pattern prevails. The same circulation controls the mid-depth level measurements with little shear at most stations between the two levels. The reader will also notice these flows in the individual monthly-averaged data, together with a cyclonic gyre in the south half of the eastern basin.

Fall experienced larger wind stresses than observed during summer, but the velocity of the bottom currents **were** only slightly larger. We will see later that the pattern of flow is perhaps less persistent during fall, which may account for a part of this curiosity, but we must also realize that **two-layer** dynamics may play a role, too. Westerly wind Impulses that cause an upward tilt of the **thermocline** surface toward the northwest add to the bottom flows and cause the bottom frictional stress vector to reinforce (be in the same direction as) the surface wind stress, thereby intensifying the summer currents.

We released some **Woodhead** seabed drifters (fig. 8) during instrument deployments, repeating on a much lesser scale the experiments of Hartley (1968). Arrows showing the drifter movements are presented in figure 9. Table 3 tabulates the release and recovery Information and the percentage of returns. The results are very similar to those reported by Hartley, verifying that the measured currents do indeed represent the dominant bottom flow regime. Northwestward flow across the basin from the vicinity of

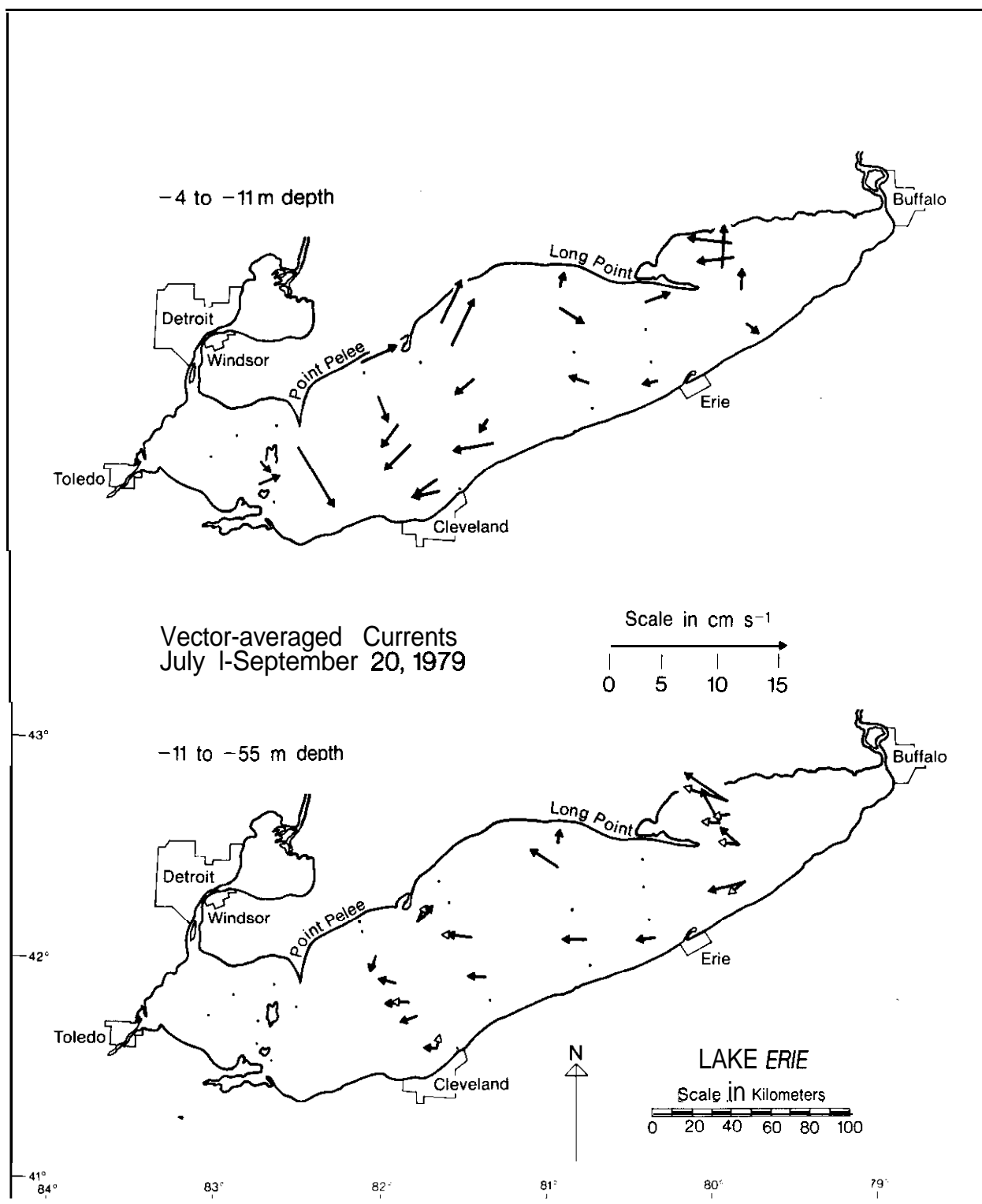


FIGURE 6.--Lake Erie resultant current vectors for the period July 1 through September 20, 1979.

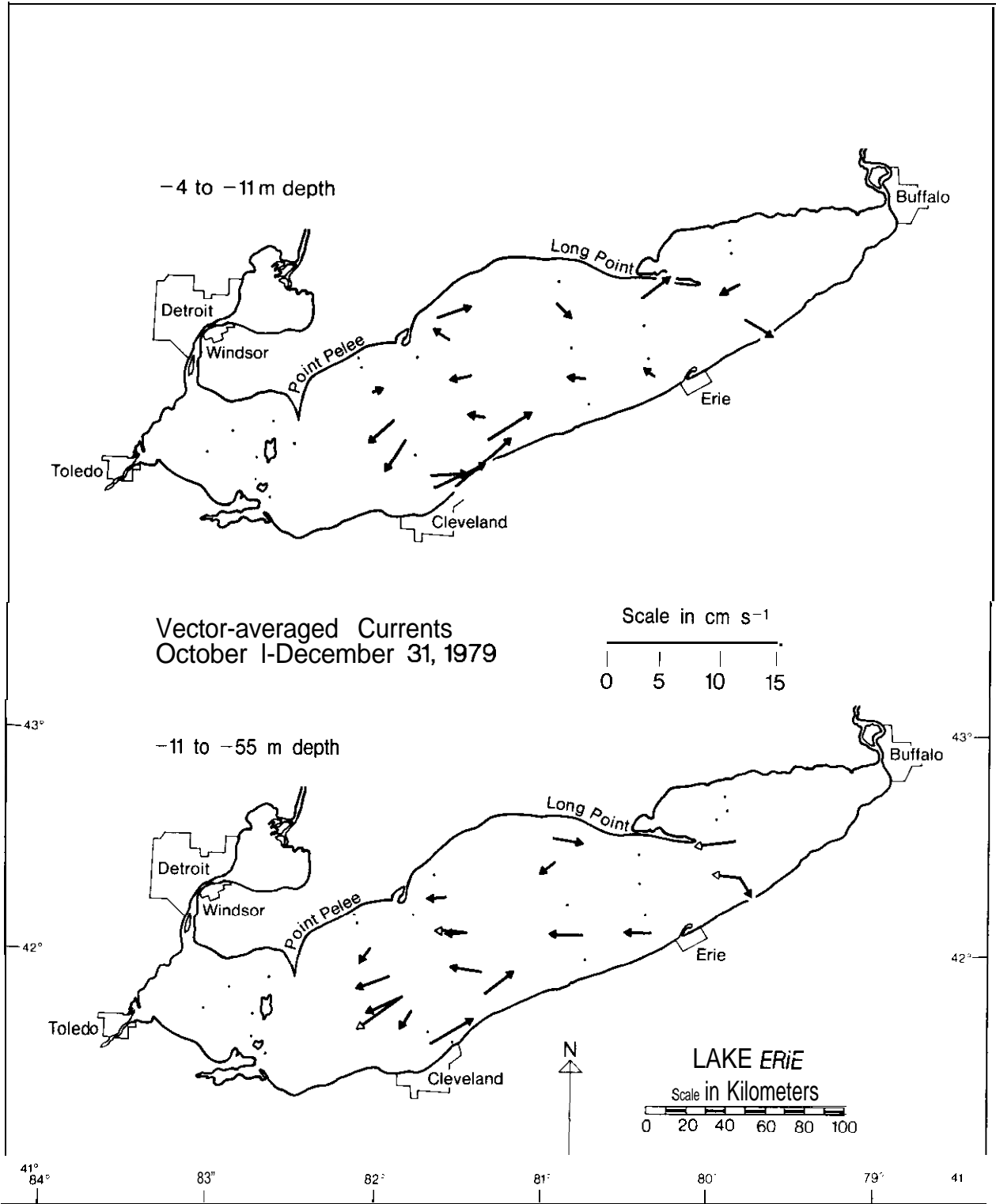


FIGURE 7.--Lake Erie resultant current vectors for the period October 1 through December 31, 1979.

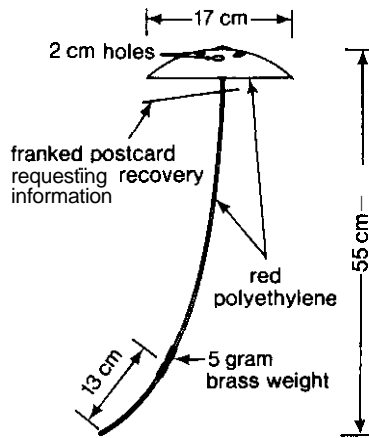


FIGURE 8.--A drawing of the *Woodhead* seabed drifter. It is weighted at the tail so that it stands upright on the lake bottom; bottom currents fill the umbrella-shaped head and drag the drifter along. The surface version floats head downward.

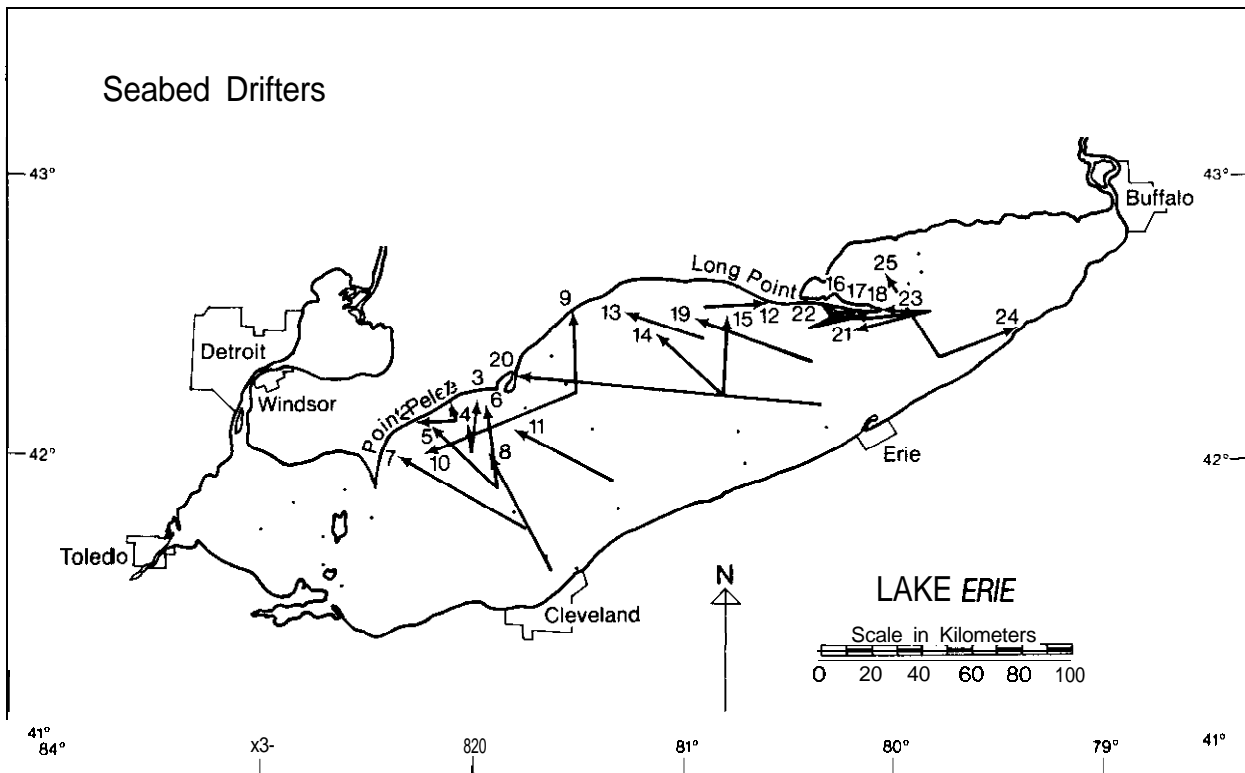


FIGURE 9.--Movements of *Woodhead* seabed drifters released in Lake Erie in 1979 and subsequently recovered.

TABLE 3.--Release and recovery information for Lake Erie seabed drifters
 197 released, 25 recovered)

Date	Deployment		Recovery		Time in water (days)	Distance traveled (km)	Speed (cm s ⁻¹)
	Position	Number	Date	Position			
5/10/79	4	2	--	--	--	--	--
5/7/79	a	5	9/23/79	1	139	7	0.06
			10/28/79	2	174	22	0.15
5/7/79	9	5	9/18/79	3	134	17	0.15
			10/24/79	4	170	11	0.07
5/7/79	10	5	12/19/79	5	226	35	0.18
			4/22/79	6	351	31	0.10
5/7/79	11	5	7/17/80	7	437	59	0.16
5/8/79	12	5	10/15/80	a	526	50	0.11
5/8/79	13	4	--	--	--	--	--
5/8/79	14	4	11/18/79	9	194	25	0.15
			6/9/81	10	763	66	0.10
5/8/79	16	5	11/9/82	1 1	1281	50	0.05
5/8/79	17	3	--	--	--	--	--
5/5/79	18	5	1/5/80	12	245	29	0.14
5/5/79	19	5	11/19/79	1 3	198	30	0.18
5/5/79	20	5	4/7/80	14	338	42	0.14
			4/11/80	1 5	342	28	0.09
5/4/79	21	5	--	--	--	--	--
5/4/79	22	5	--	--	--	--	--
5/2/79	23	4	9/30/79	1 6	151	18	0.14
			11/17/79	1 7	199	28	0.16
			7/6/80	18	431	28	0.08
5/2/79	24	5	11/1/80	1 9	549	50	0.11
5/2/79	25	5	10/5/80	2 0	521	120	0.27
5/2/79	26	5	--	--	--	--	--

TABLE 3.--Release and recovery information for Lake Erie seabed drifters
(97 released, 25 recovered) (Cont.)

Date	Deployment		Recovery		Time in water (days)	Distance traveled (km)	Speed (cm s ⁻¹)
	Position	Number	Date	Position			
5/2/79	28	5	2/3/80	21	277	30	0.13
			7/9/80	22	434	42	0.11
			8/16/80	23	471	24	0.06
5/2/79	29	5	5/5/80	24	369	36	0.11
			12/17/81	25	960	37	0.04

Cleveland is obvious, as is an eastward drift close to both the northern and southern shores in the eastern parts of the lake. Westward movements from stations 24 and 25 indicate a westward or northwestward flow of bottom water across the Pennsylvania Ridge and into the central basin **as** reported by Boyce *et al.* (1980). The course of flow of this water during summer **may** be represented by the station 19 deep current measurement shown in figure 6. Westward movements from station 28 might be indicative of the same bottom water movement and of the cyclonic gyre in the southern **half** of the eastern basin driven by eastward-directed wind stress impulses.

The monthly or longer period averaged currents we have discussed are composites of numerous wind-driven episodes. Spectra of the wind stress presented in the following section show energy accumulations in the 4- to 6-day range, which represent some average values for the major weather system passages. The response of lake currents to these impulses of wind stress is indeed complex as we will describe.

Coinciding with the last vestiges of central basin stratification, two frontal passages crossed the lake from September 17 through 22, 1979. During both, there were common sequences of events in the wind field. With the first front there were about 1.5 days of southwesterly wind, turning clockwise to northwest and then to north on the 19th. With the second front, the wind turned clockwise from southwest to northeast on the 21st and 22nd. Early in the episode, the lake spun up into an intense clockwise circulation encompassing the entire central and eastern basins; it remained fixed in that state for the episode's duration (fig. 10). The pattern is not unusual and numerous such episodes of whole central basin, or in this case central and eastern basin, clockwise flow at both 10-m and near-bottom depths are evident in charting the daily current vectors. In September, wind stresses from the 10th through the 12th and from the 27th through the 30th also provided essentially the **same** pattern of clockwise circulation. The first of the episodes clearly was the result of a strong southwesterly wind field lasting nearly 1 day and turning clockwise to northeasterly. The second accompanied a relatively light wind from the south. Because no other persistent current patterns occurred that month, September, as the monthly chart illustrates, was characterized by dominant clockwise circulation.

Equally clear in whole central basin expression is the anticlockwise circulation pattern that characterizes the episode from the 3rd through the 7th of October 1979 (fig. 11). In this case, we found that a light southwesterly wind on the 3rd and 4th rotated clockwise to northwesterly on the **5th**, followed by stronger southwesterly winds on the **6th**, rotating clockwise to northwesterly on the 7th. The wind history is therefore rather similar to that observed from September 17 through 23, but the circulation is completely reversed. The exception occurs at station 26, where outflow from the eastern basin through the deep channel in the Pennsylvania Ridge continues, especially at the deepest level. There appears to be great sensitivity of the central basin circulation to subtle changes in the nature of the driving wind stresses and to the initial momentum of the currents as the impulse is applied. After studying numerous **cases** of the excitation of one or the other of these two exactly opposite patterns, we have concluded that the question as to why either **may** dominate remains unanswered and is a good subject for research by model development.

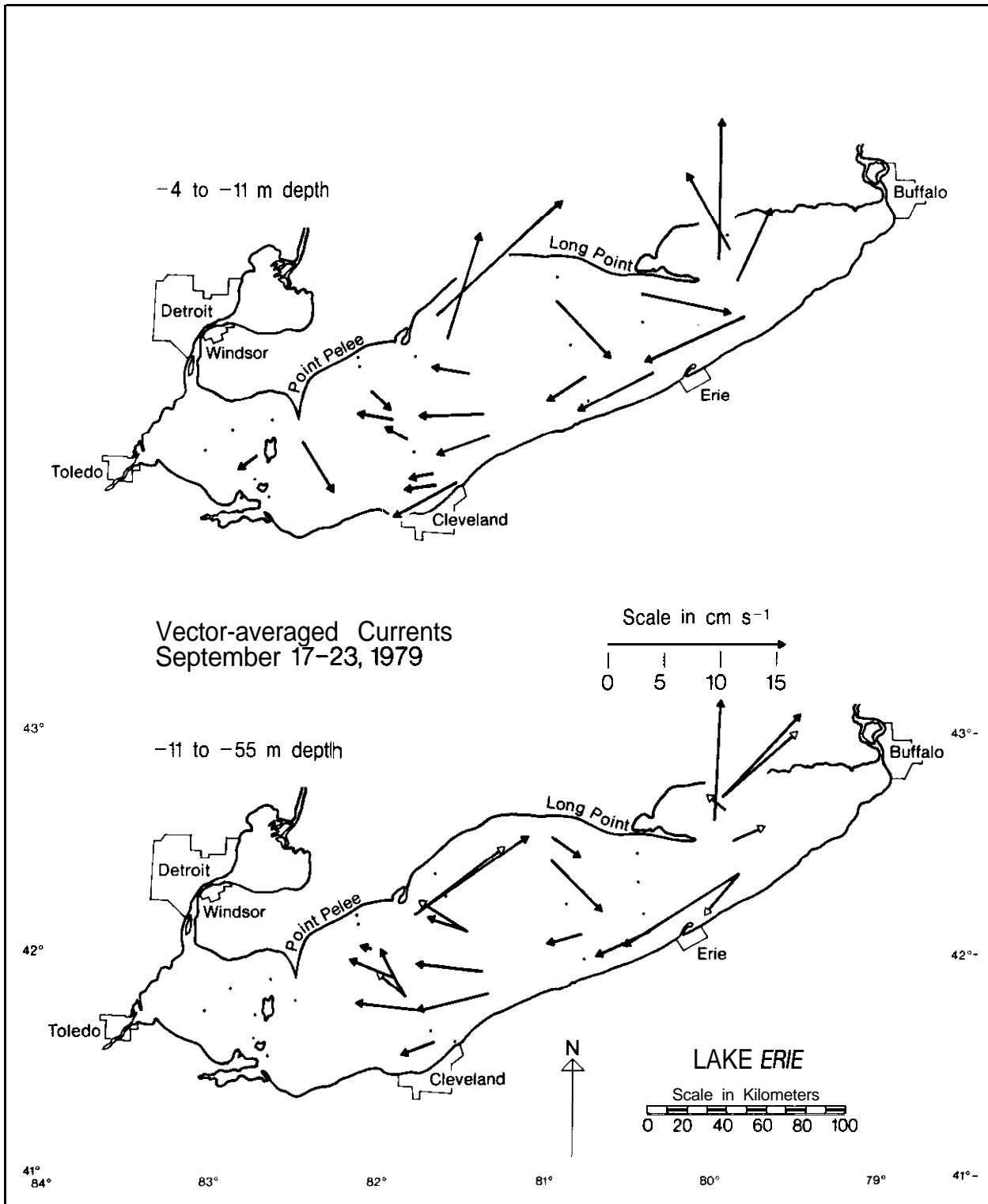


FIGURE 10.--Lake Erie *resultant* current vectors for September 17-23, 1979. Clockwise circulation prevails in both the *central* and eastern basins.

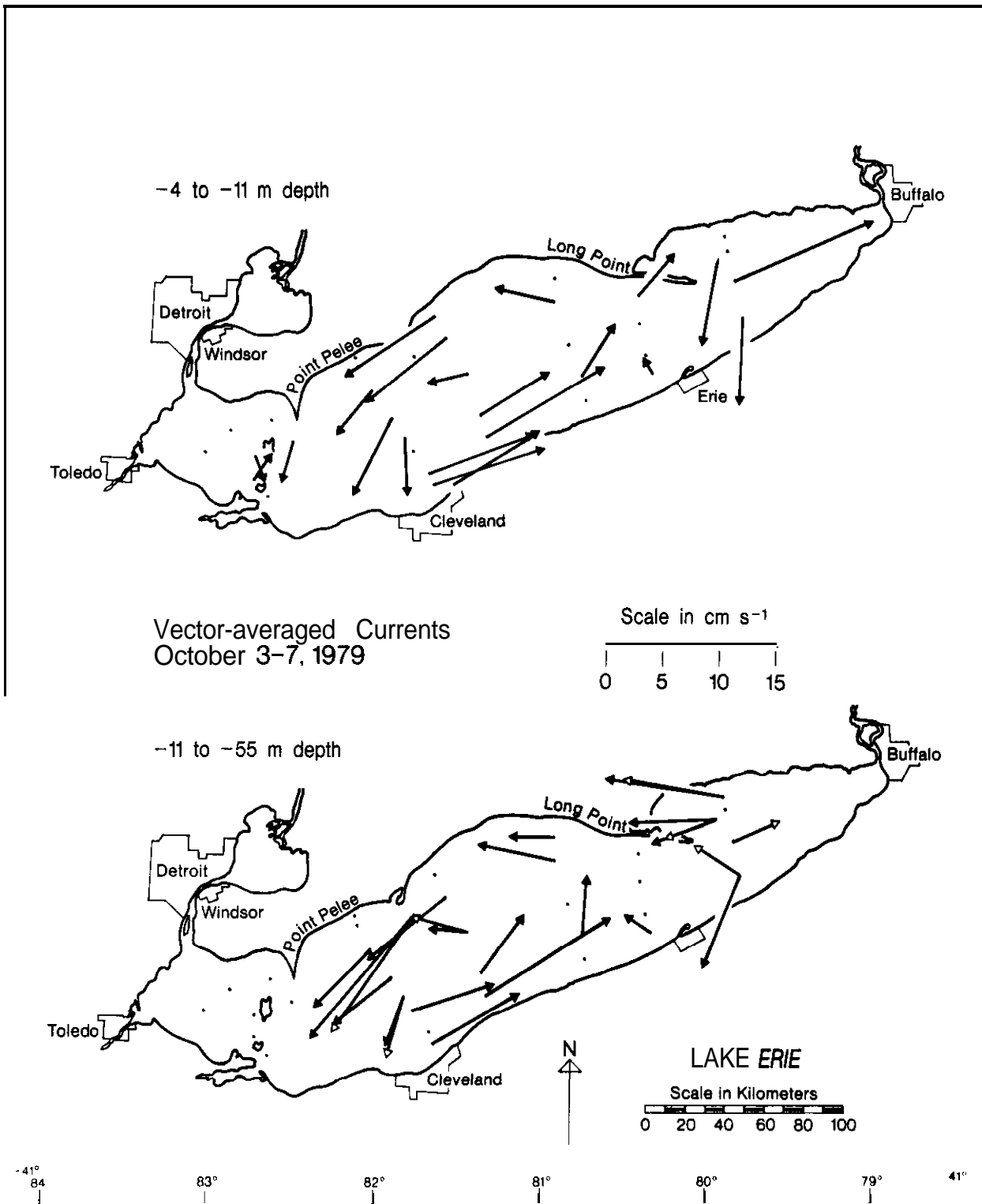


FIGURE 11.--Lake Erie resultant current vectors for October 3-7, 1979. Anticlockwise circulation prevails throughout the central basin and the northern half of the eastern basin.

The eastern basin appears somewhat separate of the anticlockwise circulation of the central basin in figure 11, **as** it also does in most charts of monthly-averaged currents and in **many** dominant pattern episodes of a few days duration. After the cyclonic flows related to geostrophy during stratification end, the eastern basin exhibits **a** characteristic two-cell circulation. Because of the prevailing westerly winds, currents along both the northern and southern shores tend to flow easterly with the wind stress. Return flow occurs westward along the axis of the basin much like the lake basin simulations described by Bennett (1974). Because Long Point projects southward, interrupting full development of the pattern along the northern shore, we find the southern half of the pattern (the anticlockwise cell) usually stronger and larger than the northern half. We will describe later how this pattern can rotate as a topographic wave, but yet retain its whole-basin two-cell features. The eastern basin alone seems to respond in the two-cell pattern whether the stress impulse is easterly or westerly, although of course the currents along the coasts are just reversed.

One month revealed domination by anticlockwise currents--April 1980. Two episodes of intense cyclonic flow occurred, one from the 1st through the 7th and the other from the 23rd through the 26th. April 1-7 **was** clearly marked by alternate wind stresses easterly and westerly along the lake axis, while winds were lighter and more variable during the second episode. These two periods clearly controlled the monthly-averaged currents and determined the basin-wide circulation. We also note that this is a month when lake water is warming (first in the shallow water along the **coasts** perhaps augmented by river inflows) and establishing thermal gradients supportive of the cyclonic flow around the basin's perimeter (cf. **Huang**, 1972). Intense "thermal bar" gradients were not recorded by our offshore instruments, however, and the slight warmth we recorded in inshore **waters** compared to offshore was not sufficient to support the magnitudes of currents observed. Interestingly, simulations of currents in Lake Erie during the year of Project Hypo by **Simons** (1976) hindcasted a nearly month long (October 23 through November 29, 1970) interval of strong cyclonic currents filling the central and eastern basins. He attributed it to **a** pattern of unusual wind stress distributions. Clockwise patterns, such **as** those in September 1979, did not distinguish themselves with as much clarity in his intervals however.

A third pattern of circulation we observed regularly is shown schematically in figure 12. It consists of a large clockwise flowing gyre in the northeastern part of the central basin and anticlockwise gyre in the southwestern part. Usually the eastern basin is rather isolated and is shown as such in the figure. The pattern is not static, but evolves in a complex manner from episode to episode and from month to month in longer period averages. The northeast clockwise cell often expands westward to envelop the whole northern shore east of Point **Pelee** and also eastward and southward to encompass the whole eastern two-thirds of the central basin and part of the eastern basin **as** well. It does this at the expense of the anticlockwise gyre, which retreats to **a** small cell in the southern half of the lake mostly west of Cleveland. At other times the anticlockwise gyre expands to fill the western half of the central basin, while the anticlockwise gyre in the southern **half** of the eastern basin **may** expand westward to envelop the region to the west of the ridge. We have **also** seen how one or the other of the two central cells becomes dominant basin wide.

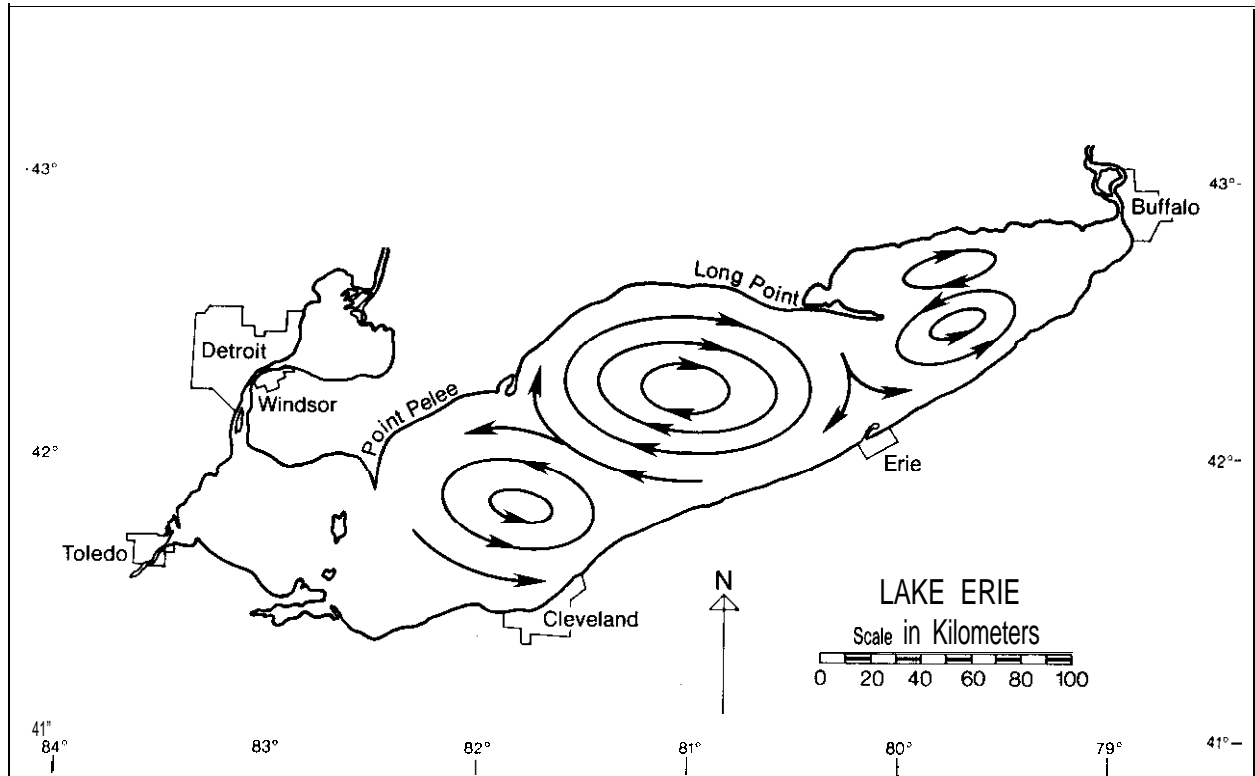


FIGURE 12.--*Generalization of the third dominant circulation pattern observed in the Lake Erie current charts.*

The proportion of the month or season that experiences one pattern or another controls the long period-averaged circulation. For example, from the time when current meter deployments were completed in mid-May 1979 through September, charts of daily current vectors revealed 27 days of clearly clockwise circulation and 8 days of clearly anticlockwise in the central basin. October through December 1979 splits 25 clockwise and 22 anticlockwise, while January 1980 through March is 11 even. February had 5 days clockwise and none anticlockwise. April had 12 days anticlockwise and none clockwise. Thus we see how the monthly or seasonal averages evolve from the dominance of episodal patterns in the interval. When there is relative balance between the simple whole-basin rotations, our third and most common pattern of several central basin gyres prevails.

3.2.3 Oscillatory Components

Several almost periodic components contribute substantially to measured current velocities. Spectra presenting the distribution of kinetic energy as a function of frequency are useful in picking out some of the more prominent **periodicities** in the velocity records. Spectra were computed by use of the

fast Fourier transform method. All were computed from multiple, overlapping, unfiltered data subsets of 256 values of either hourly or 4-hourly averaged data, which were first transformed and then ensemble-averaged and smoothed by Hanning. In figure 13 there is a very informative example computed using hourly data from a current meter placed on mooring 17, 10-km offshore from Fairport Harbor, Ohio. The clockwise rotary spectrum shows a strong peak at nearly 18 h. This is known from numerous Great Lakes studies to be the near-inertial period for oscillations of thermocline and currents that dominate this range of the kinetic energy distributions when the lake water is density stratified. It was so stratified during parts of this May through October 1979 computation [cf. FWPCA (1968) and Mortimer (1971)].

Almost submerged into the near-inertial period peak in the clockwise component is a second peak at just a slightly shorter period, i.e., at 14.2 h for the resolution possible here. It stands out clearly in the anticlockwise component though, for where the two rotary components of this oscillation are close in amplitude, the inertial component is suppressed. This oscillation is the fundamental (longest period) longitudinal seiche of the lake and its period was computed theoretically by Platzman and Rao (1963) at 14.08 h in a dynamical study of Lake Erie. Revealed also in the spectra are two additional oscillations at periods centered around 9.5 and 5.7 h; they are the second and third longitudinal seiches of the lake. Most of the energy is in the clockwise rotating component of the spectra for all of the three seiches noted, as expected from dynamical considerations. Figure 13 shows considerable energy at

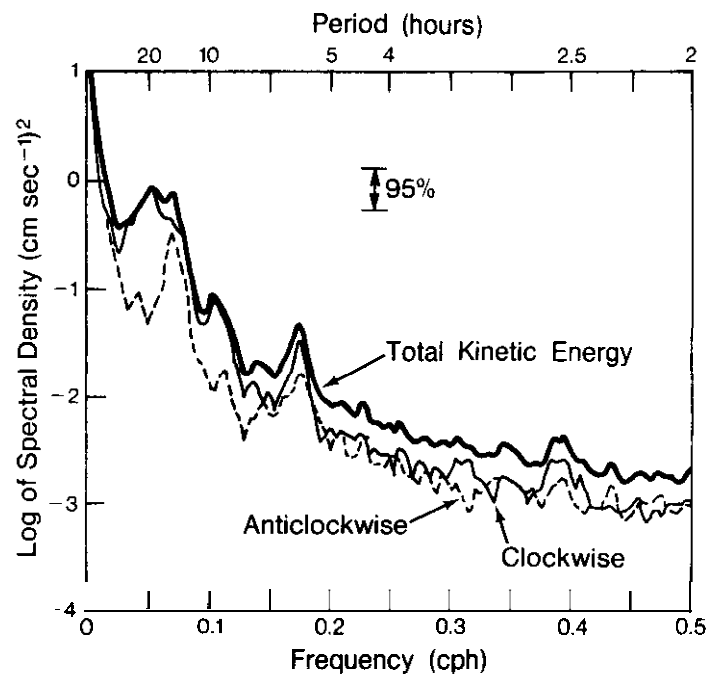


FIGURE 13.—Kinetic energy spectra computed from hourly averaged current velocity recordings at station 17 during May through October 1979. Both the rotary components and the total kinetic energy are presented.

longer periods, but the resolution is too poor to suggest oscillatory components important at low frequencies.

Inertial responses are best developed in the deep water of the eastern basin during the stratified season, with currents just out of phase in the top and bottom layers. The meters moored there reveal spectra similar to those in figure 13, with sharp and strong kinetic energy peaks for clockwise rotating currents. The seiche currents are unimportant and not easily identified here. Although present in the central basin, at most stations the inertial response is not as well defined as that in figure 13 because the energy distributions are spread over a broader frequency range, the central frequency is harder to differentiate, and the energy levels are lower. This no doubt arises because of the thinness of the lower layer and the obvious **nonlinearities** associated with wave propagations on the thermocline in this situation. The longest period seiche can be easily recognized as a significant contributor to current flows throughout the entire central basin; the second and third modes appear less regularly. The location off Fairport Harbor is close to a nodal line of all three modes and is probably atypical in its clarity of seiche currents measured there.

The frequencies of the **seiches** are not directly related to important wind forcing constituents, but it is interesting to inquire as to what the spectrum of this forcing looks like and whether obvious **periodicities** in it show up in the current responses. We computed a rotary spectrum of the Lake Erie wind stresses determined from the NWRI buoy measurements by Schwab (1982); figure 14

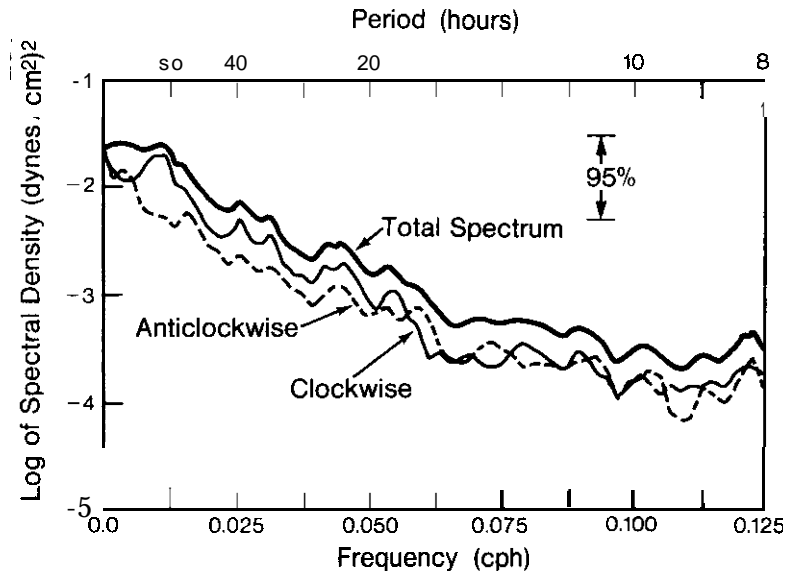


FIGURE 14.--Rotary spectra of the hourly *wind* stress vectors computed by Schwab (1982) from National Water Research Institute buoy wind measurements during May through October 1973.

gives the result for 4-h averaged stresses. The forcing is mainly from stresses that exhibit clockwise rotations of the wind vector, with a broad and energetic peak centered about the 85- to 100-h period range. Also noticeable are energy accumulations at the inertial and diurnal periods. Inertial period current responses are not highly dependent on **that** period in the wind stress for generation and the diurnal period except in special cases was not found to be significant in the kinetic energy of currents.

Wind energy in the longer time scale of 4 to 5 days has been recognized for many years as important in shaping current responses in the Great Lakes. A thorough and imaginative summary of the dynamical processes has been provided by Csanady (1982) who discussed how, in addition to setting up the quasisteady circulation gyres and forced current flows, the energy may propagate about the basins in the form of bathymetry sensitive rotational waves. The simplest form of these waves revealed with very distinctive characteristics from analytical studies of regularly configured nonuniform depth (with greatest depth in the central regions) in circular or elliptical basins is the gravest (lowest azimuthal wave number) vortex mode. **Saylor et al.** (1980) reported its existence in southern Lake Michigan and now the results of this field study suggest a time varying flow with similar properties in the eastern basin of Lake Erie.

Figure 15 shows the streamlines for the gravest vortex mode in a basin configured as a" elliptical paraboloid and its rotation over one-quarter wave period. The two-cell current pattern, originated by impulsive wind stress, fills the basin and rotates cyclonically just opposite to the clockwise torque observed in the wind stresses. For the first radial modes, this gravest azimuthal mode is unique because the current velocity does not vanish at the center of the basin as it does for higher ordered modes. In the center of the basin, there is an area of anticlockwise rotating currents. Closer to shore, the currents rotate in a clockwise fashion. These features are important in detecting the wave form.

Figure 16 shows rotary spectra of currents measured at three moorings in Lake Erie, each computed from 4-hourly averaged data recorded from May through September 1979. The spectrum from mooring 28 at the center of the eastern basin again reveals what was seen in Lake Michigan--a large accumulation of kinetic energy associated with anticlockwise rotations of the current vector. Here the peak is rather broad, although it does exhibit decay about a central period near 114 h. Closer to the north and south coasts of the eastern basin, moorings 27 and 29, respectively, energy in the period band is shifted to the clockwise rotating component. The peak at mooring 29 is submerged deeper into the more energetic low frequency lake currents occurring at the site because it is in a region more likely to experience an active steady current regime than the other two sites.

A current hydrograph almost circular in form from a current meter moored near the center of the southern basin of Lake Michigan provided graphic evidence of the persistence of the anticlockwise rotations in **Saylor et al.** (1980). Presented in a different fashion, figure 17 shows current vectors "drawn" at intervals of 2 h from the center of the eastern basin (mooring 28) for August 1979. The currents have been low-pass filtered to remove the inertial and shorter period oscillations. Anticlockwise rotations here also dominate

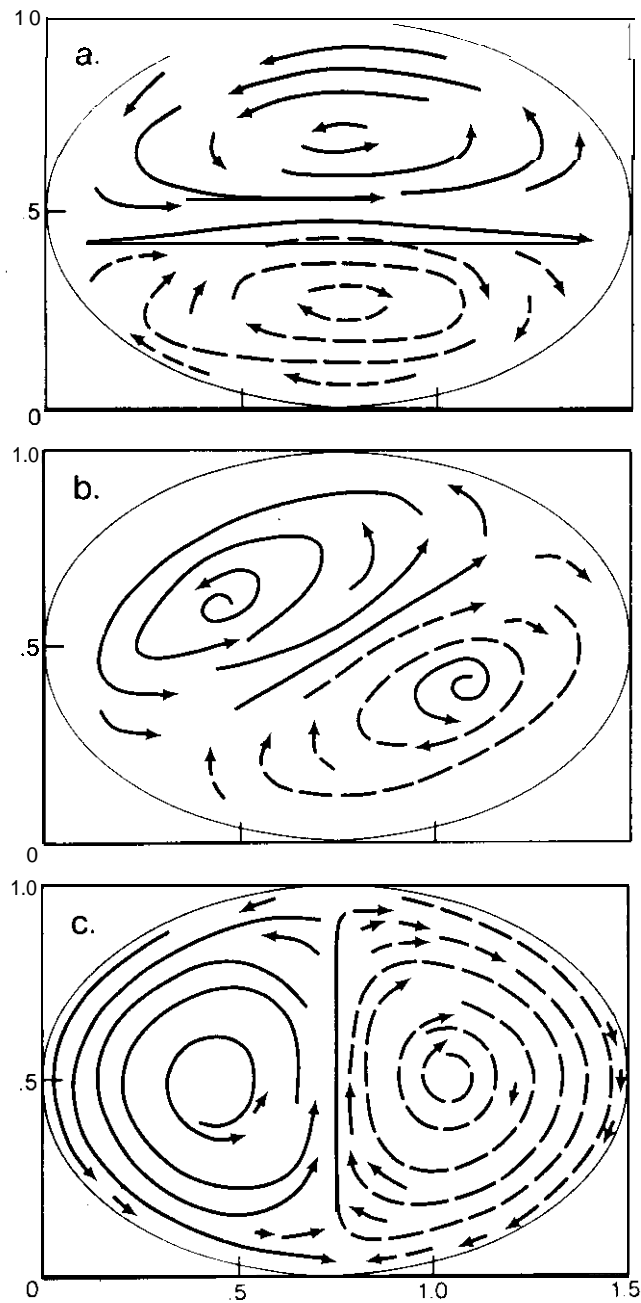


FIGURE 15.--*Transport streamline* pattern at different phases of a *gravest mode vorticity wave* in an elliptic paraboloid.

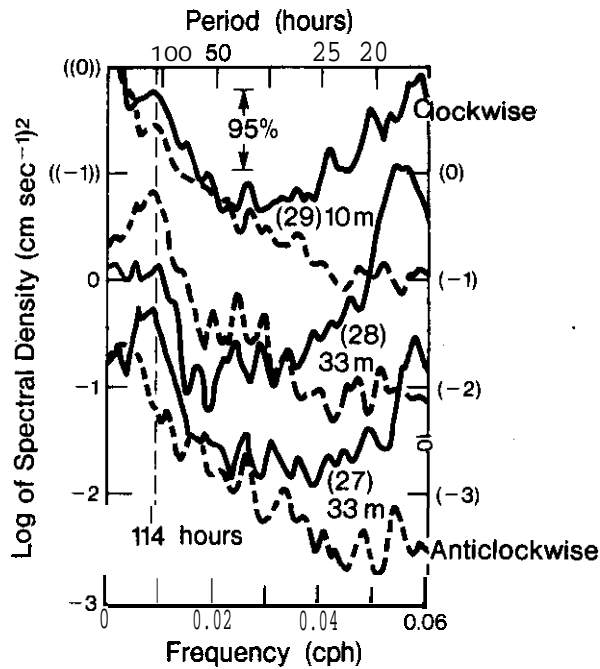


FIGURE 16.--The rotary components of kinetic energy spectra computed from 4-h-averaged current velocity recordings during May through November 1979 at three moorings situated on a cross section of the eastern basin of Lake Erie.

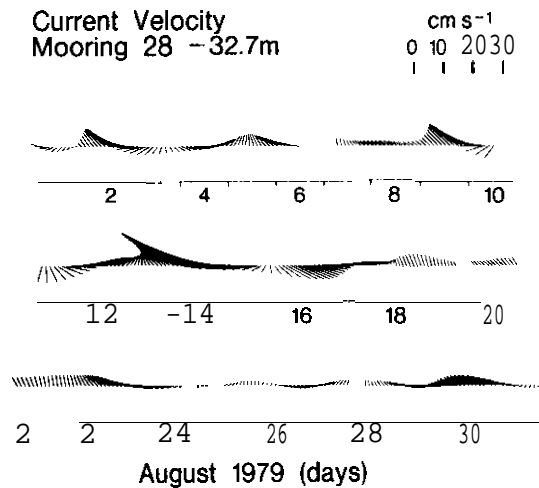


FIGURE 17.--Low-pass filtered, hourly-averaged current velocity vectors (drawn at 2-h intervals) from a middle of the eastern basin (mooring 28) current meter at 33 m depth for the month of August 1979.

the current structure, with the major axis of the current ellipses oriented nearly east-west and parallel to the axis of the basin.

Figure 18 shows a rotary spectrum of kinetic energy computed from currents recorded during the same time interval in the middle of Lake Erie's central basin (mooring 15). It reveals no indication of oscillations in the period range of interest at the low frequency end of the wind spectrum and no unequal partitioning of energy in the two rotary components.

To end our discussion of the oscillatory flows, we present the remarkable kinetic energy spectra computed from observations of current flow at station 6 between Kelleys Island and Pelee Island and at the juncture of the west and central basins. Computed from hourly averaged currents, the first three longitudinal modes of the lake seiches are revealed in exquisite detail (fig. 19). The spectra resemble those obtained through analysis of water level records, and record inconsequential, but recognizable, inertial and diurnal components (and perhaps some higher order seiche modes around 3 to 4 h). This inter-island passage is truly dominated by the tidal-like seiche-driven current flow, with clockwise rotating ebb and flow changes. Though not reproduced here, spectra from mooring 4 in the Pelee Passage present a **virtual** image of figure 19.

3.2.4 Inflow From the Western to the Central Basin

The lack of current meter data in the western basin and inter-island passages **attests** to the difficulty of maintaining moored instruments and recording quality data in this shallow water environment. The 1979 program was not immune; meters on moorings 1, 2, and 7 experienced electronics failures in the component-resolving circuitry and mooring 3 was not recovered. This left moorings 4, 5, and 6 (fig. 1), all located in the island passages. So although nothing definitive can be advanced concerning circulation in the western basin, the long continuous data from the passages afford a look at the flow between basins.

Before presenting the 1979 data, it would be useful to review results from previous investigative efforts in this region. Flow from the western to the central basin depends on the inflow to western Lake Erie. The basin receives about 80 percent of its water supply via the Detroit River; the **Maumee** River is the only other significant tributary in the basin and during summer its flow is minimal.

The majority of western basin studies, as referenced in the introduction, have relied solely on drift objects to qualitatively describe circulation and water mass exchange. The consensus is that Detroit River water first sweeps southeastward and then clockwise through the basin, with the major portion exiting to the central basin through Pelee Passage. A clockwise rotational gyre around Pelee Island is alluded to in all reports, while the southern channel's flow was considered variable by Olson (1950) and **Hamblin** (1971) and dominantly westward and part of the clockwise gyre by Verber (1955).

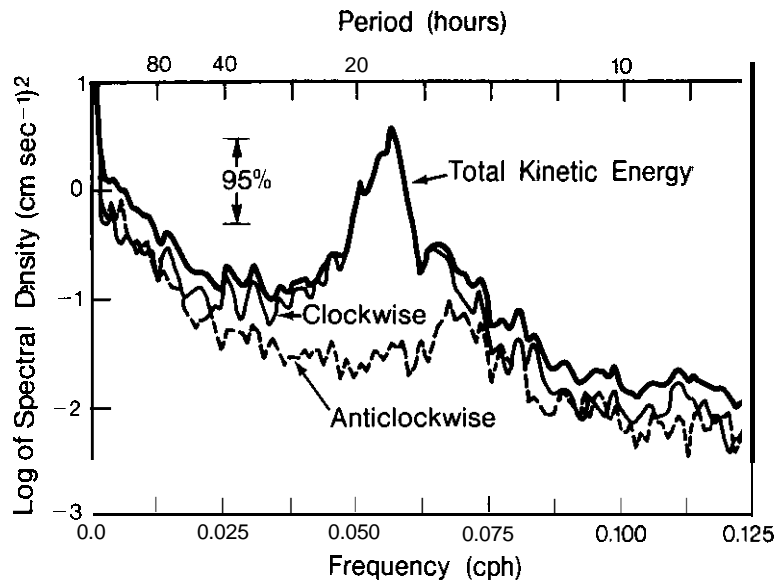


FIGURE 18.--*Kinetic energy spectra computed from &h-averaged current velocity recordings at mooring 15 during May through December 1979.*

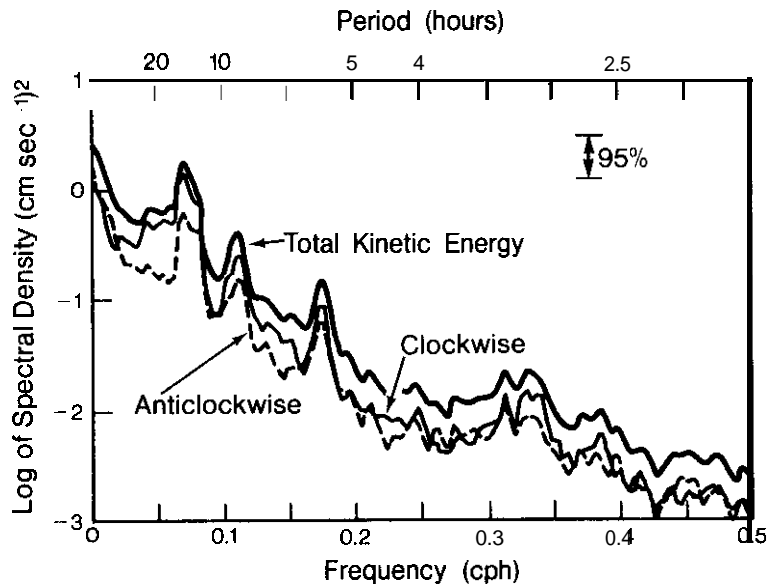


FIGURE 19.--*Kinetic energy spectra computed from hourly-averaged current velocity recordings at mooring 6 during May through October 1979.*

FWPCA (1968) moored one current meter *in* Pelee Passage and another off Catawba Island at a depth of 9 m during 1964-65. FWPCA interpreted the limited data return as surface currents rotating in a clockwise gyre through the island region with anticlockwise bottom currents. Hamblin (1971) reviewed these data (together with all previous work) and concluded that, although there is randomness in currents in the inter-island area, the clockwise gyre is a prominent feature and it extends to the bottom.

The 1979 inter-island current measurements display a variety of processes. The short-period seiche-driven currents, illustrated spectrally in figure 19, contributed markedly to turbulent mixing and diffusion. Figure 20

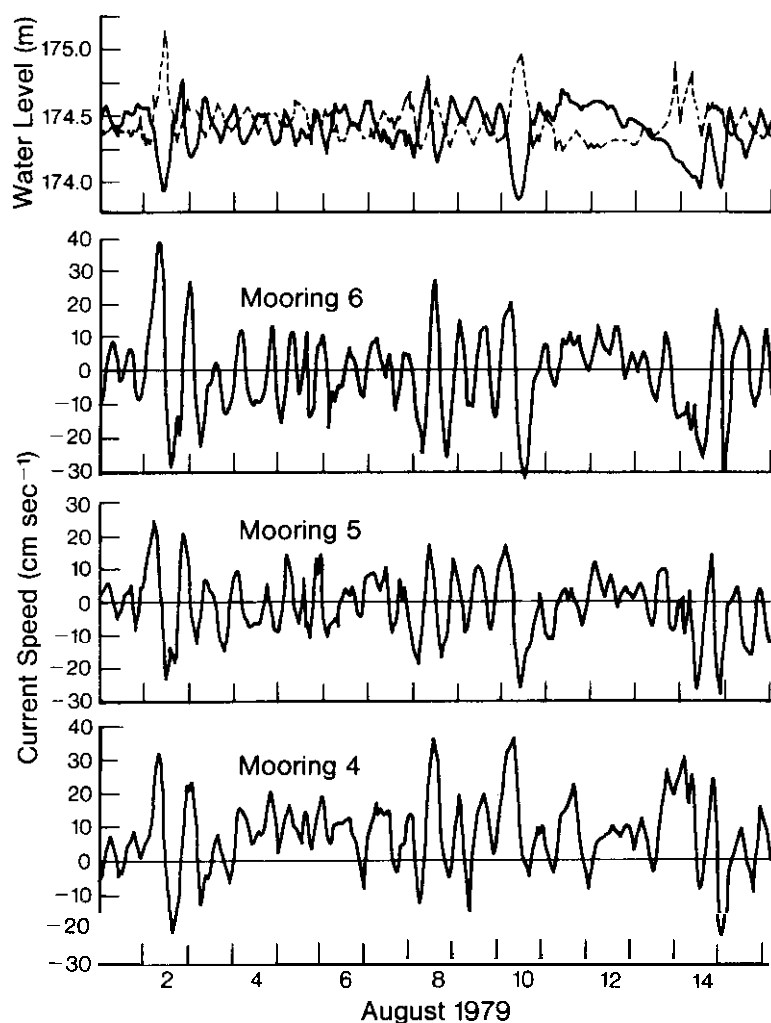


FIGURE 20. --Hourly *water* levels at Toledo (*solid line*) and Buffalo and the current velocity component *parallel* to the channel axis at moorings 4, 5, and 6, *August 1-15, 1979*.

shows the persistence and magnitudes of these current responses to wind setups and seiching. Current components from moorings 4 and 5 have been rotated to orient with the bathymetry; mooring 6 did not require rotation. The currents between islands were in phase and in concert with water-level fluctuations.

Although seiche-driven currents were persistent throughout the year, the net transport by seiche action only was near zero for each cycle and the current run during each half cycle was generally less than 5 km. Outflow from the western basin can be better illustrated by looking at longer periods.

There is no question that the major outflow from the western basin was through Pelee Passage. The resultant current at mooring 4, offset to the east to avoid ship traffic, was 4.4 cm s^{-1} directed into the central basin during the 6-month period; the scalar mean speed was 9.2 cm s^{-1} . Using a rough estimate of the cross-sectional area, we found that the net flow into the central basin is only slightly less than the Detroit River inflow.

The dominance of a clockwise Pelee Island gyre around the islands is not reflected in our data. The Kelleys Island region is certainly not a **low-velocity** area, as was illustrated in figure 20, but rather an area dominated by **seiche-driven currents and storm surges**. The resultant current was eastward at 2.4 cm s^{-1} (7.8 cm s^{-1} mean scalar) during the 6-months. (Monthly resultant currents are in appendix C.) To illustrate further, assuming that an eastward direction of the Pelee Passage currents is a necessary condition for the existence of the gyre, we found that 77 percent of the hourly values were directed toward the central basin. Of this 77 percent, mooring 6 north of Kelleys Island had concurrent eastward flow 69 percent of that time; mooring 5, 70 percent; and all three, 60 percent of that time. Although the Pelee Island gyre is not a dominant feature, examples of this gyre can be seen in the data set, particularly during strong southwest winds. Interestingly, our resultant currents are nearly identical to the flow pattern of tracers in a rotating model of Lake Erie (Rumer and Robson, 1968).

Figure 21 shows Toledo and Buffalo water levels and longitudinal currents from the three moorings during September 1979. Data were low-pass filtered to eliminate the seiche periodicities, so we are left with those resulting from long-period water level variations caused by **mesoscale** winds. Schwab (1978) discussed the wind and water level relationships that occur in Lake Erie. Our concern here is the response of currents to water level changes and its role in mass exchange between basins. Mooring 6 currents followed the trends in water level; mooring 5 currents were similar but with reduced amplitude. Large amplitude current variations in Pelee Passage superposed on the net eastward current compared similarly the first 12 days, but then took on their own oscillating character. This is typical during the measurement season. The variations may be related to the position of the Detroit River plume or the central basin's regime although the resultants are similar during oppositely rotating central basin flows (figs. 10 and 11). Figure 4 does give evidence of a different pattern of island-passage currents during very strong wind from the north-northeast; however, that would fit a storm surge increase in water level on the south shore of the western basin. Our data do not indicate any seasonal variability other than an increase in magnitude of the driving forces and current responses as winter approaches. Unfortunately,

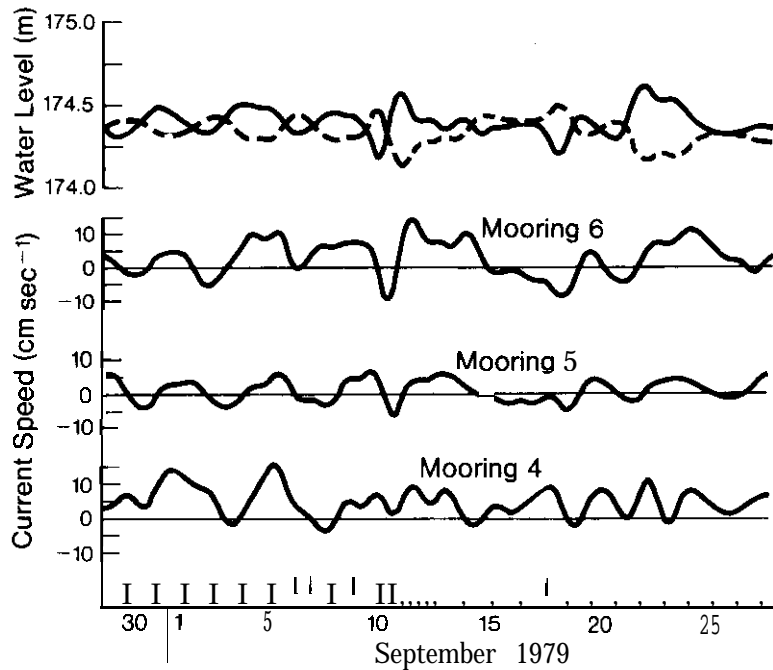


FIGURE 21.--*Low-pass filtered water levels* at Toledo (*solid line*) and Buffalo and the current velocity component parallel to the channel *axis* at moorings 4, 5, and 6, August 29-September 27, 1979.

November and December storm **surges** and **setups** are greatest, but the moorings were retrieved before then.

3.2.5 Water Volume Exchange Processes Between the Eastern and the Central Basins

Our data recovery from the current meter moorings placed on the Pennsylvania Ridge (which separates the eastern and the central basins of Lake Erie) was very meager (table 1). At the north end of the **cross** section (station 23), only the top current meter at 10-m depth provided velocity recordings. At the south end (station 26), both the 10- and the 17.5-m deep meters provided current measurements from June through November 1979, but the deeper instrument's temperature circuitry failed. Little useful current information was collected from the center two moorings, although water temperature records from station 25 were recorded during summer and fall 1979. Currents, water temperature, and dissolved oxygen concentrations were measured extensively about the ridge structure by **NWRI** in 1977 (Boyce *et al.*, 1980) and 1978 (Chiocchio, 1981), however, and much is known of the exchange characteristics. It is within this framework of knowledge that we can interpret our sparse data return.

The transport of cold, oxygenated **mesolimnion** and hypolimnion water from the eastern to the central basin has been considered for some time to be a possible oxygen renewal mechanism for the central basin bottom water (Burns and Ross, 1972). Boyce *et al.* (1980) found that deep layer flows across the ridge were basically just counter to the wind component along the lake's major axis, and that most of the cold water driven westward into the central basin flowed through the deep channel at the southern end of the ridge. During periods of sustained easterly-directed wind stresses, substantial quantities of water were found to flow westward in the lower layers. In July and August, when oxygen is rapidly consumed in the central basin hypolimnion, the transport of water into this layer from the eastern basin was found to add significant oxygen to the easternmost bottom water. Chiocchio (1981) determined that nearly 80 percent of the replenishment entered through the deeper channel south of the ridge, and that the flow turned northwestward after passing through the channel, moved clockwise, and affected mainly the northeastern part of the central basin. He also found close correlation with the along-the-lake component of the wind stress, although the channel flow was more variable in 1978 than in 1977 and long intervals of persistent, large volume flow were not as distinctly defined.

In 1977 and 1978 a semipermanent tilt of the thermocline across the ridge was observed during the stratified season, with the thermocline depressed in the south and **upwelled** closer to the northern boundary. Figure 22 provides evidence of this phenomenon in the 1979 data, as well, where we note that the thermocline passes for good through the 10-m level at stations 25 and 26 about June 10, while at station 23 this occurs in early August. Currents across the ridge and the wind stress (redrawn so that the vertical axis is parallel to the major axis of Lake Erie) for the stratified month of July 1979 are shown in figure 23. The figure first reveals great similarity between station 26 currents at 10- and 17.5-m, i.e., above and below the thermocline. (Chiocchio reported like currents through the channel from 7 m to the bottom.) It also reveals station 26 currents basically out of phase and lagging **the** wind stress component along the lake, although there are important exceptions related to the whole-basin currents. For example, during July 1 through 3, the currents flowed with the wind and were related to a strong **cyclonic** flow pattern set up in the central basin during the episode. The strongest pulse of channel flow occurred during the first week of the month and was directed into the eastern basin. Bottom water flow to the central basin through the channel was significant only during July 20-25.

Perhaps a closer fit with the wind stress impulses is demonstrated in figure 24, which shows the related currents across the ridge observed in September 1979. Through the channel, flow was again nearly out of phase and lagged the wind stress. The strong monthly-averaged currents that yielded westward channel velocities received part of this bias from the clockwise circulation that dominates the lake in September, as station 23 at the north side of the ridge cross section revealed eastward currents almost uninterrupted for the entire month. If the stratification had persisted long into September this year, the deep flows would have contributed oxygenated eastern basin water to the central basin's hypolimnion. As it was, the September flows occurred after the hypolimnion had retreated from the easternmost parts of the central basin. In August 1979 the slightly less intense westward currents

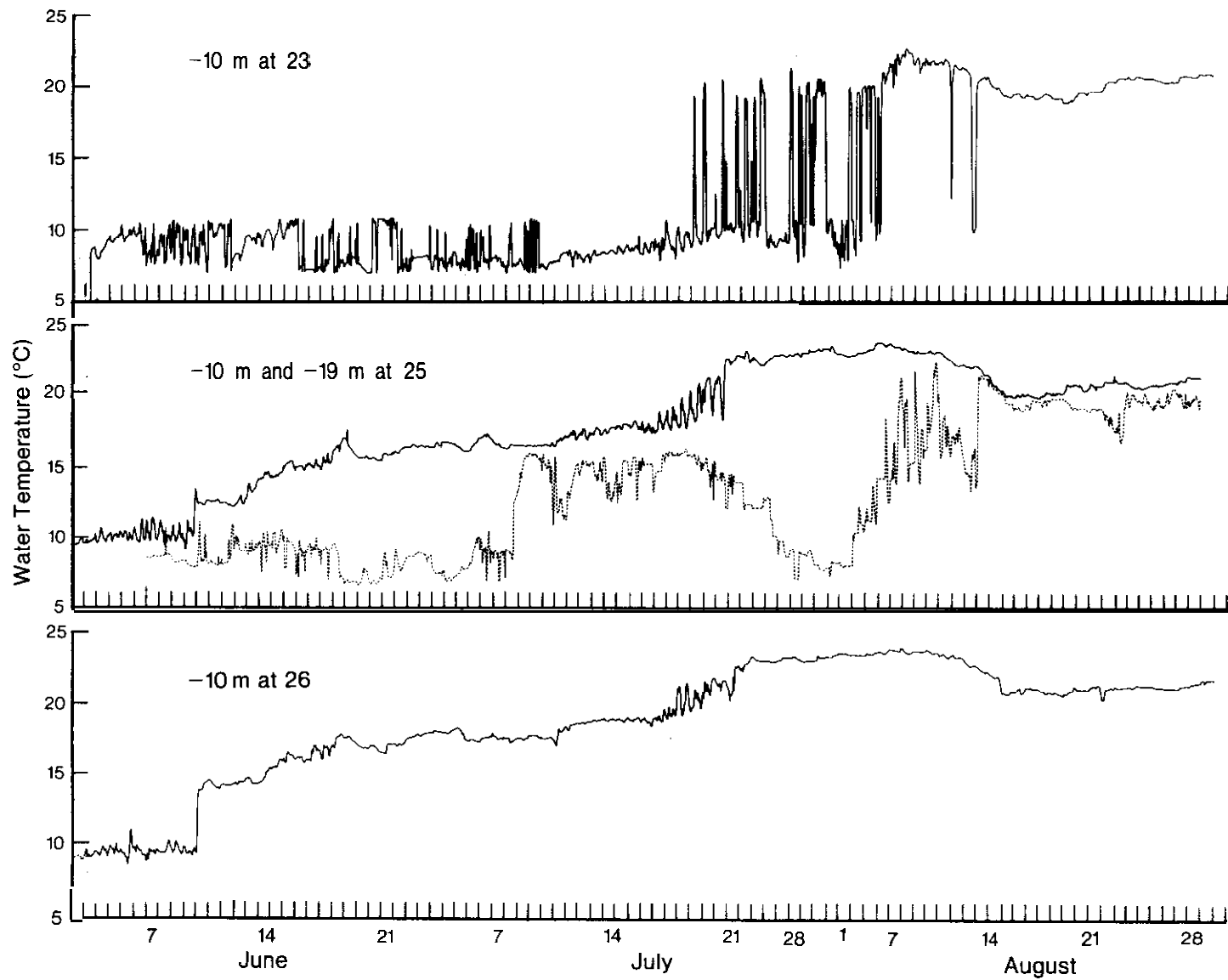


FIGURE 22.--Water temperature recordings at moorings 23, 25, and 26 on a cross section of Lake Erie at the Pennsylvania Ridge.

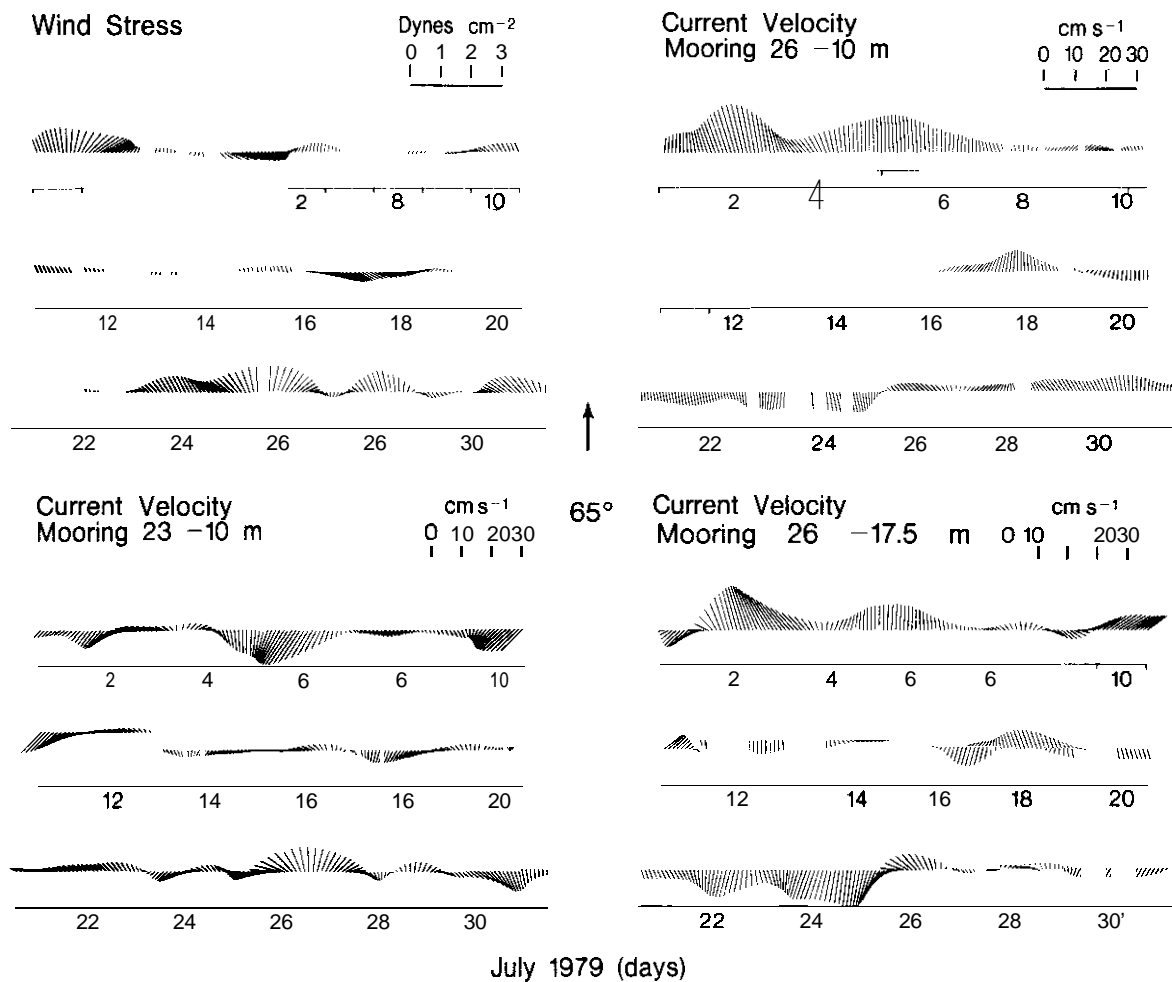


FIGURE 23.--Low-pass filtered wind stresses computed for Lake Erie in July 1979 (Schwab, 1982) and currents (both hourly-averaged but plotted at 2-h intervals) across the Pennsylvania Ridge.

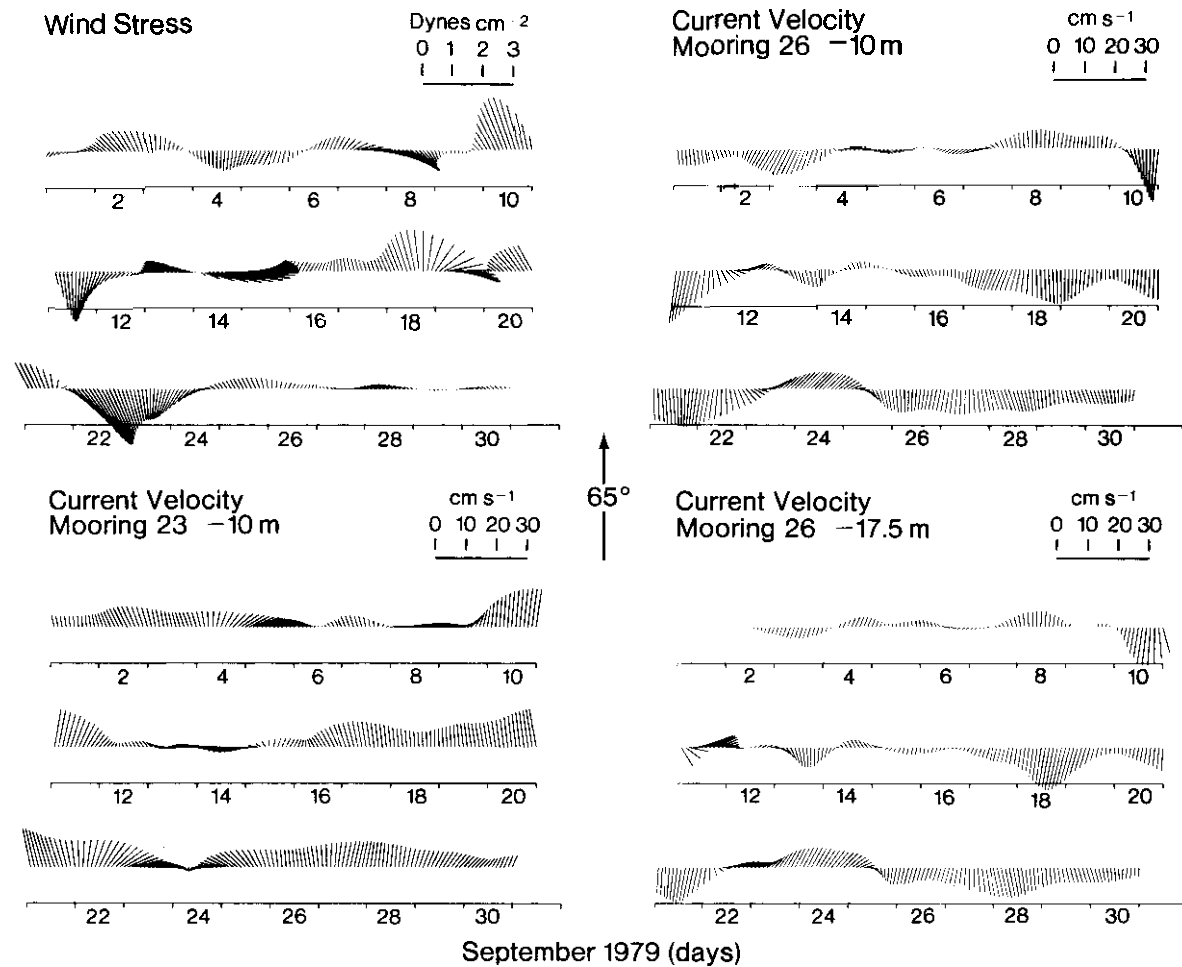


FIGURE 24.--Low-pass filtered Lake Erie wind stresses and currents at the Pennsylvania Ridge in September 1979.

through the channel no doubt contributed to bottom water renewal in the central basin.

Eid (1981) modeled exchange flow mechanisms between these two Lake Erie basins and found good correlation between the wind stress impulses along the lake and the channel transport. During the **most** strongly stratified season, the **thermocline** is deeper in the eastern basin than it is in **the** central basin, leading one to believe that **the** internal **pressure** gradients would not be too important. **Eid's** results substantiated that conclusion and showed that the principal driving force was surface wind drift and bottom **return** flow based on the surface pressure gradients. As noted in numerous other studies (**e.g.**, in Saginaw Bay, see **Danek** and Saylor, 1977), **return** flow is steered into **the** deepest return route. We also have noticed **how** the lake-scale circulation can influence the channel return flow intensity, but **this** factor was not part of the model considerations.

3.2.6 Observed Currents in Relation to Prior Modeling Results

Solutions of the steady-state circulation problem in a homogeneous Lake Erie were computed by Gedney (1971) and Gedney and Lick (1972) using Welander's (1957) shallow water formulation of Ekman dynamics. In these computations, the stream function **is** first obtained to determine the pressure gradients and then the three-dimensional velocity field can be **mapped**. Figure 25 shows the stream function computed for a steady 5.2 m s^{-1} wind from 270° and currents at near the surface, at mid-depth, and at 1.4 m off the bottom. A constant vertical eddy viscosity of $16.8 \text{ cm}^2 \text{ s}^{-1}$ was used in the calculations, making the Ekman "depth of frictional resistance" equal to 18.2 m, near the mean depth of the central basin. The horizontal distributions of the currents at each depth **show** less distinct patterns than the **vertically-**averaged currents or transports. The wind drift is confined to the surface layers and deflected a little to the right because of rotation. The deeper return currents are driven by **the** pressure gradients of the surface slope.

The model results were compared to 24-hourly averaged currents measured by the FWPCA during a few episodes of relatively constant wind stress lasting several days in 1964 and 1965. That such comparisons **can** be meaningful was demonstrated by **Haq** and Lick (1975). who showed that a shallow lake like Lake Erie reaches a steady-state circulation rather quickly. Using the available current information, Gedney and Lick found reasonably good verification of their predictions in currents recorded at mid-depths and deeper mainly in the central basin. The data with which the results could be verified were **rather** sparse though, and consisted of only a few current meter recordings at each level.

The vertically-integrated currents revealed a characteristic two-cell response to wind forcing in both the central and the eastern Lake Erie basins (fig. 25). The pattern retains this basic nature for steady winds, but varies with wind direction (Gedney, 1971). Our recent measurements highlighted two interesting features: at mid-depth and **near the bottom** of the central basin we often observe currents that exhibit less shear than expected from the model predictions and at each level organized circulation patterns may develop.

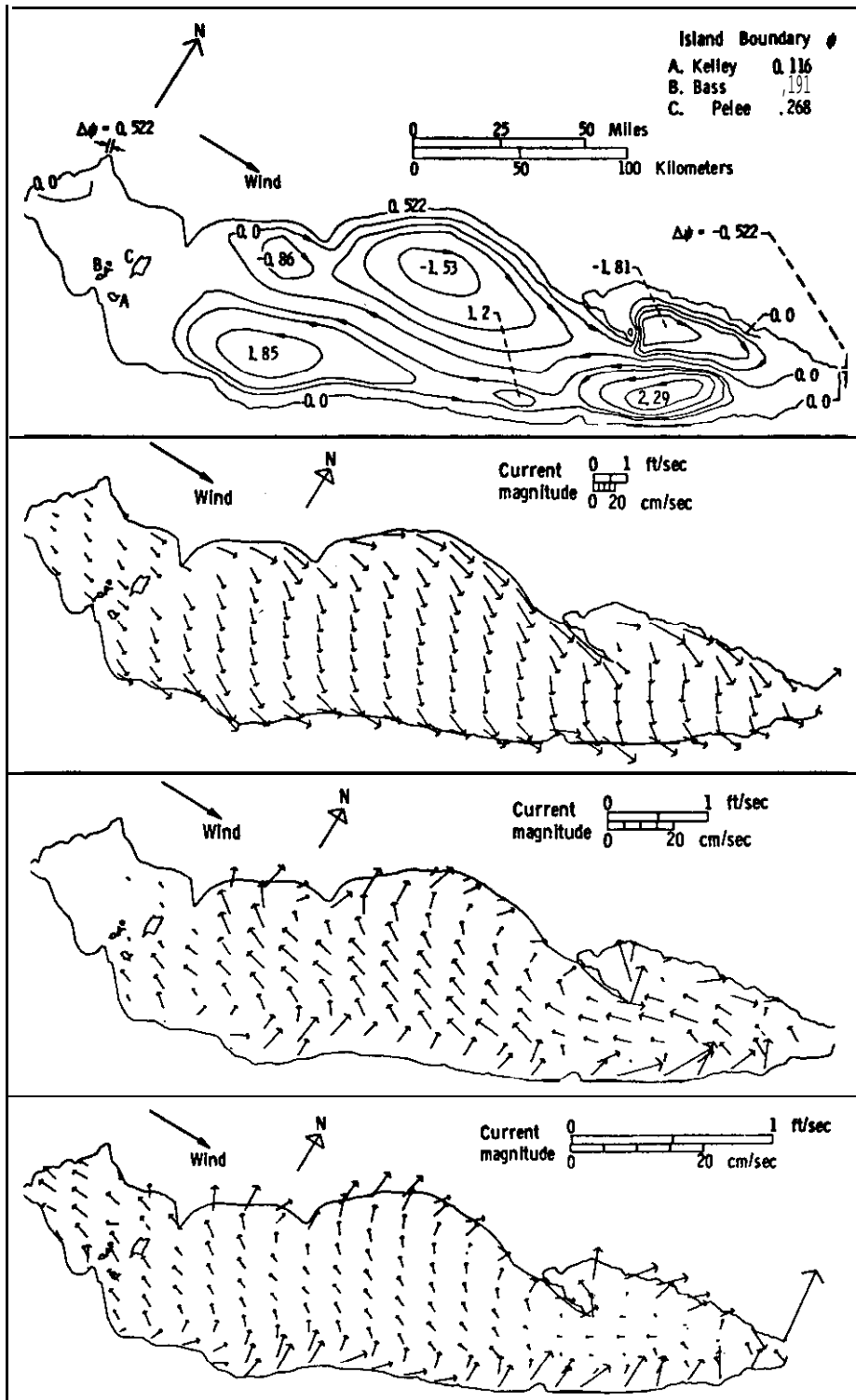


FIGURE 25.--Lake Erie stream function (top) for a 5.2 m s^{-1} west wind.

Also, during significant wind stress impulses, the pattern frequently evolves to a one-cell circulation of the lower half of the water mass in the central basin in either direction of flow. There should be further study directed toward finding why the flow is apparently more **barotropic** than predicted and determining the mechanics of how one of the circulation cells may expand to nearly fill the basin. We hope our measurements will provide a stimulus for it. It would seem that the rotary characteristics of the applied wind stress may be very important, since Schwab's (1982) wind stress computations for 1979 show strong dominance of the wind's clockwise rotating component.

A second numerical simulation of Lake Erie currents was performed by Simons (1976) for most of the ice-free season of 1970, the year of Project Hypo. The vertically-integrated model he developed first for Lake Ontario [Simons (1980) provides a thorough review of progress in lake circulation modeling] was used to **hindcast** the lake's response to measured winds for April through December. Lake surface elevations computed with the model were compared with lake level recorders for verification, while computed volume transports were used to **hindcast** chemical fluxes in a companion study (Lam and Simons, 1976). Also considered for the June through September interval was a two-layer model designed to resolve the flow in both **epilimnion** and **hypolimnion**. Comparisons with the short interval of current velocity recordings obtained during summer stratification in Project Hypo provided verification of the model results. Because this simulation used the measured wind field to **hindcast** currents during **4-week** long intervals between research vessel cruises, it would be difficult to compare these results with the 1979-80 data. The results of Simons modeling effort indicated a complicated circulation pattern of semi-independent cells or **gyres** that surely often characterize the measured currents as well.

The two-layer model provided constructive information on the nature of hypolimnion flow during summer. Results compared favorably with the Project Hypo deep current measurements and with our measurements in July and August of 1979. This model also vividly demonstrated the sensitivity of the prediction to the **parameterization** of bottom friction since the two-layer configuration yields a bottom friction vector that essentially reinforces or adds to the surface stress similar to the complete Ekman formulation of Gedney and Lick (1972).

A two-layer model was developed by Gedney et *al.* (1973) and used to determine the effects of varying eddy viscosity and wind stress distributions on currents and **thermocline** configuration. The responses were found to vary greatly for uniform winds **versus** those with distinct gradients. Though not applicable directly to Lake Erie because of the **nonlinearities** that **must** result from the thinness of the bottom layer and the **thermocline's** intersection with the bottom, their **results** indicate complex interactions that must be considered fully in interpreting lower layer movements.

4. SUMMARY AND DISCUSSION

We measured water temperatures and currents on a large-scale grid in Lake Erie from May 1979 through June 1980. Although there were operational

problems during the experiment. a large volume of high-quality data extending over many months was collected. Analyses of the data have provided some valuable insights into the physics of the Lake Erie water masses, but many topics require further in-depth study.

Water temperature recordings made with **thermister** chains documented the complete development of central basin stratification and the squeezing down of the thermocline to form a very thin hypolimnion. In the early stages of stratification, the fragile stability that slowly evolves in this shallow basin is very susceptible to strong wind stress impulses. In 1979 we observed the complete mixing of the central basin water mass caused by a wind storm in late May. It took several weeks to regain the lost stability. These physical events shorten the season of stratification and make it less likely that the hypolimnion layer will develop anoxia. In the eastern part of the central basin we observed the formation of a double thermocline that persisted for several weeks. Its eventual decay seemed coupled with **hypolimnion** volume entrainment (growth) from the thermocline layer in the manner described by **Ivey** and Boyce (1982). Mid-September dissolution of the hypolimnion because of wind stress mixing and bottom layer advection occurred first in the eastern parts of the basin. Stratification lasted about 1 week longer in the western end.

Close to the bottom, current flows during the stratified season were generally westerly along the south shore of the central basin and north-westerly in the basin's center. The movements of seabed current drifters revealed a similar pattern. These findings confirm earlier work and help explain why the last remnants of the summer hypolimnion are pushed toward the basin's western end. This pattern of bottom currents continues through most of the fall and winter and in some months it closes into a clearly clockwise circulation. Similar currents occur at mid-depth in the water column and in general there is not much current shear. The bottom currents are return flows driven by the surface pressure gradient and are therefore larger during major meteorological events. The prevailing westerly winds, strongest in fall and winter, control the nature of the bottom currents and their intensity.

Monthly-averaged resultant currents and those recorded during major wind stress impulses reveal the same prevailing current patterns. In the high current speed episodes, we often observed two-cell circulations in each of the central and eastern basins, very similar in fact to the volume transport streamlines computed theoretically for Lake Erie by Gedney (1971) and Gedney and Lick (1972). We observed the circulations in both mid-level and **near-**bottom currents without much shear between levels, suggesting that the currents are perhaps a little more barotropic than those revealed by the full **Ekman** layer model they used. Many episodes evolved such that one of the major central basin cells became dominant and the basin-wide currents flowed either clockwise or anticlockwise. There is no clear evidence for the cause of one pattern versus the other and either may arise from what appear to be very similar wind histories. The reason for the frequency of these occurrences should be investigated through model development. We suggest that an important consideration could be the strong tendency of the wind to veer in clockwise fashion, almost never constant over long time intervals. **Hamblin** and Elder (1973,) looked **briefly** at current profiles due to rotating wind stresses

over Lake Ontario and found significant differences with the direction of the rotation (surface layer flows were much stronger if the rotation was clockwise), but much more study is necessary. Episode dominance by one pattern or another plays a big part in determining the pattern of monthly resultant currents. Stratification does not seem to play a major role in shaping the current responses although **thermocline** configuration clearly responds to the wind stress.

The eastern basin appears to be somewhat separate of the central basin in most episodes of energetic currents and in monthly resultants. During the most strongly stratified time of year, cyclonic flow accompanies a density distribution that has less dense waters near the coasts because of geostrophy as noted earlier by **Hamlin** (1971). A two-cell pattern of flow in the eastern basin is generated by strong impulses of wind stress, with currents flowing with the wind near the coasts and returning down the center. Prevailing westerly winds keep the cyclonic cell mostly in the southern half of the basin, though rotation of the whole pattern **cyclonically** about the basin occurs after the wind stress relaxes.

Periodic components, including the near-inertial period current vector rotations and the first several longitudinal **seiches** of Lake Erie, were identified in the current meter recordings. The **seiche** currents are very prominent through the inter-island passages between the west and central basins and also significant over wide areas of the central basin, adding an important component to the current velocities. Currents from the western to the central basin were consistently in phase through the three island passages measured, with the largest volume of Detroit River water accounted for in the **Pelee** Passage. Persistent island **gyres** deduced by earlier authors from drift object studies were elusive in the recorded currents; perhaps the meters were too far below the surface. Longer periods are evident in the current episodes and in volume exchange processes between the eastern and central basins. Sustained westerly winds cause a subsurface return flow centered along the axis of the deep channel at the southern end of the Pennsylvania Ridge (Boyce *et al.*, 1980, and Chiochio, 1981). We observed this flow and found that its intensity is related to the whole-basin circulation across the ridge. Large volume deep inflow to the central basin occurred mostly after the end of stratification in 1979.

Our measurements ignored the near-surface wind drift currents and currents tight against the coasts. Previous investigators have found narrow eastward flows along both the northern and the southern shores from surface to bottom (cf. **FWPCA**, 1968). **Platzman's** (1963) classic paper provided a dynamical perspective of surface currents and return flow. This and subsequent model predictions with prevailing westerly winds have confirmed both the coastal currents and the surface wind drift that has been deduced from the results of drift object experiments. These features have probably been the best known parts of Lake Erie circulation and nothing here contradicts those results.

Our intent in this report has been to describe the data collected in Lake Erie in 1979 and 1980 and to present some analyses of the data pertinent to the present research interests concerning lake **physics**. Clearly much remains

to be done, and the real value of the data will come from in-depth studies that will follow. Toward this end, the data **are available** to all who express an interest in them; we encourage their exploration or use for verification of derived simulations.

5. REFERENCES

- Bennett, J. R. (1974): On the dynamics of wind-driven lake currents. *J. Phys. Oceanogr.* **4**:400-414.
- Blanton, J. O., and A. R. Winklhofer (1971): Circulation of hypolimnion water in the **central** basin of Lake Erie. ***In Proceedings of the 14th conference on Great Lakes research, 788-798.*** International Association for Great Lakes Research. Ann Arbor, Mich.
- Blanton, J. O., and A. R. Winklhofer (1972): Physical **processs** affecting the hypolimnion of the central basin of **Lake Erie**. In ***Project Hypo: An intensive study of Lake Erie central basin hypolimnion and related surface water phenomena***, 9-38. Canada Centre for Inland Waters Paper no. 6, U.S. Environmental Protection Agency Technical Report TS-05-71-208-24. **Ottawa, Ont.**
- Boyce, F. M., F. Chiocchio, B. Eid, F. **Penicka**, and F. Ross (1980): Hypolimnion flow between the central and eastern basins of Lake Erie during 1977 (interbasin hypolimnion flows). ***J. Great Lakes Res.*** **6**:290-306.
- Burns, N. M., and C. Ross (1972): ***Project Hypo: An intensive study of Lake Erie central basin hypolimnion and related surface water phenomena.*** Canada Centre for Inland Waters Paper no. 6, U.S. Environmental Protection Agency Technical Report TS-05-71-208-24. Ottawa, Ont. 182 pp.
- Carr, J. F., V. C. Applegate, and M. Keller (1965): A recent occurrence of thermal stratification and low dissolved oxygen in western Lake Erie. ***J. Fish. Res. Board Can.*** **33**:564-573.
- Charlton, M. N. (1980): Oxygen depletion in Lake Erie: Has there been any change? Can. ***J. Fish. Aquat. Sci.*** **37**:72-81.
- Chiocchio, F. (1981): Lake Erie hypolimnion and **mesolimnion** flow exchange between central and eastern basins during 1978. National Water Research Institute, Canada Centre for Inland Waters, Burlington, Ont. **99** pp. (Unpublished manuscript.)
- Csanady, G. T. (1982): ***Circulation in the*** coastal ocean. Boston: D. Reidel. 279 pp.
- Danek, L. J., and J. H. Saylor (1977): Measurements of the summer currents in Saginaw Bay, Michigan. ***J. Great Lakes Res.*** **3**:65-71.

- Eid, B. M. (1981): Investigation into interfacial transports and exchange flow for lake models. Ph.D. thesis, **McMaster** University, Hamilton, **Ont.**
- Felt, D. M., and D. S. Goldenberg (1976): *Climatology of surface temperatures of Lake8 Superior, Huron, Erie, and Ontario*. NOM, National Weather Service, Techniques Development Laboratory Office Note **TDL-76-16**. National Weather Service, Silver Spring, Md. 14 pp.
- Federal Water Pollution Control Administration (FWPCA) (1968): *Lake Erie environmental summary: 1963-64*. U.S. Department of the Interior, Great Lakes Region, Chicago, **Ill.** 170 pp.
- Gaul, R., J. Snodgrass, and D. **Cretzler** (1963): Some dynamical properties of the **Savonious** rotor current meter. In Marine sciences *instrumentation*. Vol. 2, Instrumentation Society America. New York: Plenum Press.
- Gedney, R. T. (1971): Numerical calculations of the wind-driven **currents** in Lake Erie. Ph.D. thesis, Case Western Reserve University, Cleveland, Ohio. 258 **pp.**
- Gedney, R. T., and W. Lick (1972): Wind-driven currents in Lake Erie. *J. Geophys. Res.* **77:2714-2723**.
- Gedney, **R.T.**, W. Lick, and **F. B. Molls** (1973): A simplified stratified lake model for determining effects of wind variation and eddy **diffusivity**. In *Proceedings of the 16th conference on Great Lake8 research*, 710-722. International Association for Great Lakes Research. Ann Arbor, Michigan.
- Hamblin, P. F. (1971): *Circulation and water movement in Lake Erie*. Inland Waters Branch Scientific Series no. **7**. Canada Department of Energy, Mines, and Resources, Ottawa, **Ont.** 49 pp.
- Hamblin, P. F., and **F.C. Elder** (1973): A preliminary investigation of the wind stress field over Lake Ontario. In *Proceedings of the 16th conference on Great Lake8 research*. 723-734. International Association for Great Lakes Research. Ann Arbor, **Mich.**
- Harrington, M. W.** (1895): *The currents of the Great Lakes*. Weather Bureau Bulletin B. Washington, **D.C.:** U.S. Dept. of Agriculture. 23 **pp.**
- Hartley, **R. P.**, C. E. Herdendorf, and **M. Keller** (1966): *Synoptic survey of water properties in the western basin of Luke Erie*. Ohio Dept. of Natural Resources, Div. of Geological Survey, Report of Investigations no. 58. Ohio Dept. of Natural Resources, Columbus, Ohio. 19 pp.
- Hartley, **R. P.** (1968): Bottom currents in Lake Erie. In *Proceedings of the 11th conference on Great Lake8 research*, 398-405. International Association for Great Lakes Research. Ann Arbor, **Mich.**
- Haq, A.**, and W. Lick (1975): On the time-dependent flow in a lake. *J. Geophys. Res.* **80:431-437**.

- Huang, J.C. K. (1972): The thermal bar. *Geophye. Fluid Dyn.* **3:1-25.**
- Ivey, G. N., and F. M. Boyce (1982): Entrainment by bottom currents in Lake Erie. *Limnol. Oceanogr.* **27:1029-1038.**
- Lam, D. C. L., and T. J. **Simons** (1976): Numerical computations of **advective** and diffusive transports of chloride in Lake Erie during 1970. *J. Fish. Res. Board Can.* **33:537-549.**
- Lam, D. C. L., W. M. **Shertzer**, and A. S. Fraser (1982): Simulation of Lake Erie water quality responses to loading and weather variations. National Water Research Institute, Canada Centre for Inland Waters, Burlington, Ont. (Unpublished manuscript.)
- Mortimer, C. H. (1971): Large-scale oscillatory motions and seasonal temperature changes in Lake Michigan and Lake Ontario. Center for Great Lakes Studies Special Report no. 12. University of Wisconsin-Milwaukee, Milwaukee, **Wis.** 106 pp.
- O'Leary, L. B. (1966): Synoptic vector method for measuring water mass movements in western Lake Erie. In *Proceedings of the 9th conference on Great Lakes research*, **337-344.** Great Lakes Research Division Publication no. 15. University of Michigan. Ann Arbor, **Mich.**
- Olson, F. C. W. (1950): The currents of western Lake Erie. Ph.D. thesis, Ohio State University, Columbus, Ohio. 370 pp.
- Platzman, G. W. (1963): The dynamical prediction of wind tides on Lake Erie. *Meteorol. Monogr.* **4(26):44 pp.**
- Platzman, G. W., and D. B. **Rao** (1963): The **14-hour** period of Lake Erie. In *Proceedings of the 6th conference a Great Lakes research*, 231-234. Great Lakes Research Division Publication no. 10. University of Michigan. Ann Arbor, **Mich.**
- Powers, C. F., D. L. Jones, P. C. Mundinger, and J.C. Ayers (1960): *Application of data collected along shore to conditions in Lake Erie.* Great Lakes Research Division Publication no. 4. University of Michigan. Ann Arbor, **Mich.** 78 pp.
- Resio**, D. T., and C. L. Vincent (1977): Estimation of winds over the Great Lakes. *J. Waterway Port Coast. Ocean Div.* 103 (**WW2**):265-283.
- Rathke, D. E. *et al.* (1983): Lake Erie intensive study. A report in preparation for the U.S. Environmental Protection Agency, Center for Lake Erie Research, Columbus, Ohio.
- Rumer**, R. R., and L. **Robson** (1968): Circulation studies in a rotating model of Lake Erie. In *Proceedings of the 11th conference on Great Lakes research*, 487-495. International Association for Great Lakes Research. Ann Arbor, **Mich.**

- Saylor, J. H., J. C. K. Huang, and R. O. Reid (1980): Vortex modes in southern Lake Michigan. *J. Phys. Oceanogr.* 10:1814-1823.
- Schwab, D. J. (1978): Simulation and forecasting of Lake Erie storm surges. *Mon. Wea. Rev.* 106:1476-1487.
- Schwab, D. J. (1982): Determination of wind stress from water level fluctuations. Ph.D. thesis, University of Michigan, Ann Arbor, Mich. 108 pp.
- Simons, T. J. (1976): Continuous dynamical computations of water transports in Lake Erie for 1970. *J. Fish. Res. Board Can.* 33:371-384.
- Simons, T. J. (1980): *Circulation models of lakes and inland seas.* Can. Bull. Fish. and Aquat. Sci. Bull. no. 203, Ottawa, Ont.: Department of Fisheries and Oceans. 146 pp.
- Verber, J. L. (1953): Surface water movement, western Lake Erie. *Ohio. J. Sci.* 53:42-46.
- Verber, J. L. (1955): Rotational water movements in western Lake Erie. In *Proceedings of the International Association of Theoretical and Applied Limnology* 12:97-104.
- Welander, P. (1957): Wind action on a shallow sea: Some generalizations of Ekman's theory. *Tellus* 1:47-52.
- Wright, S. (1955): *Limnological survey of western Lake Erie.* U.S. Fish and Wildlife Service Special Scientific Report Fisheries no. 139. Washington, D.C.: U.S. Fish and Wildlife Service. 341 pp.

Appendix A.--LOW-PASS FILTERED WIND **STRESS** VECTORS FOR THE PERIOD OF THE
CURRENT MEASURING PROGRAM, MAY 1979 THROUGH **JUNE** 1980.

Through October 20, 1979, hourly stresses were computed from actual winds observed at the NWRI buoys; the wind stress vectors are drawn at 2-h intervals. The remainder of the wind stress series was computed using the method of **Resio** and Vincent (1977) from meteorological observations at 3-h intervals from Toledo and Cleveland, Ohio; Erie, Pennsylvania; Buffalo, New York; and London, Ontario.

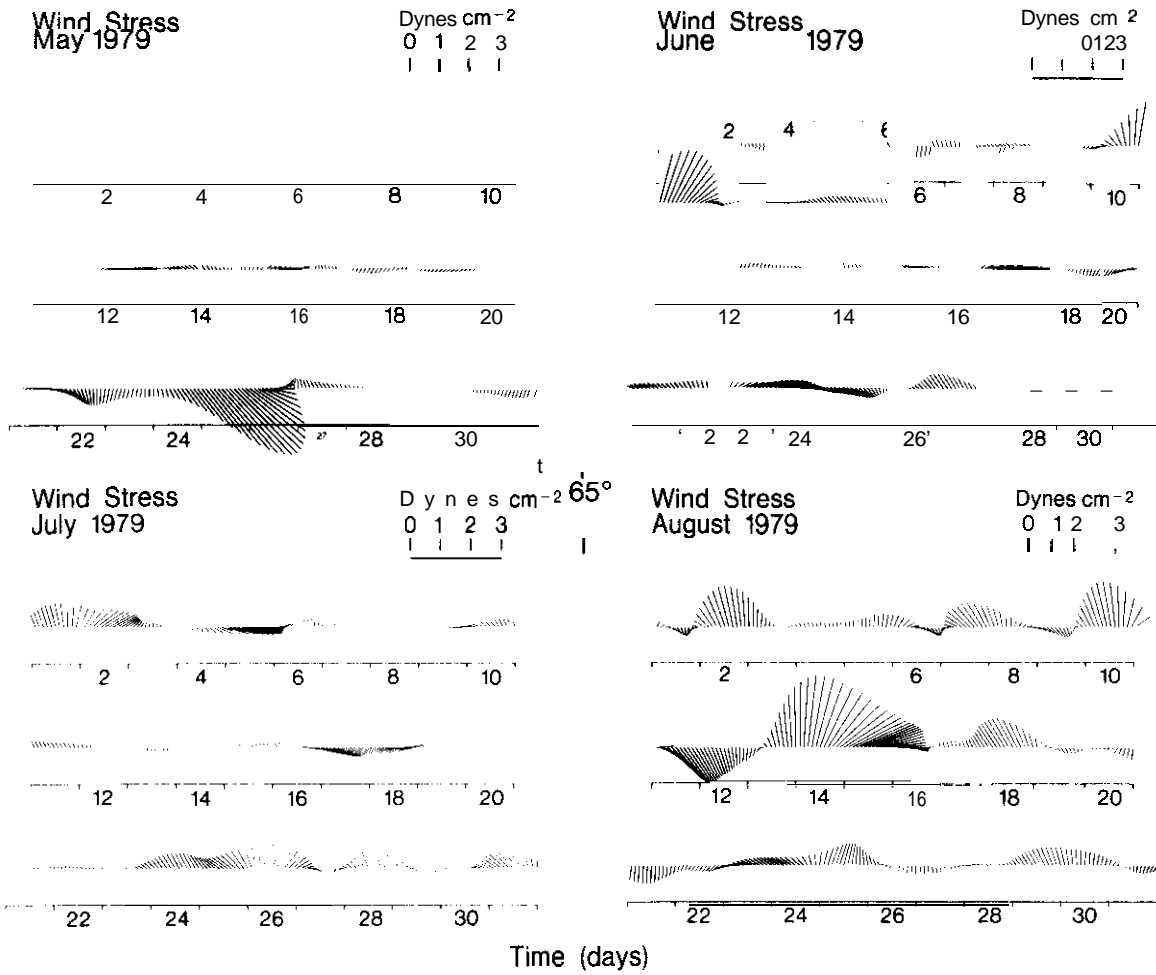


FIGURE 26.--Low-pass filtered wind stress vectors for May, June, July, and August 1979.

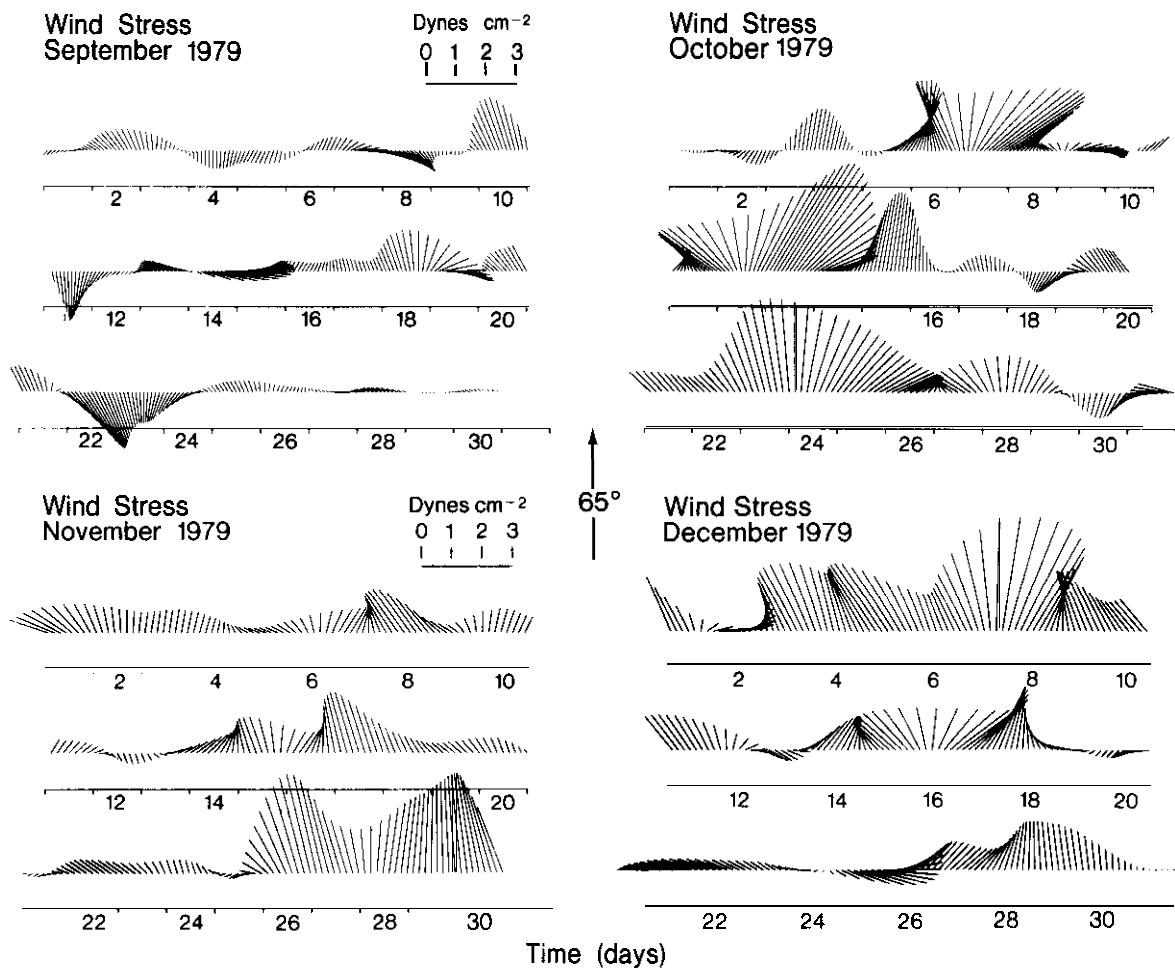


FIGURE 27.--Low-pass filtered wind stress vectors for September, October, November, and December 1979.

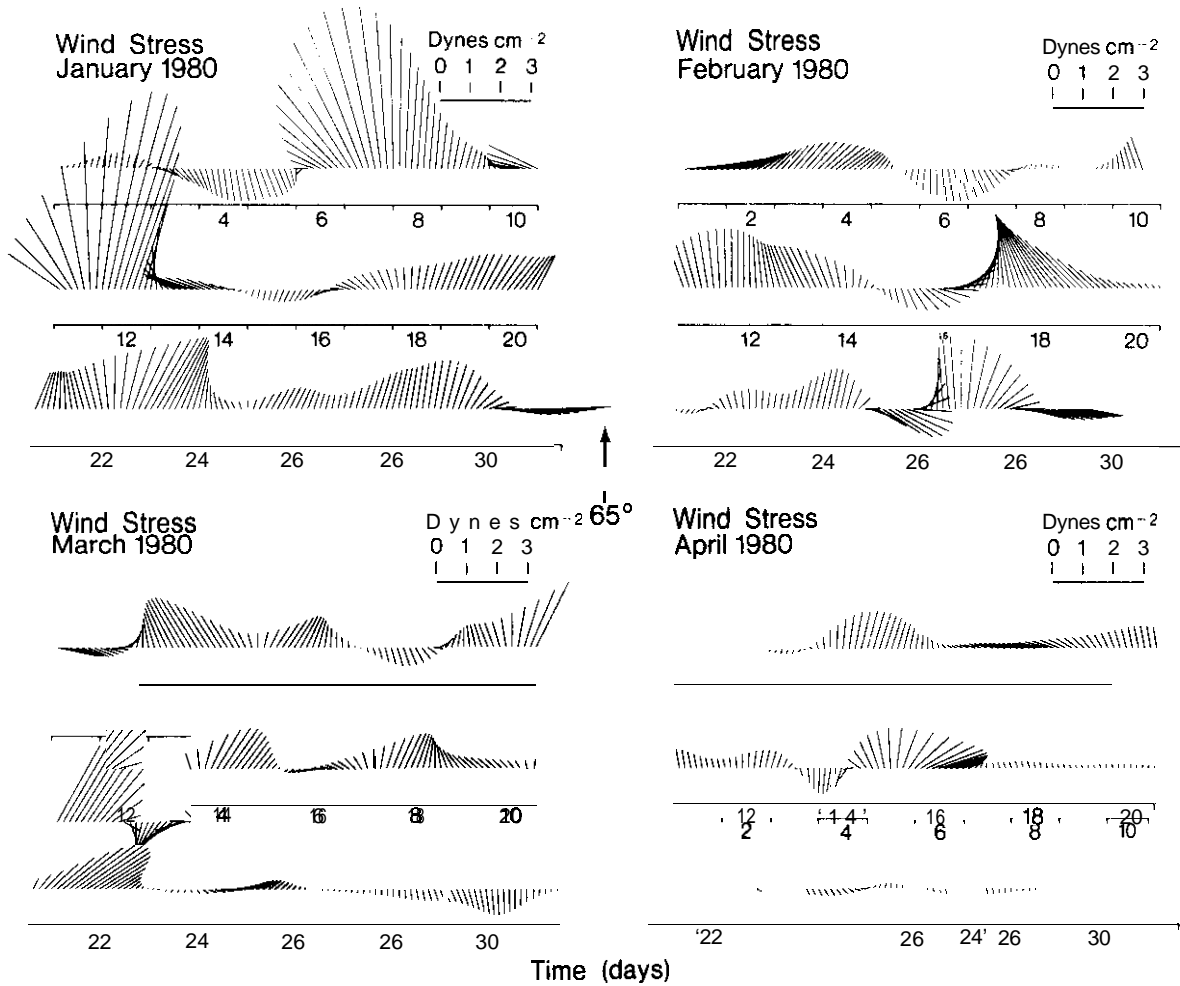


FIGURE 28.--Low-pass filtered wind stress vectors for January, February, March, and April 1980.

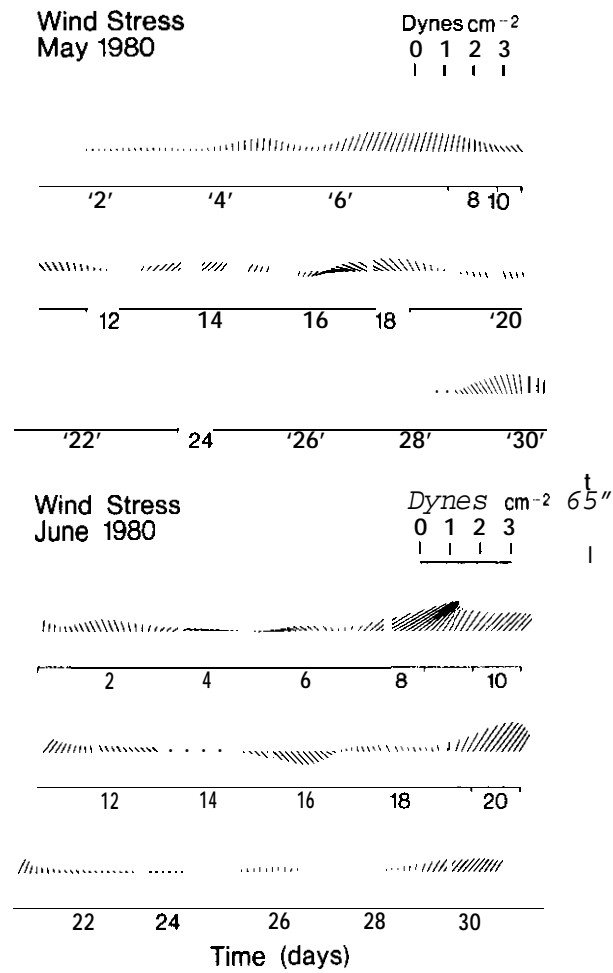


FIGURE 29.--Low-pass filtered wind stress vectors for May and June 1980.

Appendix B.--WATER TEMPERATURE ISOTHERMS ($^{\circ}\text{C}$) DRAWN FROM THERMISTOR CHAIN RECORDINGS AT MOORINGS 9, 11, 19, AND 21 IN THE CENTRAL BASIN OF LAKE ERIE FOR MAY THROUGH SEPTEMBER 1979.

The temperature structure does not extend quite to lake bottom; the water depths at moorings 9, 11, 19, and 21 were 22.9, 23.5, 20.4, and 23.5 m, respectively, **when** the moorings were deployed.

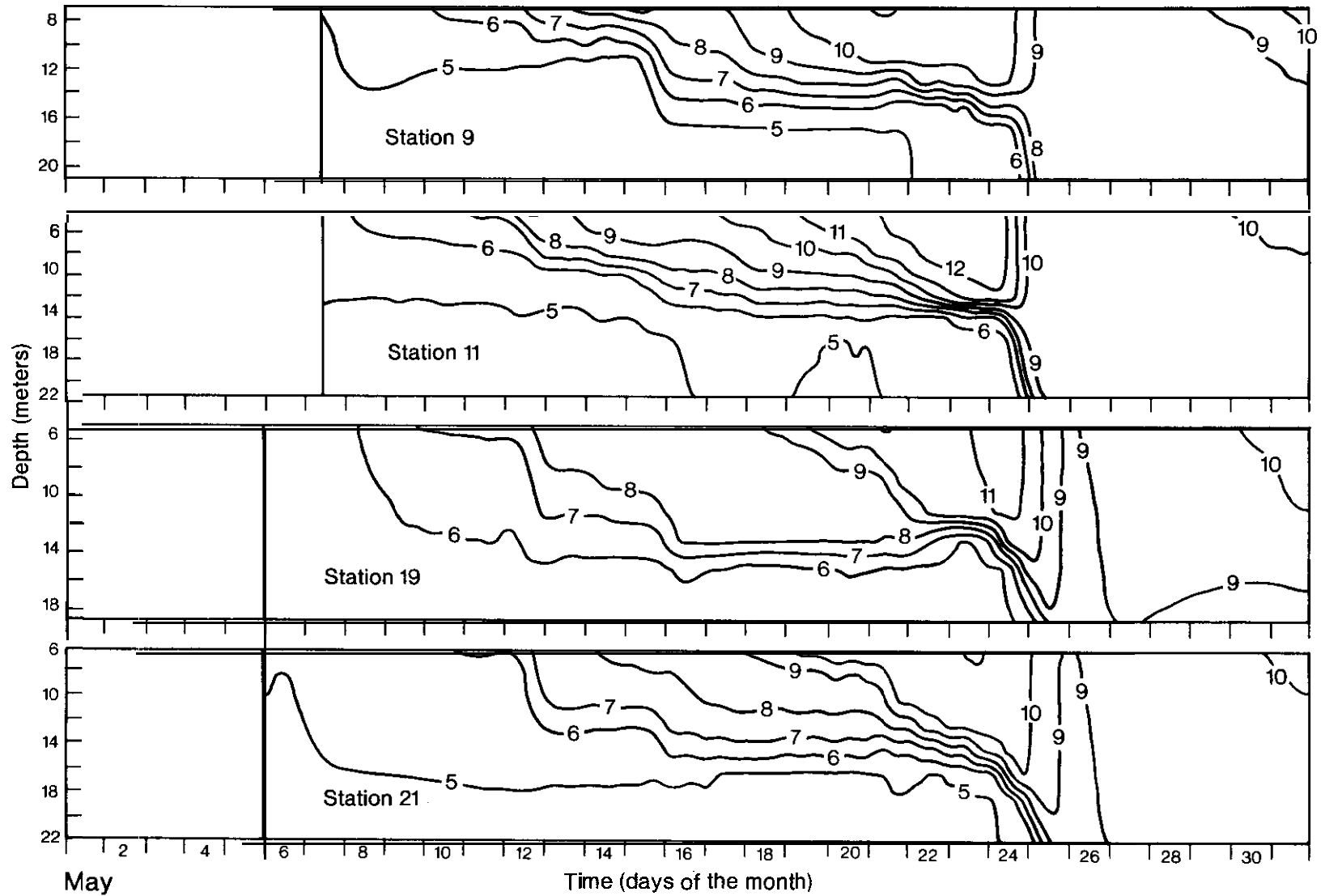


FIGURE 30 - Water temperature isotherms ($^{\circ}\text{C}$) drawn from thermister chain recordings at moorings 9, 11, 19, and 21 in the central basin of Lake Erie for May 1979.

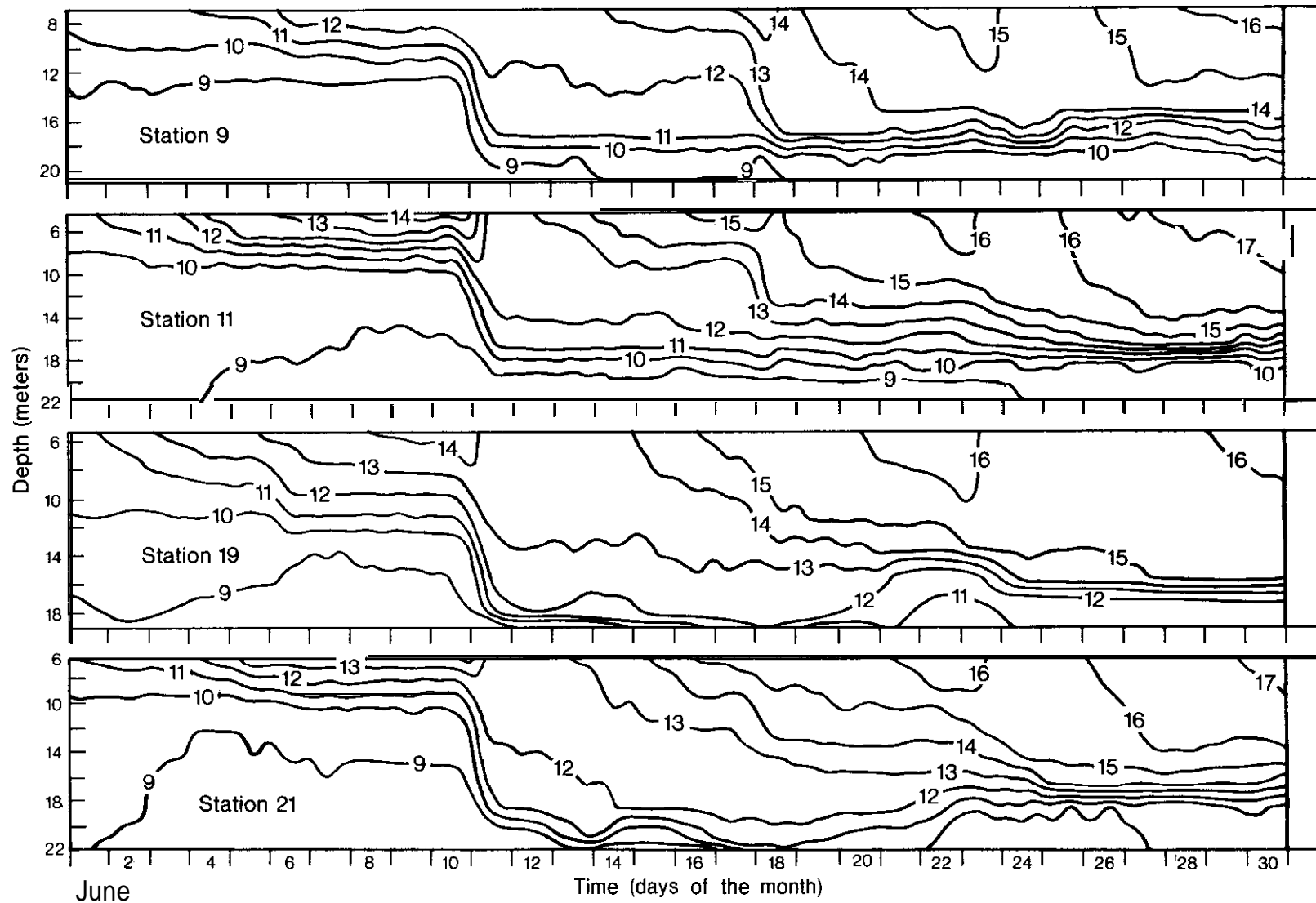


FIGURE 31.--Water temperature isotherms ($^{\circ}\text{C}$) drawn from thermister chain recordings at moorings 9, 11, 19, and 21 in the central basin of Lake Erie for June 1979.

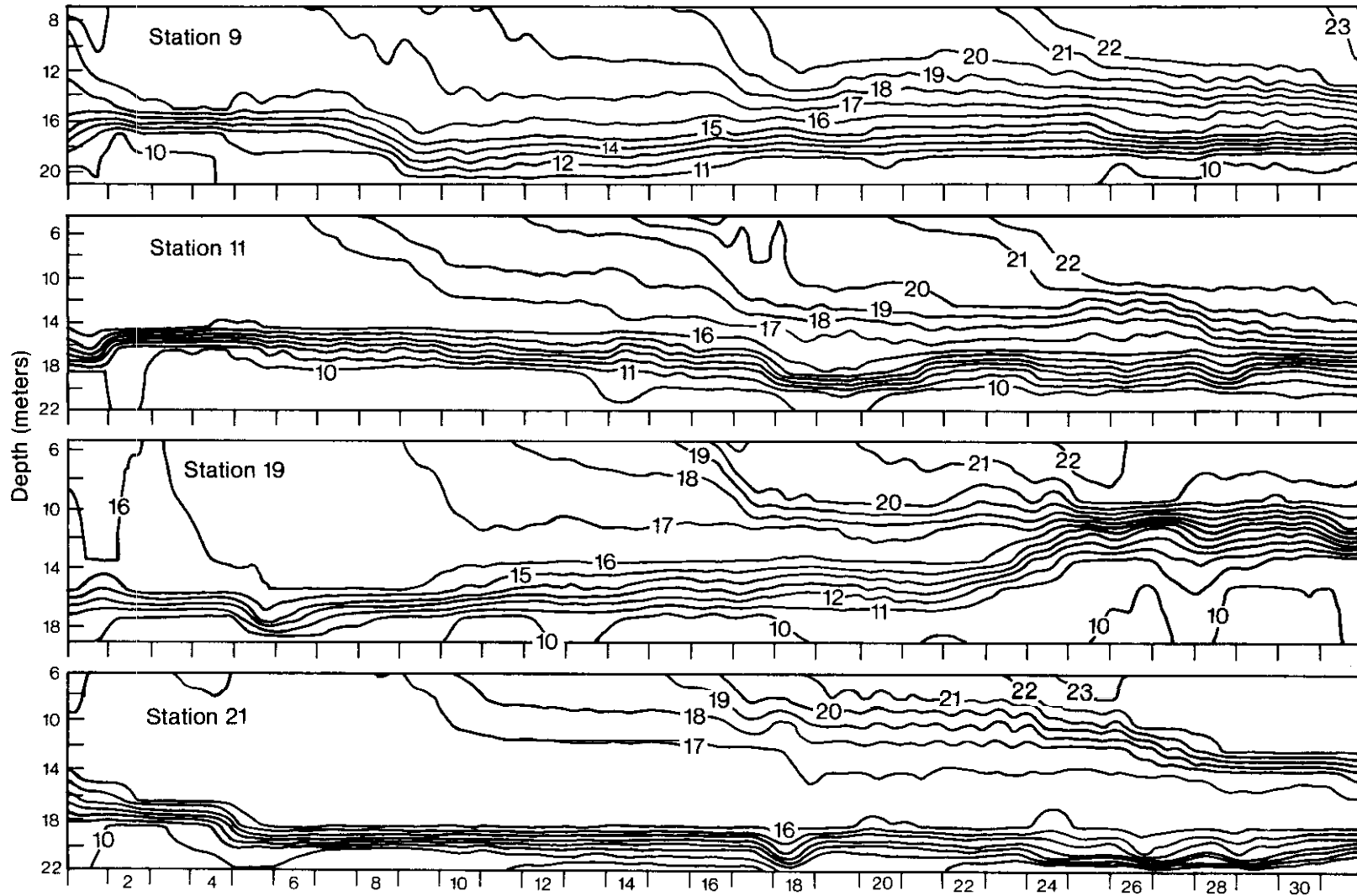


FIGURE 32.- Water temperature isotherms ($^{\circ}\text{C}$) drawn from thermister chain recordings at moorings 9, 11, 19, and 21 in the central basin of Lake Erie for July 1979.

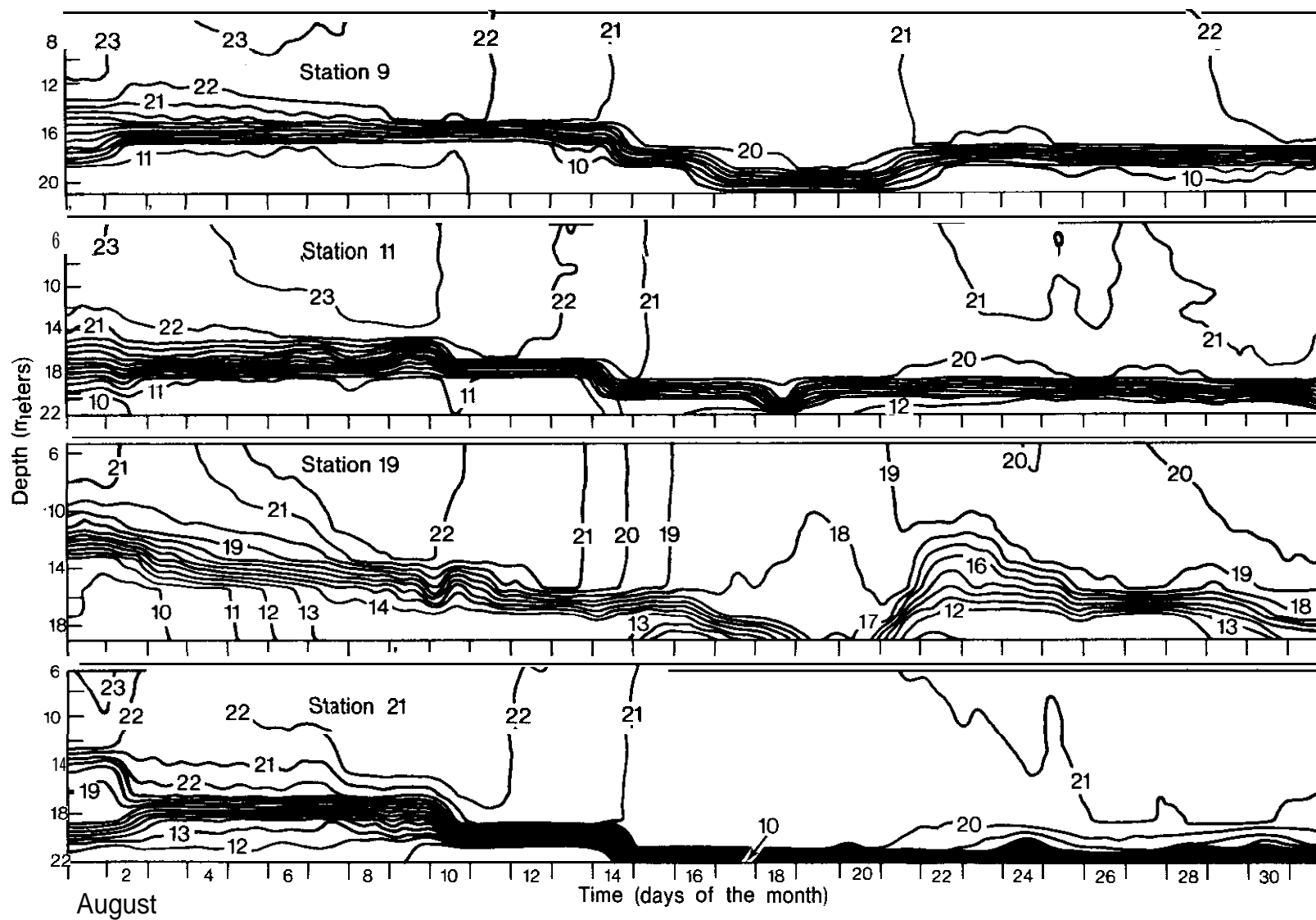


FIGURE 33.--Water temperature isotherms ($^{\circ}\text{C}$) drawn from thermister chain recordings at moorings 9, 11, 19, and 21 in the central basin of Lake Erie for August 1979.

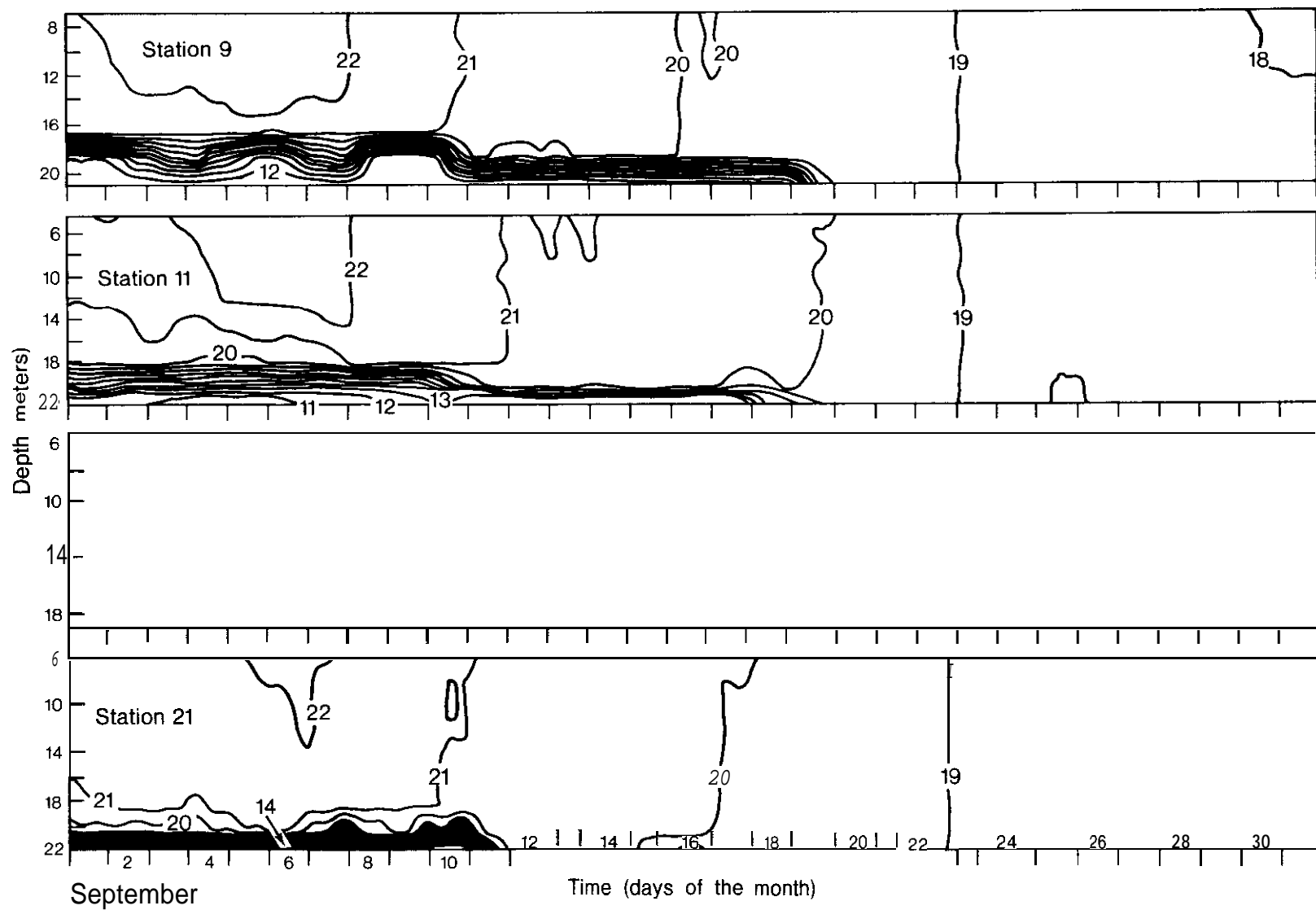


FIGURE 34.--Water temperature isotherms ($^{\circ}\text{C}$) drawn from thermister chain recordings at moorings 9, 11, 19, and 21 in the central basin of Lake Erie for September 1979.

Appendix C.--VECTOR-AVERAGED LAKE ERIE CURRENTS COMPUTED ON A
MONTHLY BASIS FOR MAY 1979 THROUGH JUNE 1980.

The arrowhead indicating direction of flow is not included as a part of the current speed scale; open arrowheads show currents closest to the bottom on moorings that had three current meters. Monthly averaged water temperatures recorded in current meters nearest the surface (top) and at 2.3 m above the lake bottom are also displayed.

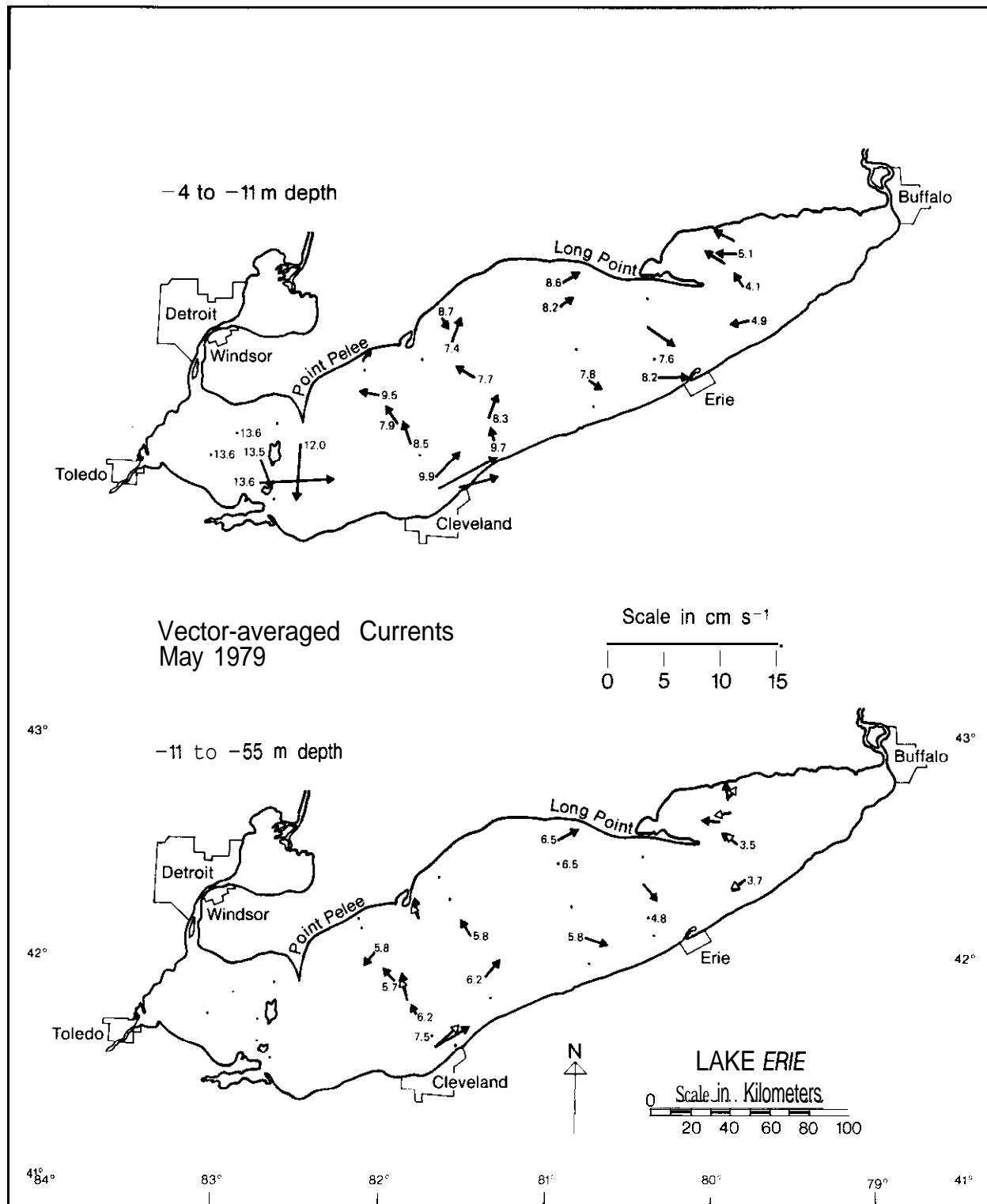


FIGURE 35.--Vector-averaged Lake Erie currents for May 1979. The arrowhead indicating direction of flow is not included as a part of the current speed scale; open arrowheads show currents closest to the bottom. Monthly averaged water temperatures recorded in current meters nearest the surface and at 2.3 m above the bottom are also displayed.

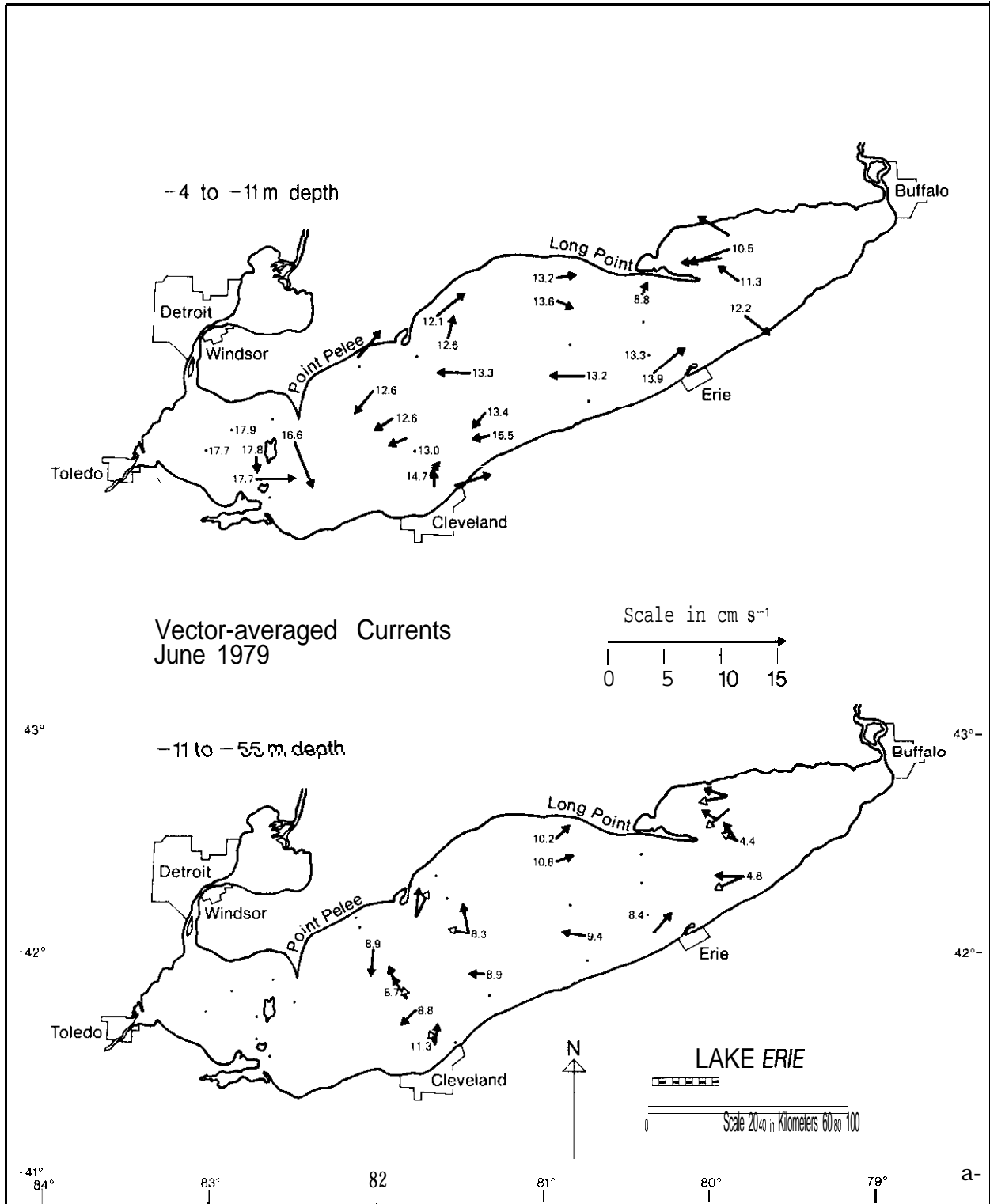


FIGURE 36.--Vector-averaged Lake Erie currents for June 1979. The arrowhead indicating direction of flow is not included as a part of the current speed scale; open arrowheads show currents closest to the bottom. Monthly averaged water temperatures recorded in current meters nearest the surface and at 2.3 m above the bottom are also displayed.

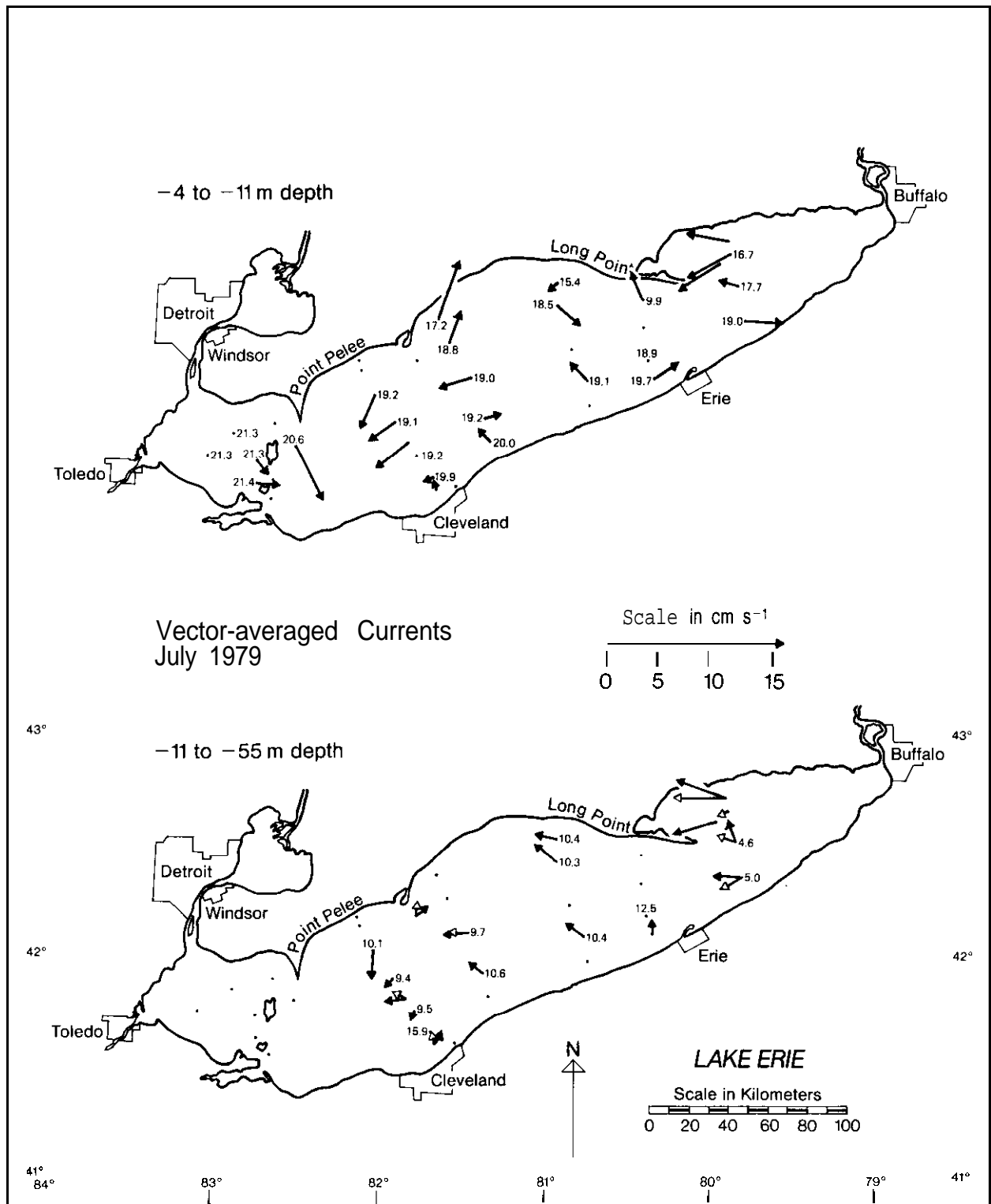


FIGURE 37.--Vector-averaged Lake Erie currents for July 1979. The arrowhead indicating direction of flow is not included as a part of the current speed scale; open arrowheads show currents closest to the bottom. Monthly averaged water temperatures recorded in current meters nearest the surface and at 2.3 m above the lake are also displayed.

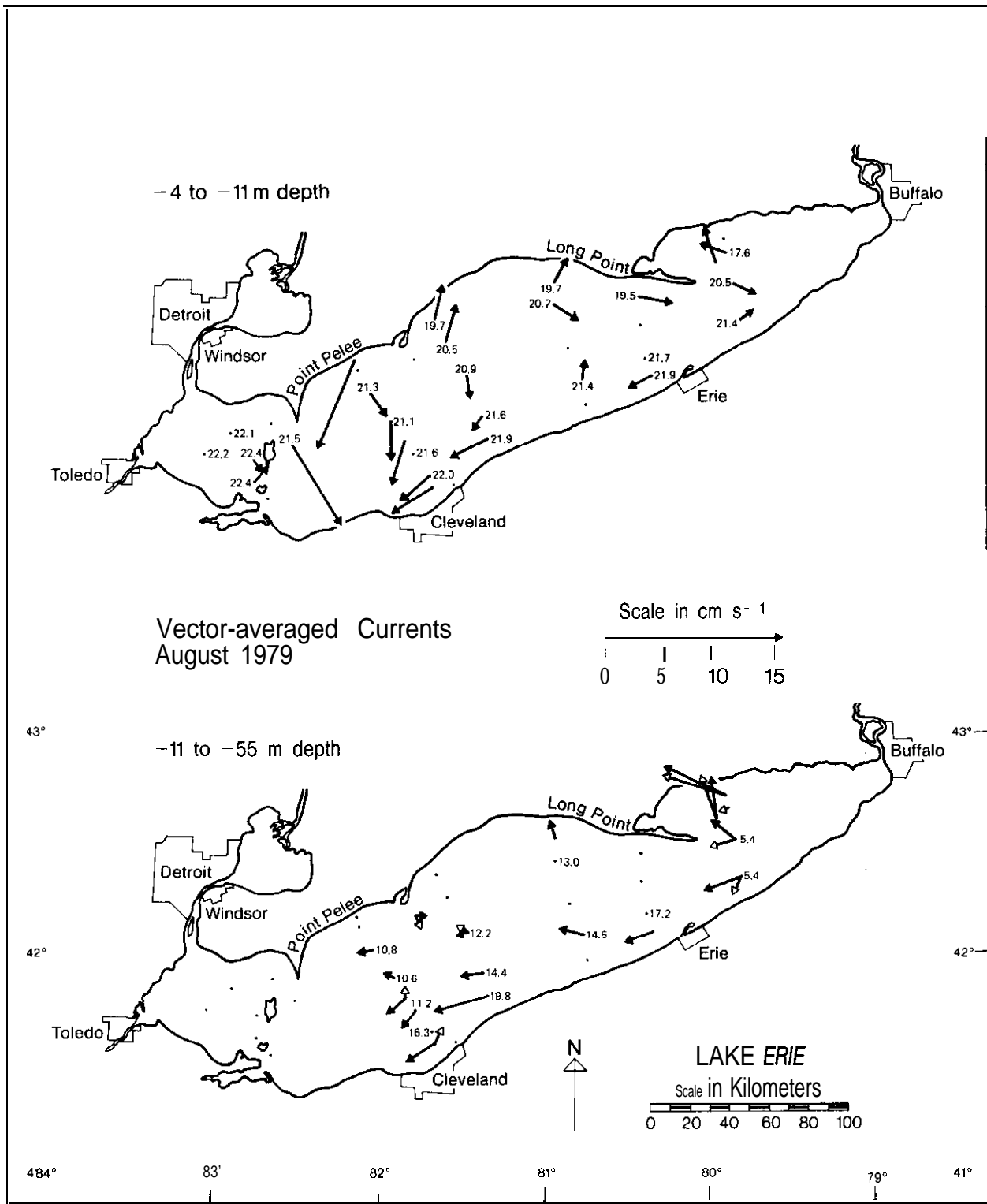


FIGURE 38.--Vector-averaged Lake Erie currents for August 1979. The arrowhead indicating direction of flow is not included as a part of the current speed scale; open arrowheads show currents closest to the bottom. Monthly averaged water temperatures recorded in current meters nearest the surface and at 2.3 m above the bottom are also displayed.

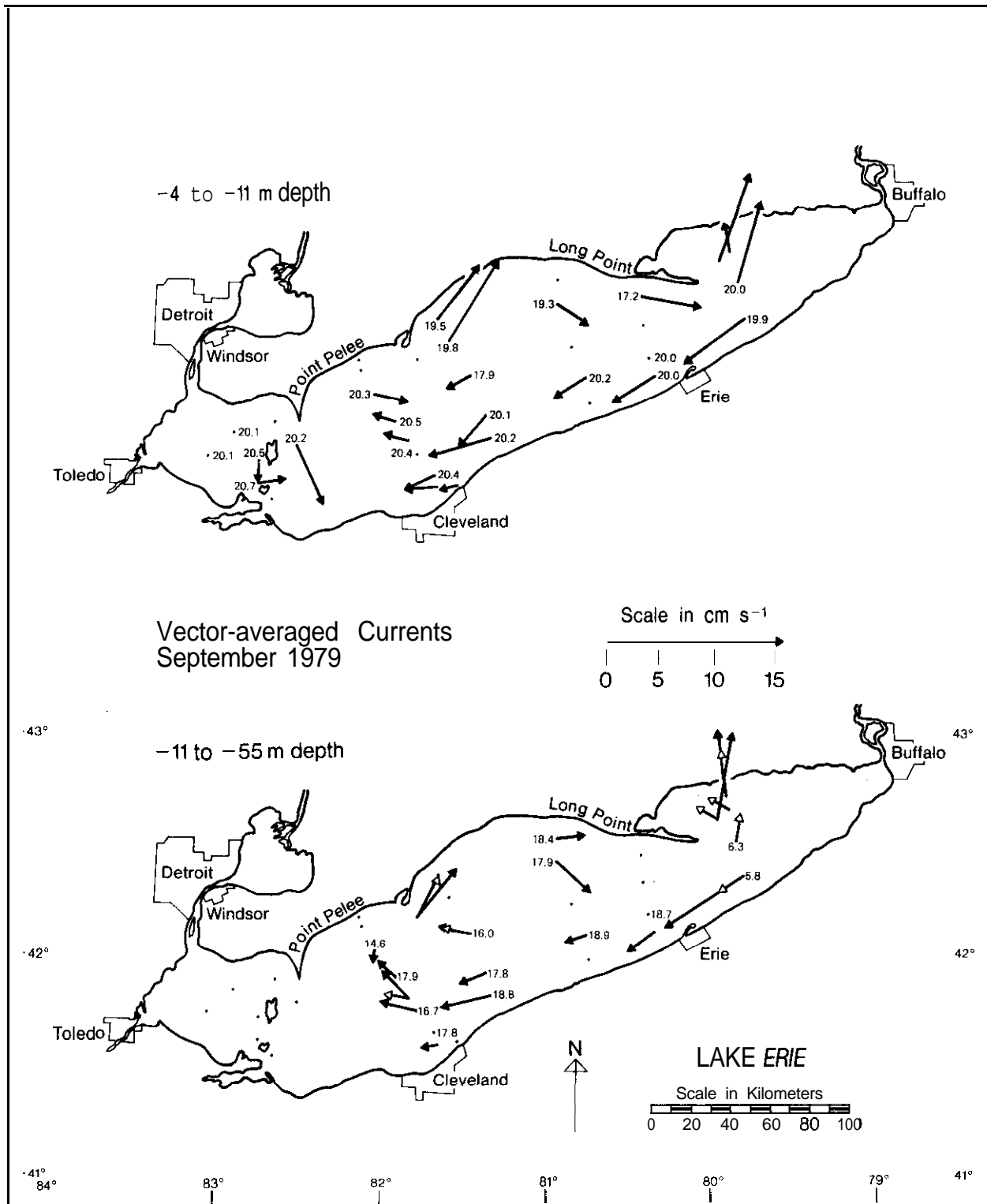


FIGURE 39.--Vector-averaged Lake Erie currents for September 1979. The arrowhead indicating direction of flow is not included as a part of the current speed scale; open arrowheads show currents closest to the bottom. Monthly averaged water temperatures recorded in current meters nearest the surface and at 2.3 m above the bottom are also displayed.

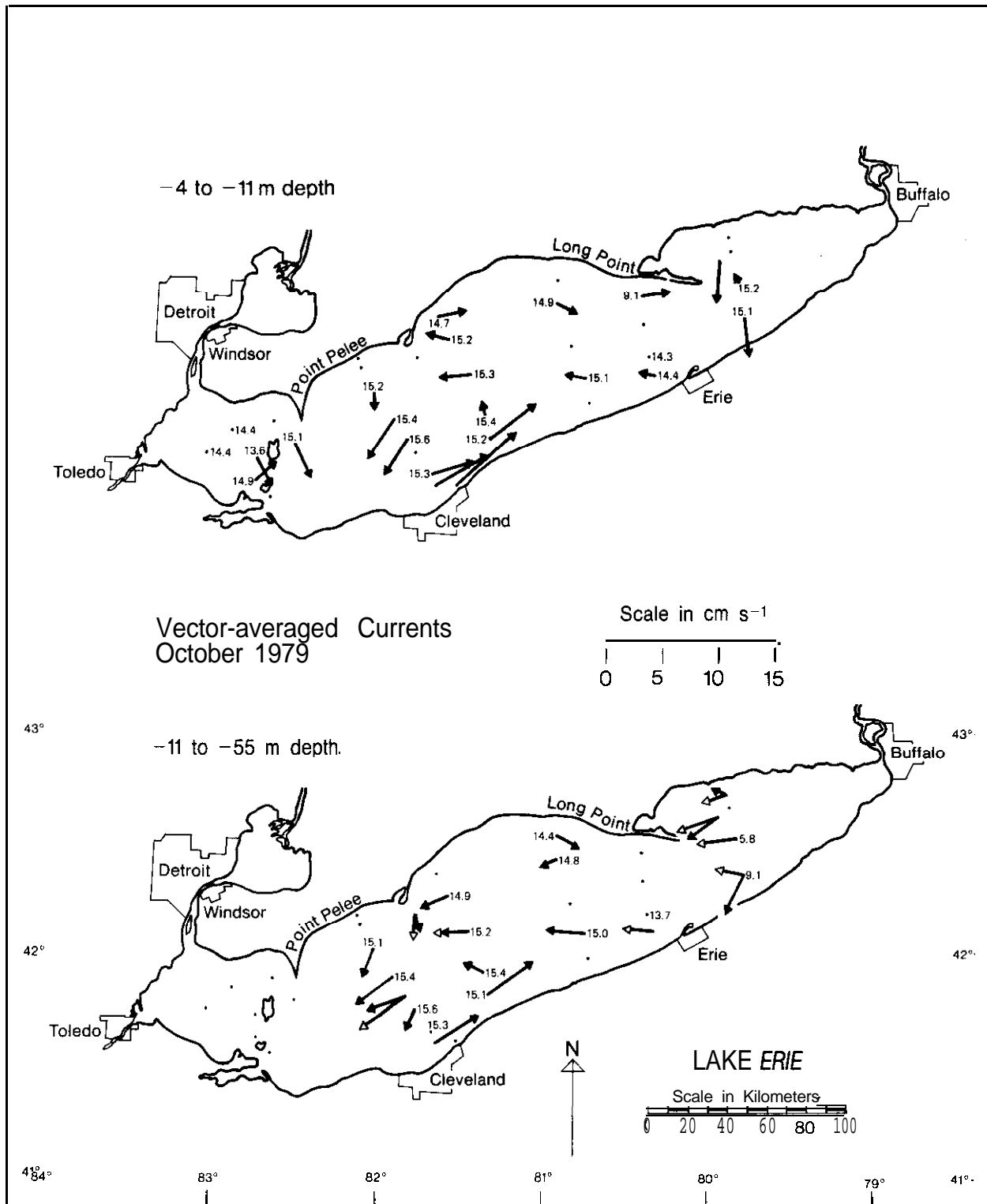


FIGURE 40.--Vector-averaged Lake Erie currents for October 1979. The arrowhead indicating direction of flow is not included as a part of the current speed scale; open arrowheads show currents closest to the bottom. Monthly averaged water temperatures recorded in current meters nearest the surface and at 2.3 m above the bottom are also displayed.

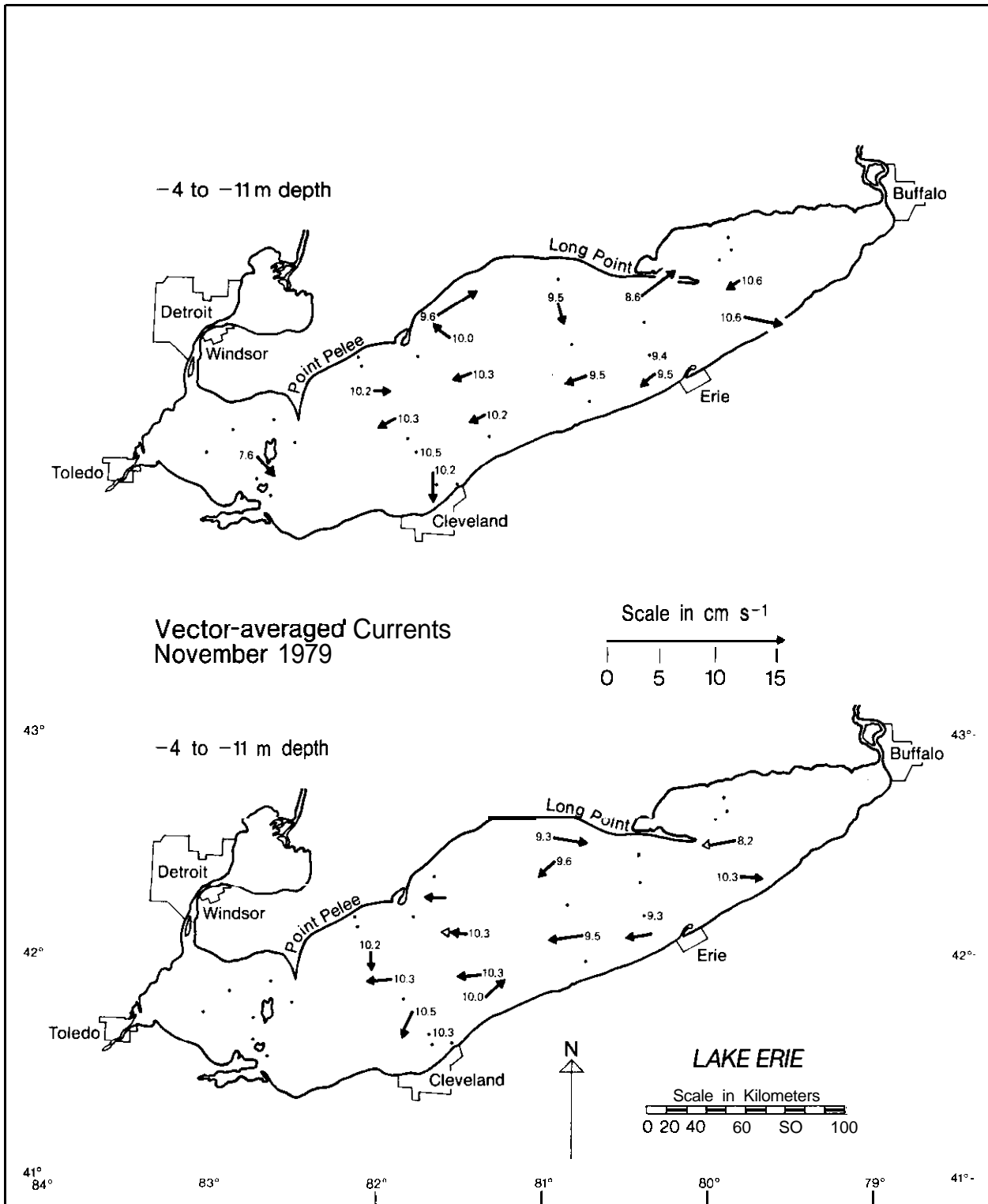


FIGURE 41.--*Vector-averaged* Lake Erie currents for November 1979. The arrowhead indicating direction of *flow* is not included as a part of the current speed scale; open arrowheads show currents closest to the bottom. Monthly averaged water temperatures recorded in current meters nearest the surface and at 2.3 m above the bottom are also displayed.

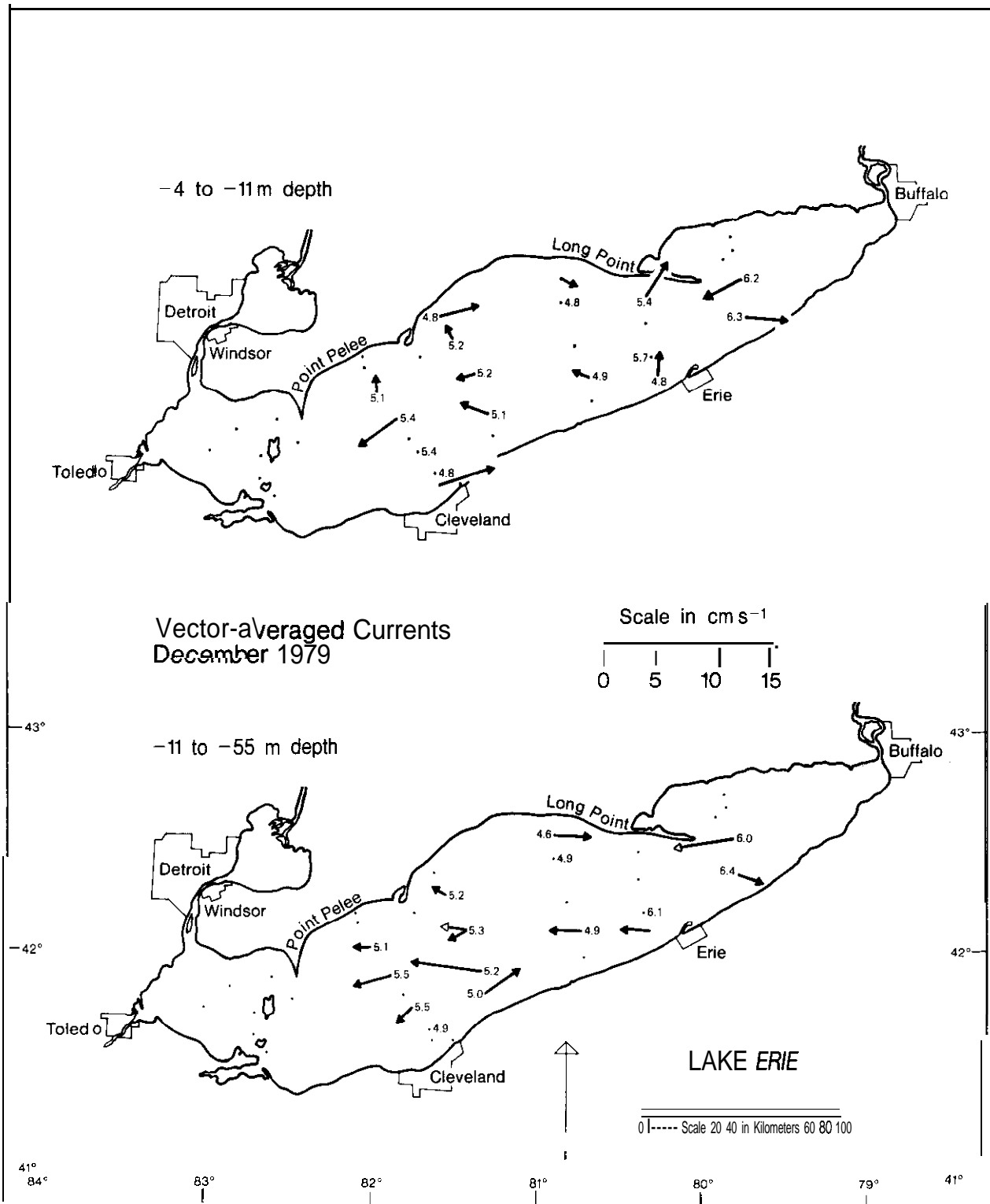


FIGURE 42.--Vector-averaged Lake Erie currents for December 1979. The arrowhead indicating direction of flow is not included as a part of the current speed scale; open arrowheads show currents closest to the bottom. Monthly averaged water temperatures recorded in current meters nearest the surface and at 2.3 m above the bottom are also displayed.

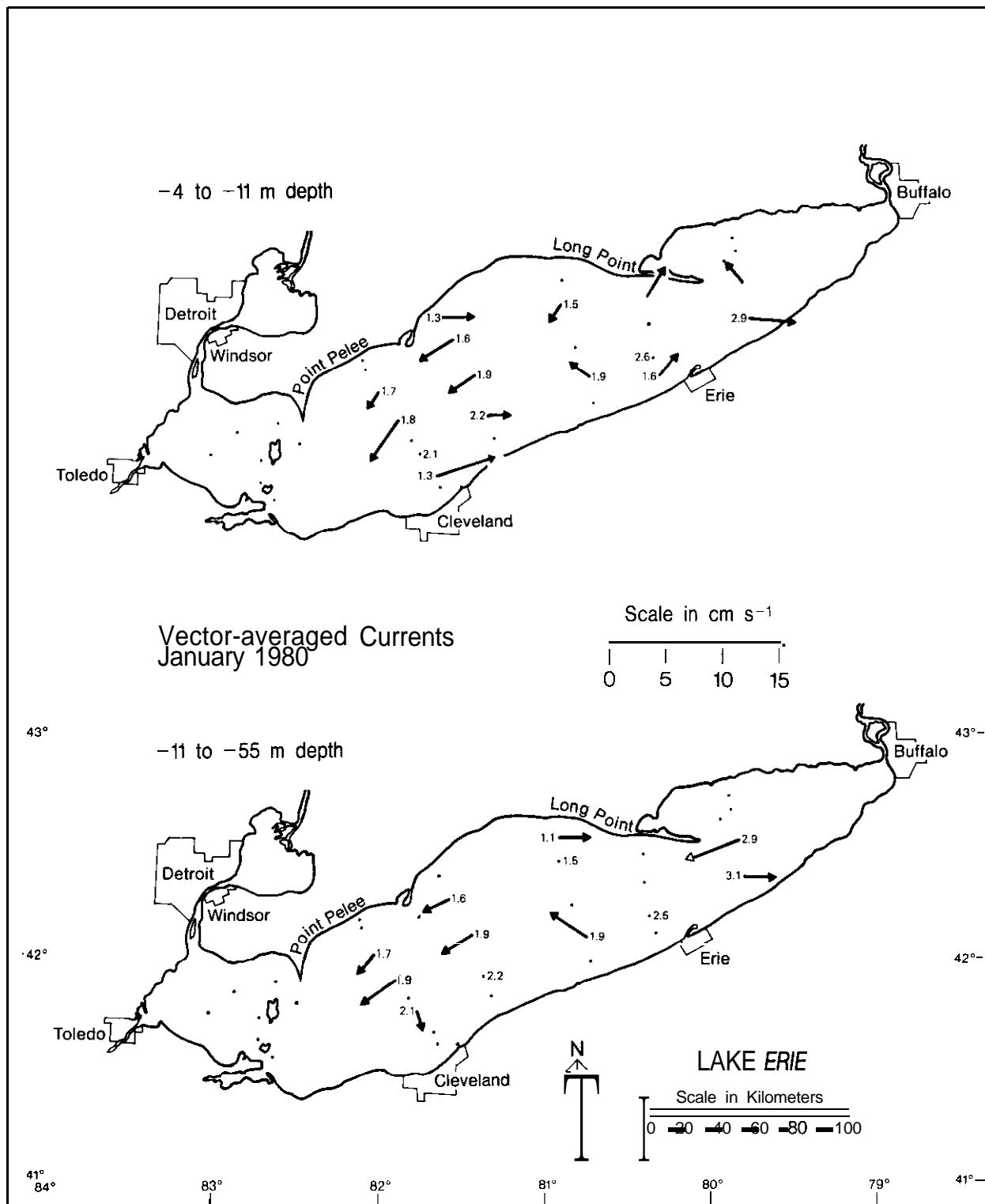


FIGURE 43.--Vector-averaged Lake Erie currents for January 1980. The arrowhead indicating direction of flow is not included as a part of the current speed scale; open arrowheads show currents closest to the bottom. Monthly averaged water temperatures recorded in current meters nearest the surface and at 2.3 m above the bottom are also displayed.

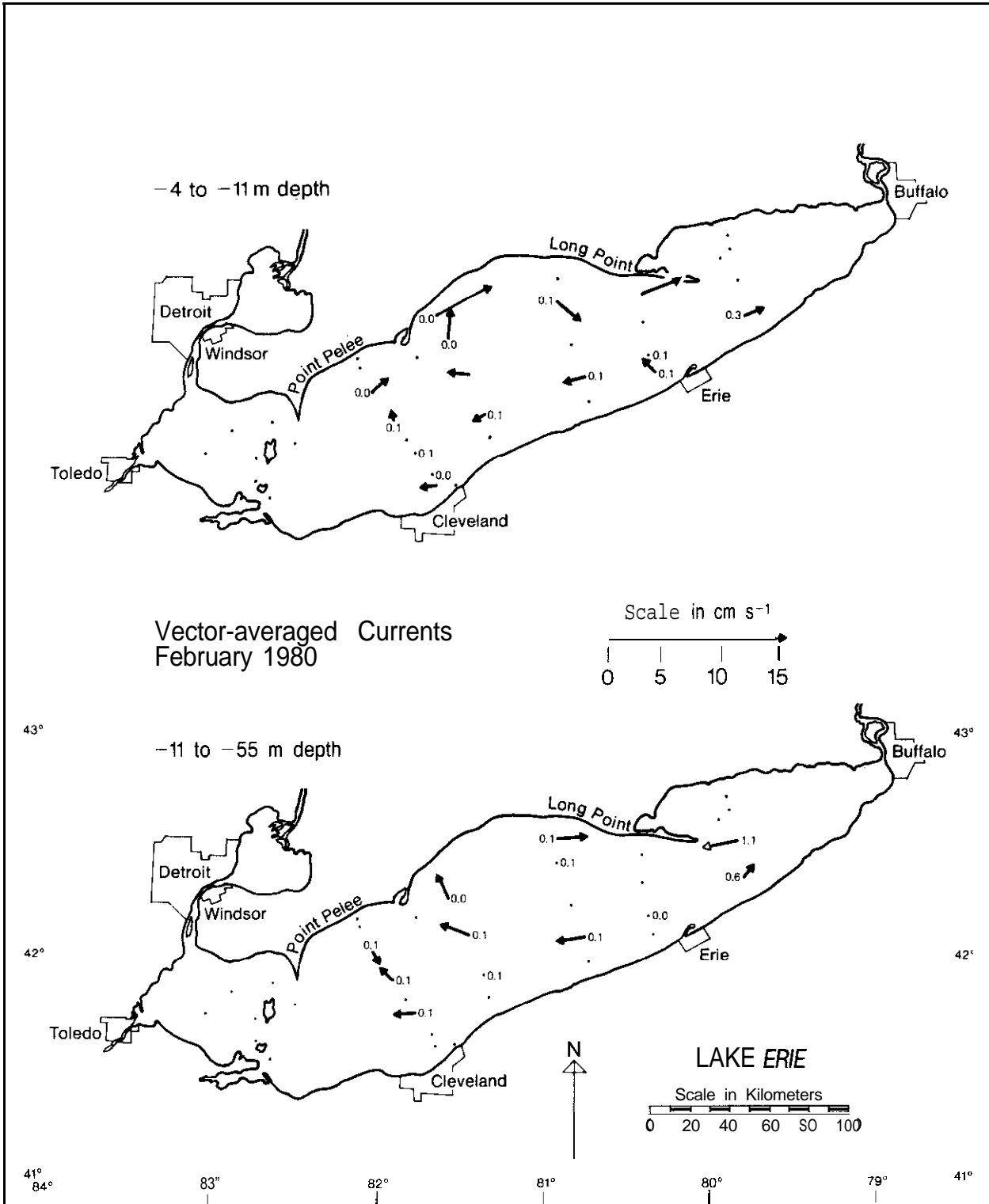


FIGURE 44.--Vector-averaged Lake Erie currents for February 1980. The arrowhead indicating direction of flow is not included as a part of the current speed scale; open arrowheads show currents closest to the bottom. Monthly averaged titer temperatures recorded in current meters nearest the surface and at 2.3 m above the bottom are also displayed.

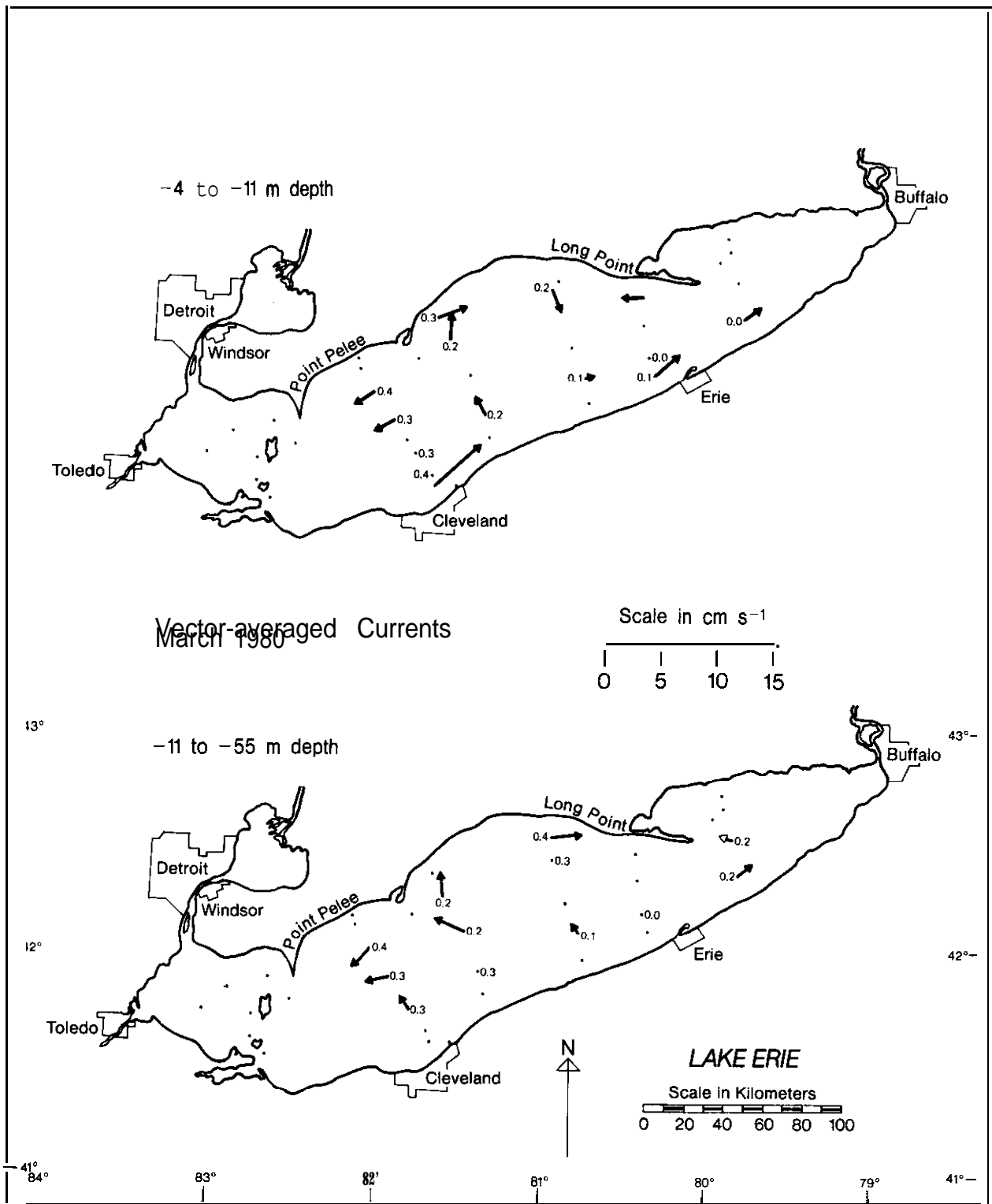


FIGURE 45.--Vector-averaged Lake Erie currents for March 1980. The arrowhead indicating direction of flow is not included as a part of the current speed scale; open arrowheads show currents closest to the bottom. Monthly averaged-water temperatures recorded in current meters nearest the surface and at 2.3 m above the bottom are also displayed.

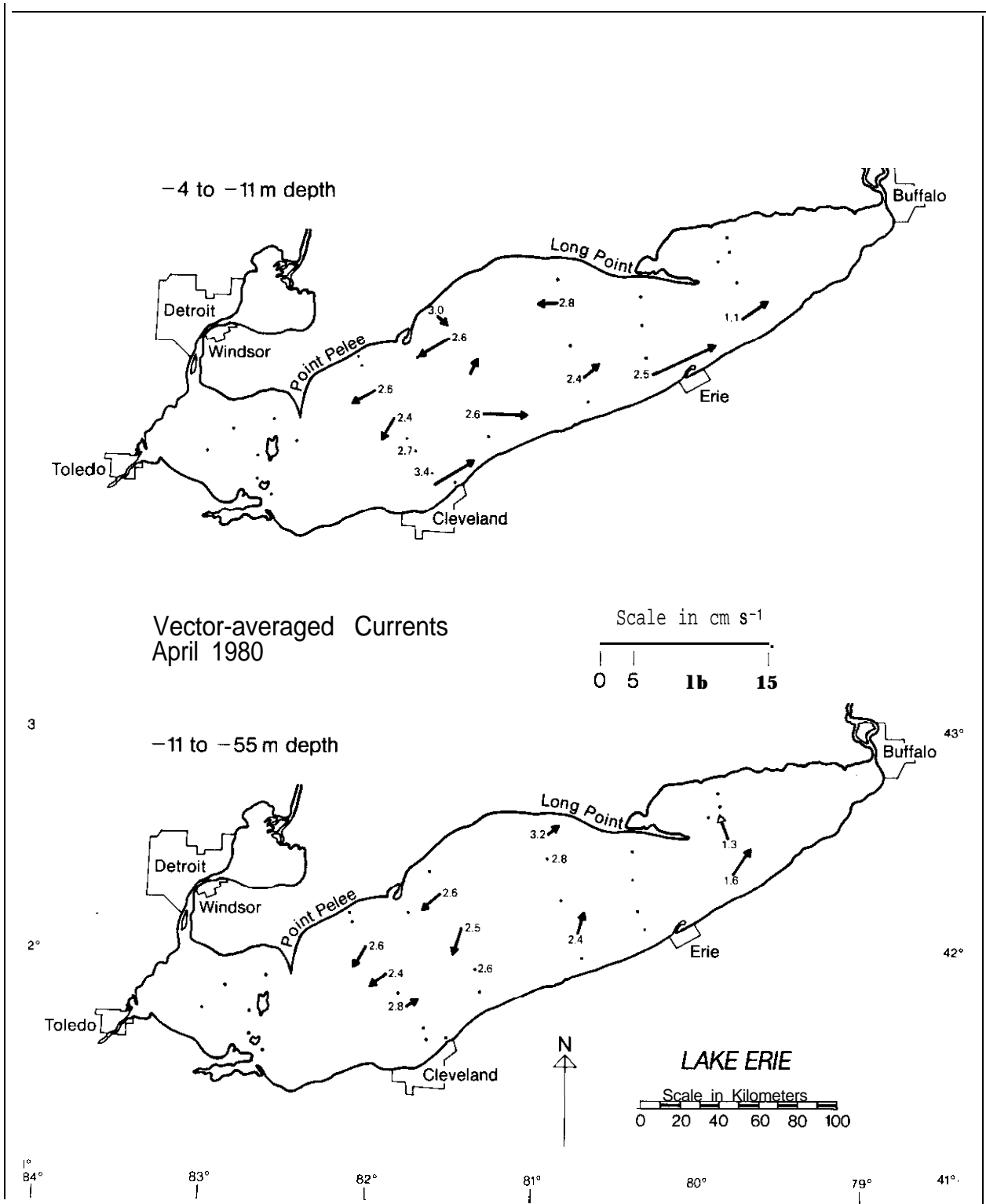


FIGURE 46.--Vector-averaged Lake Erie currents for April 1980. The arrowhead indicating direction of flow is not included as a part of the current speed scale; open arrowheads show currents closest to the bottom. Monthly averaged water temperatures recorded in current meters nearest the surface and at 2.3 m above the bottom are also displayed.

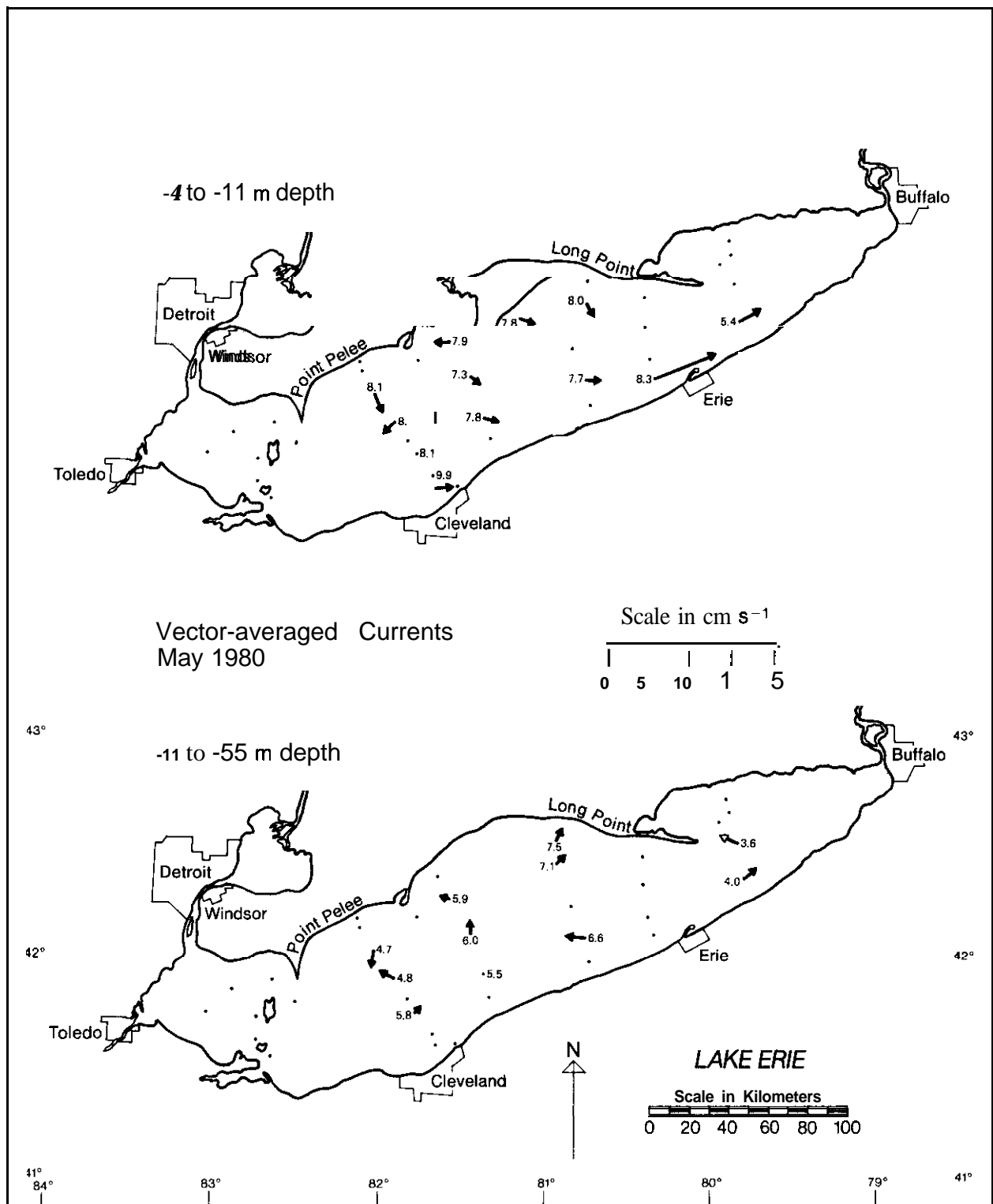


FIGURE 47.--Vector-averaged Lake Erie currents for May 1980. The arrowhead indicating *direction* of flow is *not* included as a *part* of the current *speed* scale; open arrowheads show currents closest to the bottom. Monthly averaged water temperatures recorded in current meters nearest the surface and at 2.3 m above the bottom are also displayed.

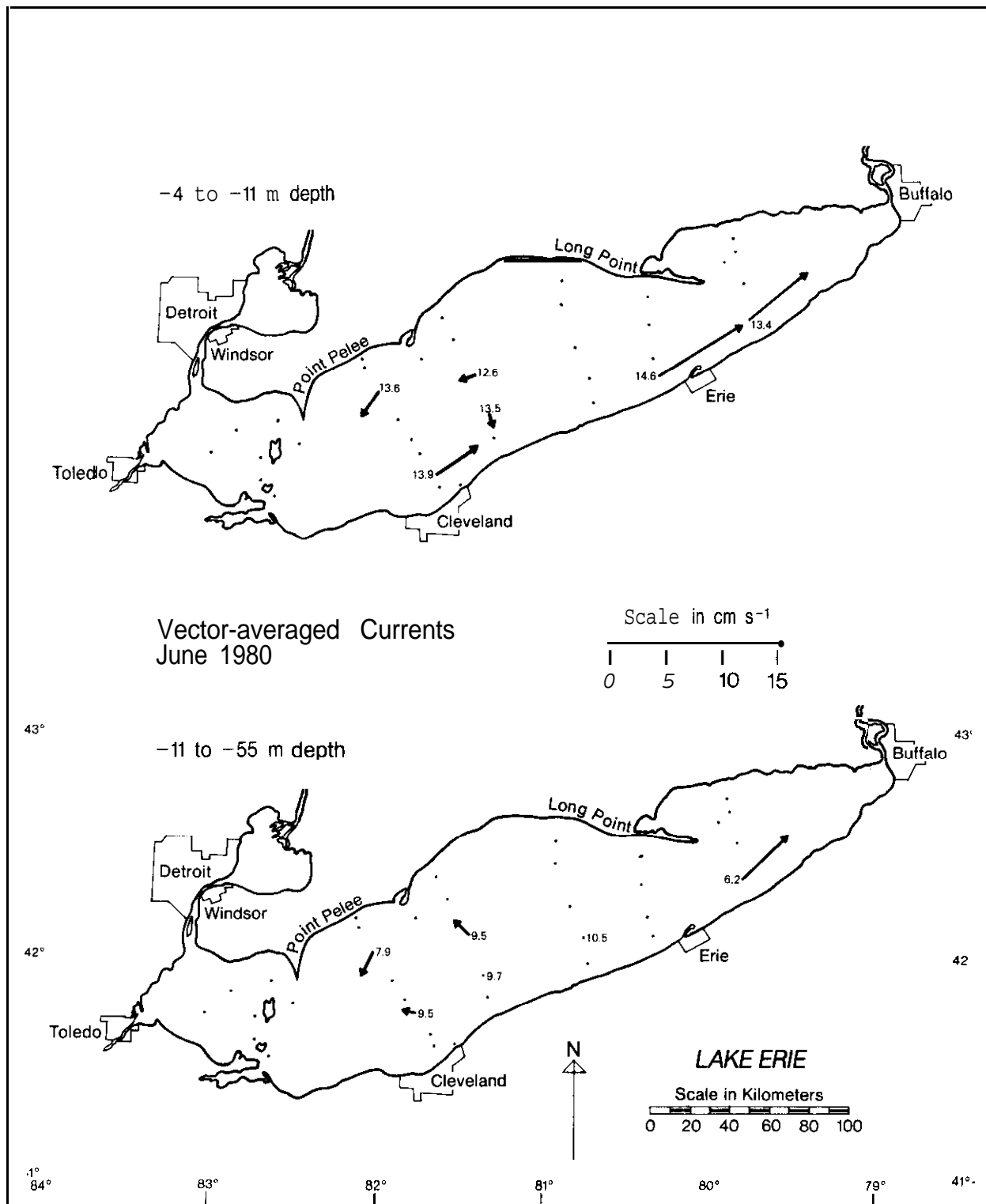


FIGURE 48.--Vector-averaged Lake Erie currents for June 1980. The arrowhead indicating direction of flow is not included as a part of the current speed scale; open arrowheads show currents closest to the bottom. Monthly averaged water temperatures recorded in current meters nearest the surface and at 2.3 m above the bottom are also displayed.